UNIVERSITÀ DEGLI STUDI DI VERONA

DIPARTIMENTO DI BIOTECNOLOGIE

SCUOLA DI DOTTORATO IN SCIENZE NATURALI ED INGEGNERISTICHE

DOTTORATO DI RICERCA IN BIOTECNOLOGIE

CICLO XXXIV

CYSTINE-KNOT PEPTIDES AND BBX MICROPROTEINS AS CONTROLLING FACTORS OF FLOWER AND FRUIT DEVELOPMENT

CO-ORDINATOR: PROF. MATTEO BALLOTTARI
TUTOR: PROF.SSA TIZIANA PANDOLFINI
CO-TUTOR: PROF.SSA BARBARA MOLESINI

DOCTORAL STUDENT: VALENTINA DUSI

INDEX

ABSTRACT ..... - 4 -

1. GENERAL INTRODUCTION ..... - 7 -

2. BIBLIOGRAPHY ..... - 11 -

Chapter 1 | Tomato Cysteine-knot peptides ..... - 13 -

1. INTRODUCTION ..... - 14 -

1.1. Plants cystine-knot proteinase inhibitors ..... - 15 -

1.2. Tomato cystine-knot miniprotein ..... - 16 -

2. AIM OF THE WORK ..... - 19 -

3. MATERIALS AND METHODS ..... - 20 -

3.1. Solanum lycopersicum cv UC82 growth conditions ..... - 20 -

3.2. Preparation of the construct used for TCMP-2 overexpression in MicroTom ..... - 20 -

3.3. Agrobacterium-mediated MicroTom genetic transformation ..... - 20 -

3.4. Arabidopsis plants expressing SlTCMP-2 ..... - 21 -

3.5. Solanum pennelli plants expressing SlTCMP-2 ..... - 22 -

3.6. Ploidy level evaluation and maintenance of diploid S. pennellii T-DNA ..... - 22 -

3.7. Genomic DNA extraction ..... - 23 -

3.8. RNA extraction and quantitative RT-PCR analysis ..... - 23 -

3.9. Phenotypic evaluations ..... - 23 -

3.10. Yeast Two-Hybrid screen ..... - 24 -

3.11. Bimolecular fluorescence complementation assay (BIFC) ..... - 24 -

3.12. In vivo Interaction Assay with Ratiometric BIFC (rBiFC) ..... - 25 -

3.13. Statistical analysis ..... - 25 -

4. RESULTS ..... - 26 -

4.1. TCMP gene family in S. lycopersicum ..... - 26 -

4.2. Tomato plants with an increased TCMP-2 level in flower buds displayed an anticipated termination of sympodial units ..... - 27 -

4.3. Phenotypic alterations in 35S::TCMP-2 MicroTom plants ..... - 30 -

4.4. Phylogenetic TCMPs analysis and S. pennelli plants over-expressing TCMP-2 ..... - 32 -

4.5. TCMP-2 interacts with a member of the BBX family ..... - 35 -

4.5.1. Searching for TCMP interacting partners by Yeast two-hybrid (Y2H) screen ..... - 35 -

4.5.2. Bimolecular fluorescence complementation (BiFC) and Ratiometric BIFC (rBIFC) ..... - 38 -

4.6. The ectopic overexpression of TCMP-2 in Arabidopsis affects the flowering time ..... - 40 -

5. DISCUSSION ..... - 42 -

6. BIBLIOGRAPHY ..... - 46 -

Chapter 2 | Tomato BBX16 and BBX17 microproteins 53
1. INTRODUCTION ..... - 54 -
1.1. Origin, evolution and structure of BBX genes ..... *- 54 -*
1.2. Function of BBX genes ..... *- 57 -*
1.2.1 Flowering process ..... *- 60 -*
2. AIM OF THE WORK ..... - 65 -
3. MATERIALS AND METHODS ..... - 66 -
3.1. Preparation of the genetic construct for SlBBX16 and SlBBX17 overexpression ..... *- 66 -*
3.2. Floral dip transformation of Arabidopsis plants for the overexpression of SlBBX17 and SlBBX16 and phenotypic analysis ..... *- 66 -*
3.3. Yeast Two-Hybrid screen ..... *- 67 -*
3.4. Agrobacterium-mediated MicroTom genetic transformation and phenotypic analysis ..... *- 67 -*
3.5. Genomic DNA extraction ..... *- 68 -*
3.6. RNA extraction and quantitative RT-PCR analysis ..... *- 68 -*
3.7. Phenotypic evaluation ..... *- 68 -*
3.8 Statistical analysis ..... *- 68 -*
4. RESULTS ..... - 69 -
4.1. Molecular and phenotypic analysis of Arabidopsis over-expressing SlBBX16 or SlBBX17 ..... *- 69 -*
4.2. Analysis of BBX16 and BBX17 interaction with components of the Arabidopsis flowering repressor complex ..... *- 72 -*
4.3. Functional analysis of SlBBX17 in tomato ..... *- 75 -*
4.3.1 SlBBX17 expression pattern analysis in MicroTom ..... *- 75 -*
4.3.2. Overexpression of SlBBX17 in MicroTom plants ..... *- 76 -*
4.4. Functional analysis of SlBBX17 in tomato ..... *- 78 -*
5. DISCUSSION ..... - 81 -
6. BIBLIOGRAFY ..... - 84 -
7. APPENDIX A ..... - 91 -
8. APPENDIX B ..... - 98 -

ABSTRACT

Cystine-knot peptides are members of the large family of Cysteine-rich proteins with a dimension typically less than 50 amino acids in their mature form, characterized by the presence of six conserved cysteine (Cys) residues linked by three disulfide bonds in a knotted arrangement (Rees & Lipscomb, 1980). Peptides containing the knot motif are widespread in various species such as fungi, insects, mollusks, and mammals, where they mainly play a defense role against microorganisms, acting as toxins, or as signals in cell defense pathways (Craik et al., 2001; Iyer & Acharya, 2011; Schwarz, 2017; Vitt et al., 2001).

In plants, cystine-knot peptides (also referred to as cysteine-knot miniproteins) are often involved in resistance to pathogens with the function of protease inhibitors, namely metallocarboxypeptidases and serine proteases (Daly & Craik, 2011; Molesini et al., 2017). A class of cystine-knot protease inhibitors specific to the Solanaceae family was described for the first time in the 1980s (Hass & Hermodson, 1981a; Rees & Lipscomb, 1980). This class includes the tomato cystine-knot miniproteins 1 and 2 (TCMP-1 and TCMP-2), of 37 and 44 amino acids, respectively. TCMP-1 and TCMP-2 display a sequential expression pattern, which is highly modulated during flower and fruit development. TCMP-1 is expressed at a very high level in flower buds before anthesis, then its expression decreases rapidly after anthesis and increases again during fruit development (Cavallini et al., 2011). TCMP-1 mRNA level is very low in leaves, although its expression is induced by wounding and elicitors of responses to biotic stress (Díez-Díaz et al., 2004; Martineau et al., 1991). The expression of TCMP-2 is low in flower buds before anthesis, and gradually increases after fertilization, reaching a maximum in green and ripe fruits, whereas it is apparently absent in leaves, roots, and stems (Cavallini et al., 2011; Pear et al., 1989; Treggiari et al., 2015). Indeed, the TCMP-2 promoter (also named 2A11; X13743; [Pear et al., 1989]) has been successfully used to improve qualitative trait in tomato fruit (Davuluri et al., 2005). Although the biological activity of metallocarboxypeptidase inhibitors supports a role for Solanaceous cystine-knot proteins in plant defense, it has recently been demonstrated that tomato TCMPs are implicated in fruit development (Molesini et al., 2018).

In the paper by Molesini et al. (2018), tomato plants transformed with a chimeric gene containing the entire TCMP-1 coding region under the control of the TCMP-2 promoter (pTCMP-2::TCMP-1) showed a marked increase in the expression of TCMP-2 before anthesis,

associated with anticipated fruit production. This evidence suggests that TCMPs are regulators of fruiting time and that the maintenance of a correct TCMP-1/TCMP-2 ratio is required for proper initial fruit growth. The mode of action of TCMPs remains largely unexplored also due to the absence of homologous genes in other model species, including *Arabidopsis thaliana*. In several cases, Cysteine-rich peptides act as signaling molecules in plant development, by interfering with receptors or modifying the activity of multimeric complexes (de Coninck & de Smet, 2016; Tavormina et al., 2015).

The general aim of this thesis was a further investigation of the functional role played by TCMP-2 during the first phases of reproductive development.

Specific aims were:

1) phenotypic and molecular analyses of *pTCMP-2::TCMP-1* and *35S::TCMP-2* plants, during the transition from vegetative growth to reproductive development;
2) identification of TCMP-2 interacting partners by Yeast Two-Hybrid (Y2H) screening using a tomato cDNA library;
3) functional study of one of these interactors (*i.e.,* a B-BOX motif-containing protein) in both Arabidopsis and tomato.

A detailed analysis of *pTCMP-2::TCMP-1* plants during the transition from the vegetative to the reproductive stage showed an anticipated termination of the sympodial units linked with an induced expression of the florigen gene *SINGLE FLOWER TRUSS* (SFT), which is the main inducer of flowering. Moreover, MicroTom plants over-expressing TCMP-2 under the control of the CaMV35S constitutive promoter exhibited a reduction of the primary shoot length, very often accompanied by a decreased number of leaves before the first inflorescence, which are indicators of early flowering.

The Y2H screen permitted the identification of 47 potential interactors of TCMP-2. Among them, we focused on the B-Box domain-containing protein 16 (*Sl*BBX16). The interaction between TCMP-2 and *Sl*BBX16 was validated *in vivo* in plant cells by bimolecular fluorescence complementation (BIFC) analysis. We demonstrated that TCMP-2 is also able to interact with *Sl*BBX17, which is the closest tomato homolog of *Sl*BBX16, and with the *Sl*BBX16 Arabidopsis homolog, *At*BBX31. A recent study showed the involvement of *At*BBX30 and *At*BBX31 microproteins (also referred to as miP1b and miP1a) in a multiprotein complex which

regulates flowering time in Arabidopsis (Graeff et al., 2016). These proteins interact with the flowering regulator CONSTANS (*At*BBX1) and additionally engage in a larger protein complex involving the co-repressor protein TOPLESS through a specific amino acid motif (PFVFL). These interactions suppress the CO-mediated induction of FT expression, causing the severe late flowering phenotype observed in plants over-expressing AtBBX30/31.

The implication of *At*BBX30/31 in flowering control may indicate that the TCMP-2-*Sl*BBX16/*Sl*BBX17 interaction could play a role in the regulation of flowering. To test this hypothesis, we ectopically overexpressed TCMP-2, *Sl*BBX16 and *Sl*BBX17 in Arabidopsis. The overexpression of TCMP-2 led to an anticipated flowering phenotype linked to an increased FT mRNA level, whereas the overexpression of *Sl*BBX16 and *Sl*BBX17 in *Arabidopsis* WT and *At*BBX30/31 KO mutant resulted in a slight delay in flowering time, suggesting that tomato BBXs were unable to fully phenocopy *At*BBX30/31 overexpression.

One of the possible reasons for the weak phenotype displayed by *A. thaliana* over-expressing *Sl*BBX16 and *Sl*BBX17 could be attributed to their inability to interact with *At*CO and *At*TPL, since the interaction between *At*BBX30/31 with *At*CO and *At*TPL is due to the PFVLF motif (Graeff et al., 2016), which is absent in *Sl*BBX16 and *Sl*BBX17. Indeed, the Y2H experiments revealed no interaction between the tomato BBXs and *At*CO and *At*TPL, even when using a mutated version of *Sl*BBXs containing the PFVLF motif.

The functional study in tomato was conducted on *Sl*BBX17, which presents a peculiar expression pattern in the floral organs. MicroTom plants over-expressing *Sl*BBX17 showed a number of leaves at the first inflorescence similar to that of WT plants, but a delay in the time to reach the flower anthesis stage and a reduced number of ripe fruits.

To investigate whether in tomato TCMP-2 and *Sl*BBX17 may participate in a multiprotein complex similar to that described in Arabidopsis (*At*BBX30/31-CO-TPL), we carried out *ad hoc* Y2H analyses to test the interaction between TCMP-2 and *Sl*CO1 and *Sl*TPL1 and the interaction between *Sl*BBX17 and *Sl*CO1 and *Sl*TPL1. Our data indicate that neither TCMP-2 nor *Sl*BBX17 can directly bind to *Sl*CO1 and *Sl*TPL1. Further investigation of the role in flowering and fruiting of *Sl*BBX16, the homologue of *Sl*BBX17, may provide additional insight into the function of BBXs microproteins in tomato.

1. GENERAL INTRODUCTION

Several years ago, the discovery of genes encoding small peptides with hormonal activity in Arabidopsis stimulated research interest for these signaling molecules, leading to the identification of genes putatively coding for hormonal peptides in many plant species (Lease & Walker, 2006; Ohyama et al., 2008). Plant signaling peptides are involved in cell–cell communication networks and coordinate many developmental processes, such as reproduction mechanisms, symbiotic interactions, and stress and defense responses (Matsubayashi, 2014; Tavormina et al., 2015). Frequently, the cell signaling activation response is the consequence of the perception of small peptides by receptor-like kinases (RLKs). This binding stimulates receptor dimerization with coreceptors, initiating cellular signaling outputs. This apparently simple peptide perception mechanism can activate several different signaling pathways due to the enormous diversity of peptide-receptor/coreceptor pairs (M. J. Kim et al., 2021).

Small peptides included amino acid sequences in the range 2-100 in length and can be divided into classes based on their mode of action, which can be extracellular or intracellular. Small peptides can either originate from precursor proteins or be directly translated from short open reading frame (sORF) embedded in transcripts. The latter refers to peptides that can be translated from a sORF (<100 codons) that is present in the leader sequence of an mRNA, in primary transcripts of microRNAs (miRNAs), in intergenic RNAs, in presumed non-coding RNAs or in other transcripts not encoding longer (>100 amino acids) proteins (Hanada et al., 2013; Lauressergues et al., 2015). The precursor protein-derived peptides can be formed from non-functional precursors or functional precursors. The non-functional precursor, also referred to as inactive precursor, presents an N-terminal signal sequence (NSS) that directs the protein to the secretory pathway. Moreover, precursor proteins can also contain pro-domains, requiring additional processing to obtain the biologically active mature peptides. The maturation process of these peptides may involve multiple proteolysis cycles and post-translational modification (de Coninck & de Smet, 2016). Indeed, peptides derived from non-functional precursors can be i) post-translationally modified (PTM), ii) non-Cys-rich and non-post translationally modified (non-Cys-rich/non-PTM) and iii) Cys-rich (Tavormina et al., 2015). Post-translational modifications are known to alter the physicochemical properties of peptides by changing net charge, hydrophilicity, and/or conformation, thus modulating the

binding ability and specificity for their target receptor proteins (Matsubayashi, 2011, 2014). PTM peptides typically consist of a maximum of 20 amino acids, present few or no Cys residues in their sequence, contain modifications on their Pro and Tyr residues, and are released from pre-protein precursors. PTM peptides are often grouped in highly conserved families, including C-TERMINALLY ENCODED PEPTIDE (CEP), CLAVATA3/EMBRYO SURROUNDING REGION RELATED (CLE), and ROOT GROWTH FACTOR (RGF)/GOLVEN (GLV)/CLE-LIKE (CLEL) peptides, with great functional redundancy within the families. For most of these peptides, the signal transduction pathway is well known.

The most studied PTM peptides belong to the CLE family, a large group of secreted peptides. Functional roles in root, shoot and floral meristem maintenance, lateral root emergence and vascular development have been described for most of the CLE peptides identified in Arabidopsis. CLE signaling pathways are also involved in plant-environment interactions, including symbiosis and responses to abiotic stresses (Mitchum et al., 2008; Wang and Fiers, 2010; Kiyohara and Sawa, 2012; Miyawaki et al., 2013; Qiang et al., 2013; Yamaguchi et al., 2016).

Non-Cys-rich/non-PTM peptides, usually from 8 to 36 amino acids in length, are characterized by functionally important residues, such as proline, glycine, and lysine. This small group of peptides, which includes Systemins, is mainly involved in the defense response of plants (Tavormina et al., 2015).

Cysteine-Rich peptides (CRPs) represent a second class of small peptides derived from nonfunctional precursors. Genes coding for CRPs are usually found in gene clusters located in discrete chromosomal regions, probably originated because of successive series of gene duplications. The amino acid position of cysteine-rich peptides is highly different between clusters and between species, but they all share four common characteristics: small size (less than 160 amino acid residues), positive charge, presence of the conserved NSS and a C-terminal cysteine-rich domain usually containing 4-16 cysteine residues (Marshall et al., 2011; Murphy & de Smet, 2014). The C-terminal portion of CRPs form intramolecular disulfide bonds that are essential for proper class-specific secondary folding and activity. The majority of known Cys-rich plant peptides are thought to function as antimicrobial peptides (AMPs) during plant-microbe interactions, and they have been isolated from roots, leaves, stems, flowers, and seeds (Nawrot et al., 2014). Additionally, it has been shown that several Cys-rich peptides also have a role in plant development, pollen recognition and guidance, and seed

development (Marshall et al., 2011; Quet al., 2015; Molesini et al., 2018, 2020). Based on the conserved Cys pattern and three-dimensional (3D) structural characteristics, which are largely dependent on the arrangement of the disulfide bridges, CRPs are grouped in distinct categories. Amongst the plant CRPs, the class of cystine-knot peptides, also known as knottins or inhibitor cystine-knot peptides or cystine-knot miniproteins, is characterized by a particular 3D structure. The cystine-knot peptides are less than 50 amino acids in the mature form and contain six conserved cysteine forming three disulfide bonds in the C-terminal region that are intertwined giving rise to a unique structural scaffold (Molesini et al., 2017). This group of cystine-knot proteins is structurally subdivided into the linear inhibitor cystine-knot peptides (ICK) and cyclic cystine-knot peptides (CCK) or cyclotides. In several cases, Cys-rich peptides act as signaling molecules by interfering with receptors or modifying the activity of multimeric complexes (de Coninck & de Smet, 2016; Tavormina et al., 2015). For instance, Koehbach and collaborators (2013) demonstrated that the oxytocin and vasopressin V1a receptors, members of the G protein-coupled receptor family, are the molecular targets of the *Viola odorata* cyclotide kalata B7, found to induce contractility in human uterine smooth muscle cells. Tomato carboxypeptidase inhibitors, TCMPs, which are linear cystine-knot miniproteins, displayed bio-activity in heterologous systems by affecting vascular endothelial growth factor receptor (VEGFR) activation (Treggiari et al., 2015). Currently, no receptors for TCMPs have been found in plants.

Recently, functional studies on TCMP-2 highlighted its involvement in fruit development and flowering time, suggesting that another mode of action of Cystine-knot miniproteins might be attributed to their participation in regulatory multimeric complexes (Molesini et al., 2018, 2020).

The capability to interfere with multidomain complexes, by sequestering target proteins into non-functional complexes, is one of the functions fulfilled by MicroProteins (miPs) (Graeff & Wenkel, 2012). miPs are potent regulators of protein activity in both plants and animals, typically present a small size (below 140 amino acids) and a single domain protein, and harbor a protein-protein-interaction domain. Thus, the term ‘microProtein’ was coined due to their small size and negative regulatory activity similar to miRNAs (Staudt & Wenkel, 2011). Several miPs have been identified in past years in plants and a characteristic of all these small proteins is their ability to engage larger, multi-domain proteins into dimers inhibiting the default function of the larger protein (Eguen et al., 2015; Seo et al., 2011; Staudt & Wenkel, 2011).

miPs can derive from individual genes but can also be produced by alternative splicing. Additionally, it might be possible that the generation of these microproteins occurs through proteolytic cleavage of proteins, thereby losing domains required for activity but retaining domains required for dimerization (Graeff and Wenkel, 2012).

The analysis of the translated Arabidopsis ORFeome for the existence of small, single-domain proteins, which might function as microProteins targeting transcriptional regulators, has led to the identification of a multitude of putative miPs (Graeff et al., 2016). In particular, two Arabidopsis miPs, miP1a and miP1b (also referred to as *At*BBX31 and *At*BBX30, respectively), have been reported to heterodimerize with the flowering regulator CONSTANS (CO). Their interactions cause late flowering in Arabidopsis due to a failure in the induction of FLOWERING LOCUS T (FT) expression.

Expanding knowledge on the role played by small Cys-rich peptides and miPs into mechanisms that regulate the plant life cycle could elucidate fundamental processes such as flowering and fruit set, which are important for maintenance of productivity in the context of changing environment.

2. BIBLIOGRAPHY

de Coninck, B., & de Smet, I. (2016). Plant peptides – taking them to the next level. *Journal of Experimental Botany*, *67*(16), 4791–4795. https://doi.org/10.1093/JXB/ERW309

Eguen, T., Straub, D., Graeff, M., & Wenkel, S. (2015). MicroProteins: small size-big impact. *Trends in Plant Science*, *20*(8), 477–482. https://doi.org/10.1016/J.TPLANTS.2015.05.011

Graeff, M., Straub, D., Eguen, T., Dolde, U., Rodrigues, V., Brandt, R., & Wenkel, S. (2016). MicroProtein-Mediated Recruitment of CONSTANS into a TOPLESS Trimeric Complex Represses Flowering in Arabidopsis. *PLoS Genetics*, *12*(3). https://doi.org/10.1371/journal.pgen.1005959

Graeff, M., & Wenkel, S. (2012). Regulation of protein function by interfering protein species. *Biomolecular Concepts*, *3*(1), 71–78. https://doi.org/10.1515/BMC.2011.053/MACHINEREADABLECITATION/RIS

Hanada, K., Higuchi-Takeuchi, M., Okamoto, M., Yoshizumi, T., Shimizu, M., Nakaminami, K., Nishi, R., Ohashi, C., Iida, K., Tanaka, M., Horii, Y., Kawashima, M., Matsui, K., Toyoda, T., Shinozaki, K., Seki, M., & Matsui, M. (2013). Small open reading frames associated with morphogenesis are hidden in plant genomes. *Proceedings of the National Academy of Sciences of the United States of America*, *110*(6), 2395–2400. https://doi.org/10.1073/PNAS.1213958110

Kim, M. J., Jeon, B. W., Oh, E., Seo, P. J., & Kim, J. (2021). Peptide Signaling during Plant Reproduction. *Trends in Plant Science*, *26*(8), 822–835. https://doi.org/10.1016/J.TPLANTS.2021.02.008

Koehbach, J., O'Brien, M., Muttenthaler, M., Miazzo, M., Akcan, M., Elliott, A. G., Daly, N. L., Harvey, P. J., Arrowsmith, S., Gunasekera, S., Smith, T. J., Wray, S., Göransson, U., Dawson, P. E., Craik, D. J., Freissmuth, M., & Gruber, C. W. (2013). Oxytocic plant cyclotides as templates for peptide G protein-coupled receptor ligand design. *Proceedings of the National Academy of Sciences of the United States of America*, *110*(52), 21183–21188. https://doi.org/10.1073/PNAS.1311183110

Lauressergues, D., Couzigou, J. M., San Clemente, H., Martinez, Y., Dunand, C., Bécard, G., & Combier, J. P. (2015). Primary transcripts of microRNAs encode regulatory peptides. *Nature 2015 520:7545*, *520*(7545), 90–93. https://doi.org/10.1038/nature14346

Lease, K. A., & Walker, J. C. (2006). The Arabidopsis unannotated secreted peptide database, a resource for plant peptidomics. *Plant Physiology*, *142*(3), 831–838. https://doi.org/10.1104/PP.106.086041

Marshall, E., Costa, L. M., & Gutierrez-Marcos, J. (2011). Cysteine-Rich Peptides (CRPs) mediate diverse aspects of cell-cell communication in plant reproduction and development. *Journal of Experimental Botany*, *62*(5), 1677–1686. https://doi.org/10.1093/jxb/err002

Matsubayashi, Y. (2011). Post-Translational Modifications in Secreted Peptide Hormones in Plants. *Plant and Cell Physiology*, *52*(1), 5. https://doi.org/10.1093/PCP/PCQ169

Matsubayashi, Y. (2014). Posttranslationally Modified Small-Peptide Signals in Plants. *Http://Dx.Doi.Org/10.1146/Annurev-Arplant-050312-120122*, *65*, 385–413. https://doi.org/10.1146/ANNUREV-ARPLANT-050312-120122

Mitchum, M. G., Wang, X., & Davis, E. L. (2008). Diverse and conserved roles of CLE peptides. *Current Opinion in Plant Biology*, *11*(1), 75–81. https://doi.org/10.1016/J.PBI.2007.10.010

Molesini, B., Dusi, V., Pennisi, F., di Sansebastiano, G. pietro, Zanzoni, S., Manara, A., Furini, A., Martini, F., Rotino, G. L., & Pandolfini, T. (2020). TCMP-2 affects tomato flowering and interacts with BBX16, a homolog of the arabidopsis B-box MiP1b. *Plant Direct*, *4*(11), e00283. https://doi.org/10.1002/PLD3.283

Molesini, B., Rotino, G. L., Dusi, V., Chignola, R., Sala, T., Mennella, G., Francese, G., & Pandolfini, T. (2018). Two metallocarboxypeptidase inhibitors are implicated in tomato fruit development and regulated by the Inner No Outer transcription factor. *Plant Science*, *266*, 19–26. https://doi.org/10.1016/J.PLANTSCI.2017.10.011

Molesini, B., Treggiari, D., Dalbeni, A., Minuz, P., & Pandolfini, T. (2017). Plant cystine-knot peptides: pharmacological perspectives. *British Journal of Clinical Pharmacology*, *83*(1), 63–70. https://doi.org/10.1111/BCP.12932

Murphy, E., & de Smet, I. (2014). Understanding the RALF family: A tale of many species. *Trends in Plant Science*, *19*(10), 664–671. https://doi.org/10.1016/J.TPLANTS.2014.06.005

Nawrot, R., Barylski, J., Nowicki, G., Broniarczyk, J., Buchwald, W., & Goździcka-Józefiak, A. (2014). Plant antimicrobial peptides. *Folia Microbiologica*, *59*(3), 181–196. https://doi.org/10.1007/S12223-013-0280-4/TABLES/7

Ohyama, K., Ogawa, M., & Matsubayashi, Y. (2008). Identification of a biologically active, small, secreted peptide in Arabidopsis by in silico gene screening, followed by LC-MS-based structure analysis. *Plant Journal*, *55*(1), 152–160. https://doi.org/10.1111/J.1365-313X.2008.03464.X

Seo, P. J., Hong, S. Y., Kim, S. G., & Park, C. M. (2011). Competitive inhibition of transcription factors by small interfering peptides. *Trends in Plant Science*, *16*(10), 541–549. https://doi.org/10.1016/J.TPLANTS.2011.06.001

Staudt, A. C., & Wenkel, S. (2011). Regulation of protein function by 'microProteins.' *EMBO Reports*, *12*(1), 35–42. https://doi.org/10.1038/EMBOR.2010.196

Tavormina, P., de Coninck, B., Nikonorova, N., de Smet, I., & Cammue, B. P. A. (2015). *The Plant Peptidome: An Expanding Repertoire of Structural Features and Biological Functions OPEN*. https://doi.org/10.1105/tpc.15.00440

Treggiari, D., Zoccatelli, G., Molesini, B., Degan, M., Rotino, G. L., Sala, T., Cavallini, C., Macrae, C. A., Minuz, P., & Pandolfini, T. (2015). A cystine-knot miniprotein from tomato fruit inhibits endothelial cell migration and angiogenesis by affecting vascular endothelial growth factor receptor (VEGFR) activation and nitric oxide production. *Molecular Nutrition & Food Research*, *59*(11), 2255–2266. https://doi.org/10.1002/MNFR.201500267

von Arnim, A. G., Jia, Q., & Vaughn, J. N. (2014). Regulation of plant translation by upstream open reading frames. *Plant Science*, *214*, 1–12. https://doi.org/10.1016/J.PLANTSCI.2013.09.006

Wang, G., & Fiers, M. (2010). CLE peptide signaling during plant development. *Protoplasma*, *240*(1), 33–43. https://doi.org/10.1007/S00709-009-0095-Y/TABLES/1

Yamaguchi, Y. L., Ishida, T., & Sawa, S. (2016). *CLE peptides and their signaling pathways in plant development*. https://doi.org/10.1093/jxb/erw208

Chapter 1 | Tomato Cysteine-knot peptides

1. INTRODUCTION

Cystine-knot peptides/miniproteins, also known as knottins or inhibitor cystine-knots (ICK; https://www.dsimb.inserm.fr/KNOTTIN/), came to light as an important class of molecules with applications as therapeutic and diagnostic agents (Daly & Craik, 2011; Kolmar, 2010; Molesini et al., 2017; Molesini et al., 2018). Polypeptides containing cystine-knot motifs have been found in fungi, plants and animals and perform a multitude of different biological functions. In animals, cystine-knot miniproteins can function as extracellular ligands and regulate numerous cellular functions such as cell growth and development (Vitt et al., 2001). In plants, some cystine-knot peptides, belonging to the carboxypeptidase inhibitor group, have been shown to confer resistance to pathogens by acting as elicitors of defence responses, probably thanks to their activity as peptidase inhibitors (Norton & Pallaghy, 1998;Quilis et al., 2007).

Knottins are generally less than 50 residues long and are characterized by a common fold due to the presence of six conserved cysteines usually in the C-terminal region, which allows the formation of three interwoven disulfide bridges, realizing an intramolecular knot (le Nguyen et al., 1990) (Figure 1). This conformation confers a compact and extremely stable structure and functional resistance to high temperature, enzymatic degradation, extreme pH and mechanical stress (Ireland et al., 2006; Werle et al., 2006).

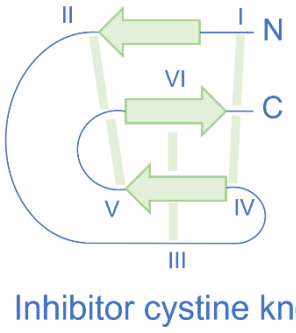

Figure 1. Schematic diagram of inhibitor cystine-knot. The β-strands are drawn as arrows, the cysteine residues are numbered (I – VI), disulfide bonds are represented as shaded lines. The penetrating disulfide bond connects Cys III – VI (modified from Craik et al., 2001).

The cystine-knot motif is also present in several human growth factors, including transforming growth factor-β (TGF-β), nerve growth factor (NGF), glycoprotein hormones (GPHs) and vascular endothelial growth factors (VEGF) (Iyer & Acharya, 2011); however, in these proteins

the connectivity is different and thus they belong to a distinct structural family (https://www.dsimb.inserm.fr/KNOTTIN/). During evolution, the growth factors have acquired loops with versatility in conformational changes that presumably serve to modulate their biological specificity or enable them to trigger changes in their cognate receptors as part of the process of signal transduction (Pallaghy et al., 1994).

1.1. Plants cystine-knot proteinase inhibitors

Rees and Lipscomb (1980) obtained the crystal structure of the first cystine-knot protease inhibitor in potato (PCI), consisting of 39 amino acids which form a globular peptide characterized by turns, beta strands, and the peculiar cystine-knot motif. It was also demonstrated that PCI acts as potent protease inhibitor on different enzymes of the metallocarboxypeptidases (MCPs; *e.g.*, carboxypeptidase A family [Ryan et al., 1974]). MCPs catalyze the hydrolysis of peptide bonds at the C-terminus of peptides and proteins, and their catalytic mechanism involves a metal ion, often zinc. The activity of MCPs can be regulated by protease inhibitors that play different functions, such as preventing uncontrolled proteolysis or acting as antifeedant and antimicrobial molecules contributing to plant protection (Hartl et al., 2010; Norton & Pallaghy, 1998; Quilis et al., 2007; Ryan, 1980).

Consisting with a role of MCP inhibitors in plant defense, PCIs accumulate in potato tubers and in leaves after wounding and after treatment with abscisic acid and jasmonate (Graham & Ryan, 1981; Villanueva et al., 1998). In this regard, Quilis and collaborators (2013) demonstrated that the expression in rice of a fusion gene encoding two proteinase inhibitors, PCI and MPI (maize proteinase inhibitor), provides dual resistance against the lepidopteran *Chilo suppressalis* and the fungal pathogen *Magnaporthe oryzae*, two detrimental agents affecting rice crops.

Other cystine-knot metallocarboxypeptidase inhibitors with homologous sequences have been isolated from other species of the Solanaceae family such as: MCPI in S*olanum lycopersicum* (Hass & Hermodson, 1981), YBPCI in *Capsicum annuum* L. var. Yellow Bell Pepper (Cotabarren et al., 2018) and imaPCI in a variety of Andean potato, *Solanum tuberosum* subsp. *Andigenum cv. Imilla morada* (Lufrano et al., 2015).

1.2. Tomato cystine-knot miniprotein

Hass and Hermodson (1981) reported the amino acid sequence of a 37 residue-long cystine-knot carboxypeptidase inhibitor from tomato. The homology between this new peptide and PCI was demonstrated, showing that 26 residues are identical in the two miniproteins. Ten years later, the cDNA of this tomato metallocarboxypeptidase inhibitor (MCPI also referred as tomato cystine-knot miniprotein, TCMP-1) was identified and characterized through the screening of an ovary cDNA library of *Solanum lycopersicum* cv UC82 (Martineau et al., 1991). These authors identified the entire sequence of TCMP-1, which, in addition to the previously deposited 37 amino acid-long sequence corresponding to the mature miniprotein (Hass & Hermodson, 1981), presents an N-terminal signal peptide of 32 amino acids and an extension of 8 amino acids at the C-terminus. The MCPI protein is present at high level in tomato ovary at anthesis (2-5% of the total cellular protein) and undetectable in ripe fruit (Martineau et al. 1991, Cavallini et al., 2011). In leaves, MCPI mRNA and protein levels are barely detectable, but a dramatic (100-fold) increase in mRNA level was observed after wounding without a concomitant increase in MCPI protein, suggesting a control at the post-transcriptional or translational level. An increased level of MCPI mRNA also accumulated in tomato leaves in response to treatments with systemin, methyl jasmonate, oligogalacturonic acid and chitosan (Díez-Díaz et al., 2004). The function of TCMP-1 in plant is still not well understood but it is expected to be, like other carboxypeptidase inhibitors, a potential protective agent in defense against pests and plant predators (Bayés et al.,2006).

A study that comprehensively analyzed tomato protease inhibitors (PI) through phylogenetic relationships, gene structure, and expression patterns (Fan et al., 2000) showed that TCMP-1 (corresponding to tomato PI #28) was highly expressed in tomato plants tolerant to heat stress.

A role of TCMP-1 in response to abiotic stress was proposed by Manara and collaborators (2020), who demonstrated that TCMP-1 is implicated in response to saline stress and Cd toxicity. Through a Y2H screening, TCMP-1 was found to interact with the metal-ion binding protein *Sl*HIPP26, which is highly similar (92% sequence similarity) to the Arabidopsis HIPP26 (also known as *At*FP6; a heavy metal-associated isoprenylated plant protein that belongs to metal chaperones) (Manara et al., 2020). HIPPs expression is induced by abiotic stresses, such as cold and saline conditions, and is differentially modulated by heavy metal application (de

Abreu-Neto et al., 2013). Indeed, Arabidopsis plants ectopically over-expressing TCMP-1 showed an increased expression of *At*HIPP26 when exposed to Cd, ABA and NaCl treatments (Manara et al., 2020). The over-expression of the transgene also resulted in a lower Cd accumulation in shoot, where a Cd content approximately 10% lower than in the WT shoot was measured (Manara et al., 2020).

A second metallocarboxypeptidase inhibitor of the cystine-knot type was discovered by screening a cDNA library created from the pericarp of ripe tomato fruit (Pear et al., 1989). It was also demonstrated that this protease inhibitor (also referred to as 2A11 or TCMP-2) is fruit-specific (Cavallini et al., 2011; Pear et al., 1989). TCMP-2 is 32% identical to TCMP-1. TCMP-2 expression is very low before anthesis, gradually increases after anthesis reaching the maximum level in the fruit, accounting for approximately 1% of the mRNA in mature tomato fruit. In fact, TCMP-2 promoter has been successfully used to improve qualitative traits in tomato fruit (Davuluri et al., 2005). Differently from TCMP-2, TCMP-1 is highly expressed in flower buds collected before anthesis (1.0 – 1.1 cm long) and after this phase its expression decreases, reaching the lowest level after fertilization (4 – 5 days after anthesis). The mRNA level then increases from very young fruit to ripe fruit. TCMP-1 protein accumulates later than mRNA, with the highest level in flowers collected 4–5 days after anthesis (Cavallini et al., 2011). These sequential patterns of the two mRNAs might be indicative of a tight and coordinated regulation.

Indeed, Molesini and collaborators (2018) noted, through an *in-silico* analysis of TCMP-1 and TCMP-2 regulatory regions, the presence of several binding sites for INO (INNER NO OUTER), which is a member of the YABBY transcription factor family, specifically expressed in the outer integument of the ovule (Villanueva et al., 1999). The same authors demonstrated by chromatin immunoprecipitation analysis that INO effectively binds the promoters of both TCMP-1 and TCMP-2 genes thus regulating their transcription. This suggests that the *cis*-elements present in the promoters of TCMP-1 and TCMP-2 might compete for the binding of a common trans-activating factor.

In the same work, to gain information on the roles of the two TCMPs, their endogenous levels were altered in transgenic plants by expressing a chimeric gene harboring the TCMP-1 coding sequence under the control of the TCMP-2 promoter (*p*TCMP-2::TCMP-1). Since *p*TCMP-2 is almost exclusively a fruit-specific promoter, the expression of the transgene should cause an imbalance in the levels and ratio of TCMPs during later stages of fruit development. As

expected from the fruit-specific regulation of the transgene, the expression of TCMP-1 was increased in the fruit, giving a slight delay in ripening (Molesini et al., 2018). Unexpectedly, the expression of *p*TCMP-2::TCMP-1 caused an earlier fruit set associated with a reduction in TCMP-1 expression, and an increase in TCMP-2 level in pre-anthesis flower buds. In the transgenic plants, the changes in the levels and ratios of TCMPs before anthesis, with downstream effects on fruit set, suggested that TCMPs are regulators of fruiting time and that the maintenance of a correct TCMP-1/TCMP-2 ratio is required for a proper fruit initial growth. A possible explanation for the unexpected changes in TCMP-1 and TCMP-2 expressions in transgenic flower buds can be traced to the altered competition of the two promoters for the INO binding (Molesini et al., 2018).

Genes homologous to both TCMP-1 and TCMP-2 were found in *Solanum pimpinellifolium*, which is the closest wild relative to the cultivated tomato, whereas the genome of *Solanum pennellii,* a wild tomato species, contains TCMP-1 homologs but not TCMP-2 homologous genes (Molesini et al., 2020 and this PhD thesis). The small green-fruited desert species *S. pennellii* has evolved unique adaptations in terms of morphology, mating system, chemistry (especially secondary compounds) and responses to biotic/abiotic stresses (Lippman et al., 2007). Interestingly, in the *S. pennellii* introgression sub-line R182, selected for better performance in terms of fruit quality parameters and high yield, derived from the M82 parental line (Calafiore et al., 2016; Calafiore et al., 2019), the region of *S. lycopersicum* containing TCMP-2 was replaced by a *S. pennellii* introgressed segment apparently lacking a TCMP-2 ortholog. Consistent with this, the RNA-Seq analysis showed a severe downregulation of TCMP-2 in R182 at breaker and mature green fruit stages when compared to the M82 control line (Aliberti et al., 2020; Calafiore et al., 2019). These findings suggested that the lack of this specific protease inhibitor in R182 line could, to some extent, influence the regulation of pathways that are linked to fruit development and ripening, maybe acting on the modulation of the hormonal network and, ultimately, on the production of ascorbic acid in the fruit (Aliberti et al., 2020).

The novel role of TCMPs in the reproductive phase of tomato plants (Molesini et al., 2018) combined with the still not fully elucidated mechanism of action of these miniproteins, the absence of TCMP-2 in *S. pennellii* genome and the lack of homologous genes in other plant model species (*e.g.,* Arabidopsis), prompted us to investigate TCMP-2 more thoroughly in this PhD thesis.

2. AIM OF THE WORK

The first stage in the transition from vegetative to reproductive development in Angiosperms is the formation of flowers. Afterwards, the pollination of the flower at anthesis and successful fertilization of the ovules leads to fruit initiation, also referred to as fruit setting. Fruit setting marks the transition between the quiescent ovary and the rapidly growing fruit, a process regulated by environmental and endogenous signals. Hormones and transcription factors orchestrate these intricate processes, but several small proteins and peptides can also participate in flowering and fruit setting (de Jong et al., 2009). A recent study demonstrated the involvement of two tomato cystine-knot miniproteins, named TCMPs, possessing metallocarboxypeptidase inhibitor activity, in the timing of fruit formation (Molesini et al., 2018). The mode of action of TCMPs in plants remains largely unknown also for the absence of homologous genes in other model species, including Arabidopsis (Tavormina et al., 2015; De Coninck & De Smet, 2016).

The aim of this section of my thesis has been to delve into the molecular function of TCMP-2, using different plant systems: *Solanum lycopersicum* plants with altered TCMP-1/TCMP-2 ratio (cv:UC82 – *p*TCMP-2::TCMP-1) (Molesini et al., 2018), *Arabidopsis thaliana* ectopically over-expressing TCMP-2 (Col-0 – *CaMV35S::TCMP-2*), MicroTom over-expressing TCMP-2 (cv:MT – *CaMV35S::TCMP-2*) and *S. pennellii* over-expressing TCMP-2 (accession LA716 – *CaMV35S::TCMP-2*). The analyses were focused on the role of this protein in reproductive development, since Cys-rich peptides can act as signaling molecules in plant development by interfering with receptors or modifying the activity of multimeric complexes (Tavormina et al., 2015; De Coninck & De Smet, 2016). To have insight into the TCMP-2 mechanism of action, a high throughput Y2H screening was performed to discover its potential interacting partners.

3. MATERIALS AND METHODS

3.1. *Solanum lycopersicum cv UC82 growth conditions*

S. lycopersicum cv UC82 WT plants and two previously obtained transgenic lines (#1-2 and #20-2) harboring the chimeric construct p*TCMP-2::TCMP-1* (Molesini et al., 2018) were grown in greenhouse under controlled conditions with a 10/14 hours light/dark cycle at 24°C and 18°C respectively. After seed germination, the seedlings at the third-fourth true leaf were selected by spraying with kanamycin (300 mgL^{-1}) and the transgenic state was confirmed by PCR. Then, the plants were transplanted in pots (25 cm diameter) and grown in the glasshouse during the springtime. The phenotypic analyses were carried out for two years on two different sets of plants.

3.2. *Preparation of the construct used for TCMP-2 overexpression in MicroTom*

For the overexpression of TCMP-2 in MicroTom, a sequence corresponding to the 96 amino acid-long coding region (from nucleotide 55 to 342 of the TCMP-2 mRNA; NM_001247833) was used. Gateway BP primers were designed according to the manufacturer's instructions (Gateway® Technology with Clonase® II – Invitrogen). After subcloning in the pDONR221, the resulting pENTRY vector was used for the subsequent recombination with the destination vector pK7WG2D.1 (Ghent University, Belgium) which is suitable for the overexpression of the gene of interest using the CaMV35S promoter. The construct (schematically depicted in Figure 2) was inserted into *Agrobacterium tumefaciens* strain GV2260 by electroporation.

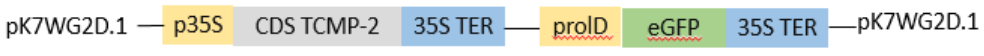

Figure 2. Schematic representation of the genetic cassette cloned in the T-DNA of pK7WG2D.1 and used for MicroTom genetic transformation.

3.3. *Agrobacterium-mediated MicroTom genetic transformation*

MicroTom seeds (ID:TOMJPF00001) were sterilized, sowed on Mourashige and Skoog agar medium supplied with vitamins (Table S.1, Appendix A), and placed in the growth chamber at 25°C for 8 days. After this period, the cotyledons appeared fully expanded and the first true

leaves started emerging from the apical meristem. Cotyledon explants were cut in a square shape and then placed in Petri dishes containing KCMS solid medium (Table S.2, Appendix A), in the dark at 25°C for 24 hours. *A. tumefaciens s*train GV2260 containing pK7WG2D.1 harboring TCMP-2 was grown for 24 hours in the dark at 28°C and 210 rpm until an OD_{600} between 1.2-1.5. After centrifugation, the bacterial pellet was resuspended with liquid KCMS (Table S.3, Appendix A) to an OD_{600} of 0.1 and this infection solution was used to sprinkle the tomato explants. After 15 minutes, the infection solution was removed and the plates were incubated in the dark at 25°C for 48 hours. After this period, the explants were moved into new Petri dishes containing RGM1 medium (Table S.4, Appendix A) supplied with kanamycin (100 mgL^{-1}) and maintained for 2 weeks. Once the calli were formed, they were placed for 2 weeks in RGM2 medium (Table S.5, Appendix A), maintaining the kanamycin selective agent (100 mgL^{-1}). Generated shoots were removed from the original callus, and transferred to Rooting Medium (Table S.6, Appendix A) supplied with kanamycin (75 mgL^{-1}). After 3-4 weeks, rooted plants were ready to be acclimated, transferred into pots containing a mixture of soil and sand and maintained in the greenhouse following the conditions described in paragraph 3.1. After acclimatation in greenhouse, the transgenic state of T0 plants was evaluated by PCR using primers spanning the nucleotide region from the CaMV35S to the 3' region of TCMP-2 CDS. TCMP-2 gene expression was evaluated by reverse transcription-PCR (RT-PCR). The phenotypic analyses were conducted in T1 generation after confirming the transgenic state and spraying plantlets with kanamycin (400 mgL^{-1}). The phenotypic analysis was carried out during autumn 2021.

*3.4. Arabidopsis plants expressing Sl*TCMP-2

A pCAMBIA1200 vector containing the genetic cassette for TCMP-2 overexpression was used for the genetic transformation of *Arabidopsis*. The terminator sequence of the nopaline synthase (*nos*) gene of *A. tumefaciens* was used. *A. tumefaciens* strain GV2260 was transformed by electroporation with the recombinant plasmid and used for *Arabidopsis* WT (*Col-0*) plants infection through the floral dip method (Zhang et al., 2006). The transgenic plants were identified using hygromycin B (13 µg mL^{-1}) in the germination medium (Table S1, Appendix A). The transgenic state was confirmed by PCR using primers spanning the entire genetic cassette, and TCMP-2 gene expression was evaluated by RT-PCR. Two homozygous *35S::TCMP-2* transgenic lines (#B2 and #M3 at the T3 generation) and WT plants were

germinated in pots and maintained in a growth chamber at a constant temperature of 25°C under long-day conditions (16/8 hours light/dark cycle, photosynthetic photon fluence rate of 150 µmol m^{-2} s^{-1} over the waveband 400-700 nm) for the phenotypic analysis.

3.5. Solanum pennelli plants expressing Sl*TCMP-2*

Leaves from axenic seedlings of *S. pennellii* (accessions: 20164 and LA0716) were used as source of plant explants as described by Gisbert et al., (1999) and Atarés et al., (2011). Leaf explants were inoculated with the LBA4404 strain of *A. tumefaciens* transformed with the genetic construct reported in Figure 2 (see paragraph3.1). Briefly, after the infection, leaf explants were co-cultured for 2 days at 23 ± 1°C in the dark and then washed in a medium containing cefotaxime (500 mgL^{-1}). Three to four weeks after organogenic response induction, leaf explant generated buds were excised. After subculture of the buds, the elongated shoots were transferred to a rooting culture medium. All plants regenerated from a single poked area of an inoculated leaf explant were considered to be derived from a single independent transformation event. The transgenic state of in vitro T0 plants was evaluated by PCR using primers spanning the nucleotide region between TCMP-2 CDS and *nos* terminator.

3.6. Ploidy level evaluation and maintenance of diploid S. pennellii T-DNA

To select the diploid plants within the transgenic lines, the ploidy level was evaluated by DNA quantification in a flow cytometer. Ploidy was determined in young leaf fresh tissue sliced with a razor blade into thin strips, smaller than 0.5 mm, in a glass Petri dish containing 0.4 ml of nuclei isolation buffer (high-resolution DNA kit, solution A: nuclei isolation, Partec, Münster, Germany). The nuclei extract was mixed with 1 ml of staining buffer (high resolution DNA kit, solution B: DAPI staining; Partec, Münster, Germany) and filtered through 50 µm nylon mesh (Nyblot). The filtrates (more than 5,000 nuclei per extract) were analyzed using a Partec PA-II flow cytometer. From every diploid transformed plant (T0), several clonal replicates were obtained by culturing axillary buds in rooting medium to maintain the *in vitro* collection as well as acclimatize a sufficient number of replicates in greenhouse to identify dominant insertion mutants and obtain T1 seeds by hand-pollination.

3.7. Genomic DNA extraction

Genomic DNA was isolated from 100 mg of plant tissue using the "NucleoSpin Plant II" kit (Macherey-Nagel) following the manufacturer's instructions.

3.8. RNA extraction and quantitative RT-PCR analysis

Total RNA was isolated from tomato and Arabidopsis tissues using the NucleoSpin RNA Plant kit (Macherey-Nagel); three leaf pools were used as biological replicates. After DNase treatment, first-strand cDNA was synthesized using the ImProm-II Reverse Transcriptase (Promega). Quantitative RT-PCR was performed with a QuantStudio 3 Real-Time PCR System (Thermo Fisher Scientific, Waltham, MA, USA) using Luna®Universal qPCR Master Mix (New England Biolabs, Ipswich, MA, USA). Each reaction was carried out for 40 amplification cycles, in technical triplicates using the primers reported in Table S.7 (Appendix A). Data were normalized using the endogenous reference genes *Sl*Actin (*Solyc11g005330*) for tomato and *At*Actin (*At3g18780*) for Arabidopsis. Data analysis was performed using the $2^{-\Delta\Delta CT}$ method (Livak & Schmittgen, 2001).

3.9. Phenotypic evaluations

Transgenic UC82 pTCMP-2::TCMP-1, Microtom 35S::TCMP-2 and the respective wild type plants were maintained in the greenhouse condition during the phenotypic analysis. All plants were transplanted in pots and then arranged in a completely randomized design. Plants were homogeneous in age, size, and exposition to light. For each line of each genotype, at least 7 individuals were grown. Phenotypic evaluation was conducted focusing on the transition between the vegetative and reproductive development.

For pTCMP2::TCMP-1 tomato (cv UC82) plants, the parameters considered were: number of leaves before the first inflorescence, and Sympodial Units (Sus) and lateral shoot flowering pattern.

For 35S::TCMP-2 tomato (cv MicroTom) plants, the parameters considered were: height of the plants before the first inflorescence, number of leaves before the first inflorescence, number of flowers and fruit set of the first 4 flower trusses, and total productivity evaluated 4 months after sowing.

For 35S::TCMP-2 Arabidopsis (Col-0) plants, flowering time was determined by counting the number of rosette leaves at bolting and the days between sowing and bolting.

3.10. Yeast Two-Hybrid screen

The yeast two-hybrid (Y2H) screen was performed by Hybrigenics Services, S.A.S., Paris, France (www.hybrigenics-services.com), using a DNA fragment encoding the mature portion of the TCMP-2 protein (Solyc07g049140; from amino acid 53 to 96) as bait to screen a tomato fruit cDNA library comprising different fruit developmental stages from mature green to red ripe stages. 183 positive clones out of 30 million tested interactions were selected on a medium supplemented with 10 mM 3-aminotriazole (3-AT) to prevent bait autoactivation. A confidence score (PBS, for Predicted Biological Score) was attributed to each interaction following the method described by (Formstecher et al., 2005). The PBSs were classified from A (greatest confidence) to D (least confidence). The PBSs positively correlate with the biological significance of interactions (Rain et al., 2001; Wojcik et al., 2002). The Matchmaker Gold Yeast Two-Hybrid System (Clontech) was used to test the interaction between TCMP-2 and selected target proteins, following the manufacturer's instruction with minor modifications. The mature TCMP-2 protein represents the bait and was expressed as a fusion to the GAL4 DNA-binding domain in pGBKT7-BD vector, and then the recombinant plasmid was introduced into Y2H Gold yeast strain. Full-length ORFs of *Sl*BBX16, *Sl*BBX17, *At*miP1b, *Sl*CO1, *Sl*TPL1 were cloned in frame into pGADT7-AD vector and introduced into Y187 yeast strain representing the prey. After mating the yeast cells, the cultures were spread on agar plates and then incubated at 30°C for 3 days. Growth of yeast on SD/-Leu/-Trp medium was used as a control for the presence of both recombinant plasmids, and growth of yeast cells on selection medium (SD/-Leu/-Trp/-His/-Ade/X-Gal/Aureobasidin A) plus 10 mM 3-AT was used to determine positive interactions.

3.11. Bimolecular fluorescence complementation assay (BIFC)

The BIFC analysis was performed by Zoonbio Biotechnology Company (www.zoonbio.com). The coding sequence of the mature TCMP-2 protein was amplified by PCR, sequenced and cloned into the pCAMBIA1300 vector fusing with N-terminus of YFP. The entire coding sequence of *Sl*BBX16 (*Solyc12g005750)* was amplified in the same way, sequenced, and fused to the C-terminus of YFP. The constructs were inserted into *A. tumefaciens* strain GV3101. *A. tumefaciens* cells holding the recombinant vectors were pelleted and resuspended in an infiltration solution (10 mM $MgCl_2$, 10 mM MES, pH 5.6, 200 µM acetosyringone) to an OD_{600} value of 0.3-0.4. The co-infiltration of four-week-old *Nicotiana tabacum* leaves was followed

by an incubation of 36-48 hours and then leaves were visualized using a confocal laser scanning microscope (Zeiss LSM 5Exciter).

3.12. In vivo *Interaction Assay with Ratiometric BIFC (rBiFC)*

The coding sequence corresponding to the mature TCMP-2 was cloned using Gateway system (Thermo Fisher Scientific), into pBiFCt-2in1_NC or NN allowing for simultaneous cloning of the entire coding sequence of *Sl*BBX16 or its deletion mutant, indicated as ΔBBX16 (corresponding to the last 49 amino acids), into the same T-DNA vector backbone and for the ratiometric analysis of the complemented signal due to additional expression of mRFP (Barozzi et al., 2019; Grefen & Blatt, 2012). Constructs were introduced into *A. tumefaciens* cells (strain GV2260), and agroinfiltrations were performed in WT *N. tabacum* as described previously (Paris et al., 2010). Leaves were examined using a confocal laser scanning microscope LSM 710 Zeiss (ZEN Software) mounting material in water (de Caroli et al., 2020). YFP was detected within the short 505–530 nm wavelength range assigning the green color, RFP within 560–615 nm assigning the red color. Excitation wavelengths of 488 and 543 nm were used. The laser power was set to a minimum and appropriate controls were made to ensure that there was no bleed-through from one channel to the other. Images were processed using Adobe Photoshop 7.0 software (Mountain View). Fluorescence intensity (complemented YFP vs. RFP) was measured and expressed as ratio index. Complemented signal was weak and dishomogeneous. Seven independent cells were used for quantification of each combination. Images were acquired with similar settings to perform the statistics and the independent samples Student t-test.

3.13. Statistical analysis

All statistical calculations were performed using the GrafhPad Prism version 5 software. The means values ± SE are reported in the figures. Statistical analyses were conducted using Student's t-test.

4. RESULTS

4.1. TCMP gene family in S. lycopersicum

In depth sequencing of tomato accessions (Menda et al., 2013; Eshed & Zamir, 1994; Tomato Genome Consortium et al., 2012) allowed the identification of additional genes highly homologous to the first two TCMPs discovered. From data retrieved from the KNOTTIN database (www.dsimb.inserm.fr/KNOTTIN), we identified ten tomato "Uncharacterized cystine-knot proteins", hereafter named from A to J, with putative function of metallocarboxypeptidase inhibitors. Their expression profile, together with that of TCMP-1 and TCMP-2, was *in silico* analyzed (http://tomexpress.toulouse.inra.fr/; Figure 3) showing a specific expression pattern in the reproductive organs for TCMP-1 and TCMP-2 only (Cavallini et al., 2011).

Symbol	Locus							Root
A	Solyc01g058000	0.0571	0.0394	0.0222	0.0517	0.0747	0.03	0.9815	0.0728
B	Solyc03g031480	12.5687	0.0005	0.057	0	0	0	0.0008	0
C	Solyc03g031490	13.9582	0.0035	0.0635	0	0	0	0	0
D	Solyc03g031500	26.4017	0.0239	0.1272	0.0183	0	0	0	0
E	Solyc03g031510	23.4188	0.2592	0.1738	0.0203	0	0.0016	0.005	0.5612
F	Solyc03g031520	34.01	0.1576	0.3138	0.0028	0	0	0	0
G	Solyc05g008150	0	0	0	0	0.0013	0.0017	0.0017	0.0018
H	Solyc06g061230	0.4184	0.1592	0.0911	0.0191	0.0347	0	0.0018	0
I	Solyc07g007240	0.1266	0.076	0.2466	0.5783	0	0.0018	0.3772	0.0636
J	Solyc07g007260	1.7004	0.5819	2.3834	2.887	0.0107	0.007	0.0354	0.0499
TCMP-1	Solyc07g007250	141.887	8.9519	46.2695	50.1831	0.3601	0.0445	0.0505	0.776
TCMP-2	Solyc07g049140	0.0178	0.0008	0.4011	3.3532	111.742	886.979	0.0028	0.0005

Figure 3. In silico expression analysis of TCMPs and their homologs in MicroTom. The evaluation was conducted at different developmental stages (from the left to the right): bud 3mm, bud 7mm, anthesis, 4 days post anthesis (dpa), mature green (35 dpa), red ripe fruit, leaf, and root.

4.2. Tomato plants with an increased TCMP-2 level in flower buds displayed an anticipated termination of sympodial units

Transgenic tomato plants (*pTCMP-2::TCMP-1*) with an altered expression level of *TCMP-1* and *TCMP-2* (Molesini et al., 2018) were previously produced to investigate the effect of their altered balance on fruit development. The *TCMP-2* promoter is highly expressed in fruit, and at low level also in pre-anthesis flower buds (Molesini et al., 2018). The *TCMP-2::TCMP-1* transgenic lines (#1-2 and #20-2) exhibited an anticipated fruit production compared with WT plants and a slight deceleration in the time intercurrent between the fruit set and the breaker stage (Molesini et al., 2018). As expected by the TCMP-2 promoter activity, an increased expression of *TCMP-1* was monitored in fruits, whereas an unexpected increase in *TCMP-2* mRNA level was observed in the flower buds before anthesis, reaching a 100- and 30-fold increase in the two transgenic lines, respectively (Molesini et al., 2018).

To try to understand the reason of this anticipated fruit production, we decided to analyze in more detail the *pTCMP-2::TCMP-1* plants during the transition from the vegetative to the reproductive stage. These transgenic tomato plants were obtained by genetic transformation of the determinate UC82 cultivar (Jones et al., 2007), whose inflorescence architecture is schematically depicted in Figure 4. After about 9-10 leaves the WT plants terminate with a primary inflorescence. The first termination event activates the sympodial cycle. The first sympodial unit (SU) includes two leaves and an inflorescence (second inflorescence). The sympodial cycling accelerates progressively causing leaf production to decrease in successive units until growth ends (Figure 4a, upper panel). Differently from the main shoot, in the lateral ones, which originate from axillary buds, the first SU consists of 3 leaves and a terminal inflorescence, and subsequent SUs form fewer leaves until the shoot is terminated (Figure 4a, lower panel).

Examining the transgenic *pTCMP-2::TCMP-1* plants, the first inflorescence was formed after the same number of leaves as in WT (Figure 4b). However, changes in flowering pattern were observed in approximately 70% of transgenic plants showing the failure in sympodial cycle activation in the main shoot of some of the transgenic plants (Figure 4b, upper panel), with the second inflorescence appearing just after the first one.

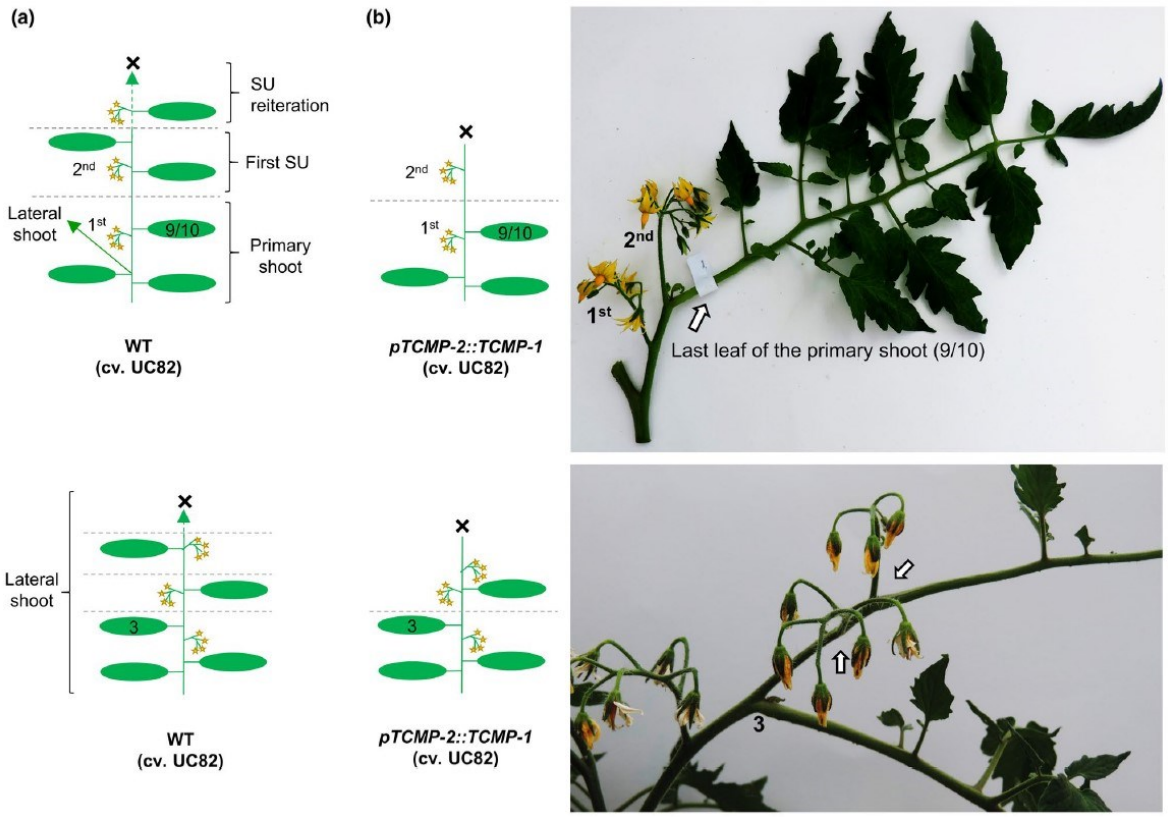

Figure 4. Shoot architecture of pTCMP-2::TCMP-1 plants. a) Schematic diagram showing shoot architecture of a WT determinate tomato plant cv UC82. (Upper panel), in WT plants, the primary shoot meristem is terminated by the first inflorescence after 9-10 leaves. Reiterated sympodial units (SUs) are then formed from sympodial meristems. The sympodial cycling accelerates progressively causing leaf production to decrease in successive units until growth ends (marked with "X"). (Lower panel), in WT plants, lateral shoot displays a first SU which consists of three leaves and an inflorescence, and subsequent SUs form fewer leaves until the shoot is terminated. (b) Schematic diagram showing shoot architecture displayed by the transgenic pTCMP-2::TCMP-1 plants and relative pictures showing alterations in the flowering pattern.

In other transgenic plants, irregular SUs were observed (Figure 5) showing a reduced number of leaves before the two terminating inflorescences. Also in the lateral shoots, a tendency of reduction in the number of leaves between inflorescences was observed in some plants of both transgenic lines compared to WT, (Figure 4b, lower panel). Collectively, the alterations observed in transgenic plants were related to an anticipated termination of the SU.

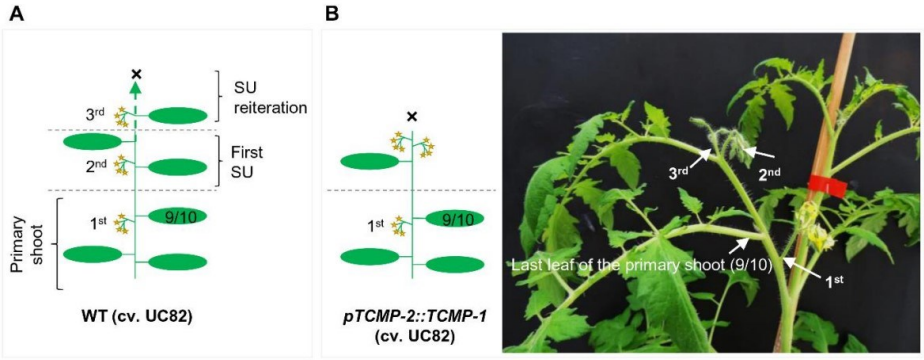

Figure 5. Representative picture of irregular SU displayed by pTCMP-2::TCMP1 plants. a) Schematic diagram showing shoot architecture of a WT determinate tomato plant cv UC82. b) Schematic diagram showing shoot architecture of pTCMP-2::TCMP-1 plant. The first inflorescence of the primary shoot is formed after 9/10 leaves as in WT. After the primary inflorescence, the shoot terminates with an irregular SU composed by a single leaf and two consecutive inflorescences

Sympodial cycling in tomato is controlled by a balance between the activity of two antagonistic genes: flower-promoting (SINGLE FLOWER TRUSS; SFT; *Solyc03g063100*) and flower-repressing (SELF-PRUNING; *Sl*SP; *Solyc06g074350*) (Lifschitz et al., 2014). The *sft* gene of tomato is the homolog of Flowering locus T (FT) of Arabidopsis, whose transcription is controlled by the activity of CONSTANS (CO) transcription factor. Therefore, the expression of SFT, *Sl*SP and of the closest homolog of the Arabidopsis *CO* (*SlCO1; Solyc02g089540*), was examined. The transcript levels of *SlSP*, and *SlCO1* did not show variations, whereas *SFT* expression was on the average doubled in both transgenic lines as compared with WT (Figure 6). The increased SFT/SP ratio in *pTCMP-2::TCMP-1* plants might explain the anticipated SU termination.

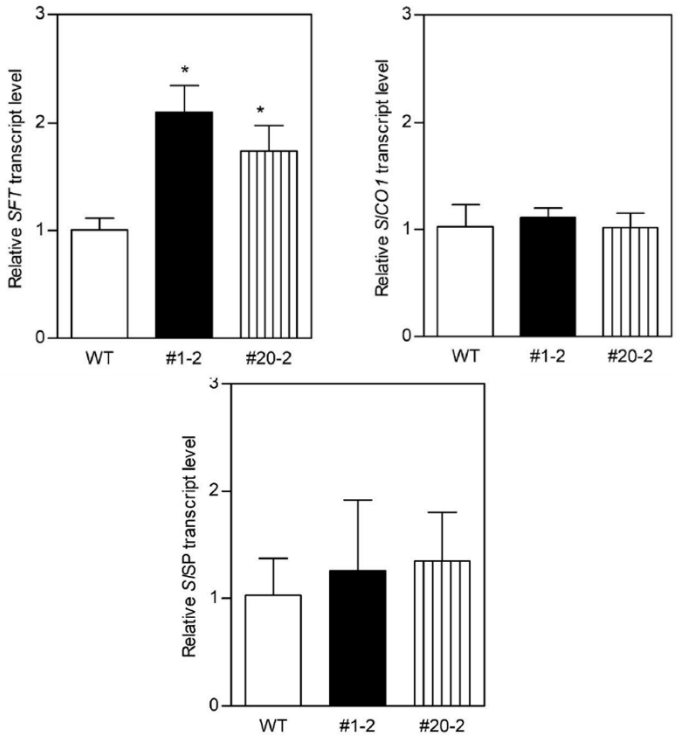

Figure 6. Expression analysis of pTCMP-2::TCMP-1 transgenic plants. Expression levels of SFT, Sl*CO1 and* Sl*SP in WT and #1-2 and #20-2 lines. The values reported are means ± SE (n = 3). Each biological sample represents a pool of either leaves (SFT and* Sl*CO1) or meristems (*Sl*SP) collected from seven plants. The level of the target genes in WT was used as calibrator. Student's t-test was used to compare the differences in transcript level between transgenic lines and WT (*p < 0.05).*

4.3. Phenotypic alterations in 35S::TCMP-2 MicroTom plants

The WT tomato cultivar MicroTom (TOMJPF00001) was used as genetic background (Kobayashi et al., 2014) for over-expressing TCMP-2 (see Figure 7 modified from Vicente et al., 2015 for a schematic representation of different growth habits in tomato cv. MicroTom). From the genetic transformation, we obtained 36 putatively transformed plants, that were acclimatized in the greenhouse and molecularly analyzed for the determination of the transgenic state.

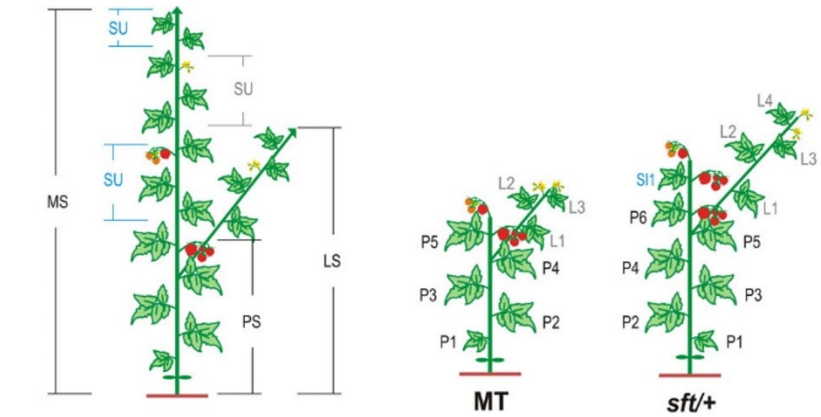

	MT	sft/+
Number of leaves on the primary shoot (PS)	5.30 ± 0.15 c	6.10 ± 0.10 b
Number of leaves on the main shoot (MS)	5.30 ± 0.15 c	7.20 ± 0.48 b
Height of the PS	6.19 ± 0.22 d	7.70 ± 0.25 c
Height of the MS	10.36 ± 0.48 c	13.78 ± 0.66 b
Height of the lateral shoot (LS)	10.73 ± 0.23 c	15.48 ± 0.42 b
Internode length	1.35 ± 0.70 b	1.42 ± 0.01 b
	Determinate	Semi-determinate

Figure 7. Schematic representation of growth habit of MicroTom (modified from Vicente et al., 2015).
The genotypes MT and sft/+ are homozygous for the recessive allele self-pruning (sp). sft=single flower truss, sft/+= heterozygote sft.

PCR analysis, using primers covering the sequence between the CaMV35S promoter and the 3' region of TCMP-2 CDS, permitted the selection of 26 plants. In figure 8, a representative agarose gel image of several transgenic lines is reported.

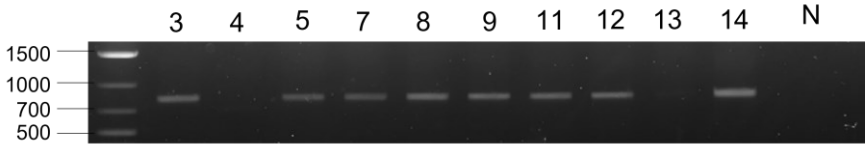

Figure 8. Agarose gel displaying amplicons corresponding to a portion of 764 bp of the genetic construct. N= not template control.

The expression of TCMP-2 was checked in all 26 PCR positive plants by RT-PCR using primers covering a portion of the CDS (data not shown). For the phenotypic analysis, 4 independent *35S::TCMP-2* transgenic lines (Figure 9a) at T1 generation (#20, #12, #25, #6) were compared with WT plants using about 7-10 individuals per line. The phenotypic analysis was conducted focusing on the transition between the vegetative and reproductive development. Several different parameters were scored: height of the plants, number of leaves before the first inflorescence, number of flowers of the first 4 flower trusses, fruit set and total productivity.

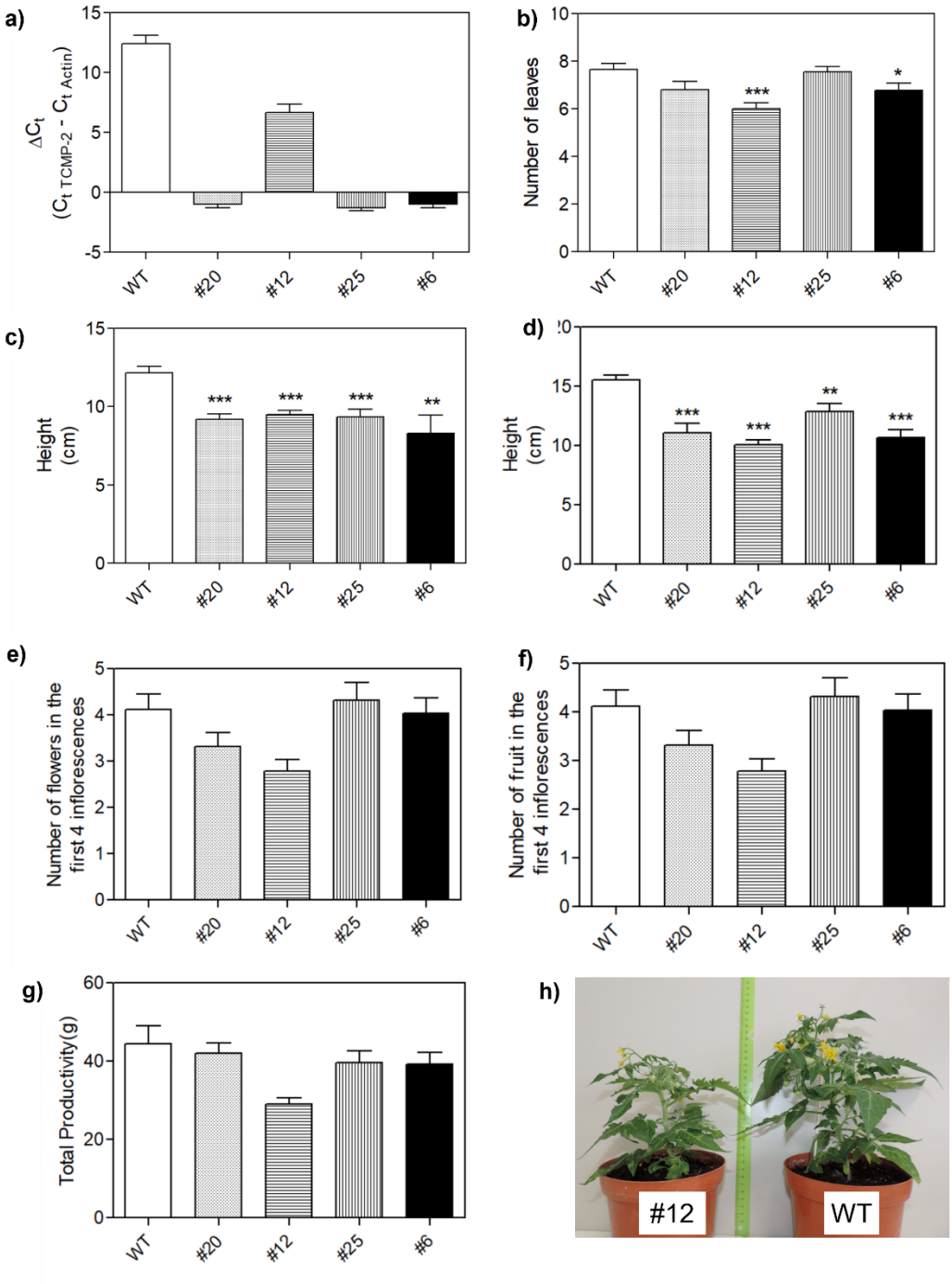

*Figure 9. Phenotypic analysis of T1 MicroTom over-expressing TCMP-2. a) expression of TCMP-2 in leaves of the 4 independent transgenic lines; b) number of leaves before the first inflorescence; c) and d) height (cm) measured 42 and 50 days after sowing; e) number of flowers in the first 4 inflorescences per plant; f) number of fruits in the first 4 inflorescences per plant; g) total productivity; h) WT and TCMP-2 over-expressing #12 plants. The values reported are means ± SEM (n= 7-10). Student's t-test was used for the statistical analysis (*P < 0.05; **P < 0.01; ***P < 0.001).*

Two (*i.e.,* #6 and #12) out of four lines showed a reduced number of leaves before the first inflorescence compared to WT plants, which is an indication of early flowering (Figure 9b). In all the transgenic lines, reduced primary shoot length was observed (Figure 9c and d).

These results may suggest that the overexpression of *TCMP-2* determines an acceleration in the transition from the vegetative stage to the reproductive phase. Concerning the number of flowers, fruit set (data not shown) and productivity, no significant differences were recorded between the transgenic lines and the WT (Figure 9 e-g).

4.4. Phylogenetic TCMPs analysis and S. pennelli plants over-expressing TCMP-2

Searching in the available genome database of wild tomato, we have retrieved the TCMPs homologs in *S. pimpinellifolium* and *S. pennellii*. Figure 10 (upper panel) shows the phylogenetic tree constructed with the amino acid sequences of TCMPs from *S. lycopersicum* and wild tomatoes.

Proteins homologous to all the members of the *S. lycopersicum* TCMPs family are present both in *S. pimpinellifolium* and *S. pennellii*, except for TCMP-2 homolog that is absent in *S. pennellii* (Figure 10).

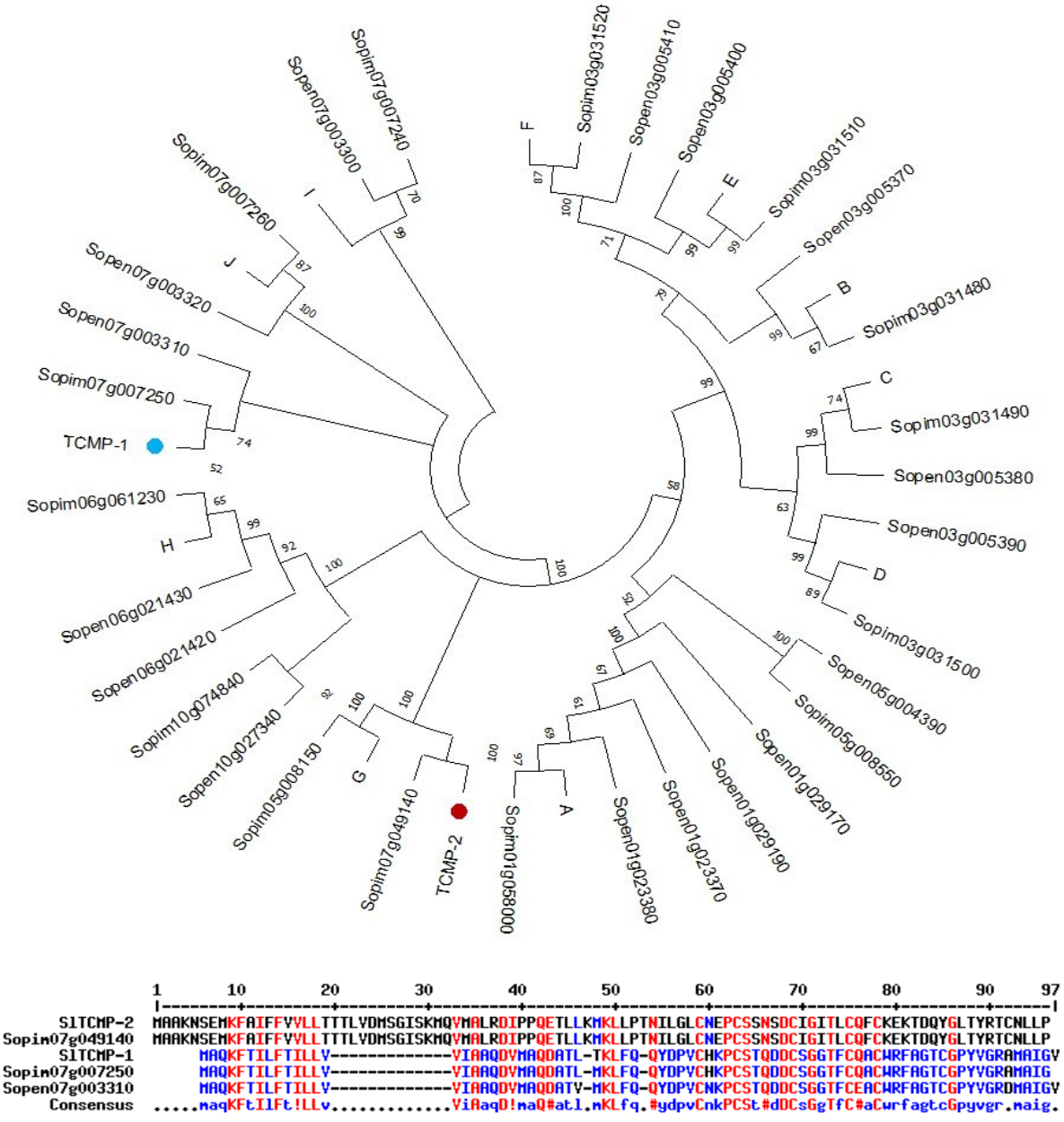

Figure 10. Sequence comparison of tomato TCMPs homologs.
Upper panel: the evolutionary history was inferred using the Minimum Evolution method (Rzhetsky A. and Nei M., 1992). The bootstrap consensus tree inferred from 500 replicates is taken to represent the evolutionary history of the taxa analyzed (Felsenstein J., 1985). Branches corresponding to partitions reproduced in less than 50% bootstrap replicates are collapsed. The evolutionary distances were computed using the JTT matrix-based method (Jones D.T., Taylor W.R., and Thornton J.M., 1992) and are in the units of the number of amino acid substitutions per site. The ME tree was searched using the Close-Neighbor-Interchange (CNI) algorithm (Nei M. and Kumar S., 2000) at a search level of 1. The Neighbor-joining algorithm (Saitou N. and Nei M., 1987) was used to generate the initial tree. This analysis involved 42 amino acid sequences. All ambiguous positions were removed for each sequence pair (pairwise deletion option). There was a total of 138 positions in the final dataset. Evolutionary analyses were conducted in MEGA11 (Tamura K., Stecher G., and Kumar S., 2021).
Lower panel: Sequence alignment of TCMP-2 and TCMP-1 proteins from S. lycopersicum with the closest homologs identified in S. pennellii and S. pimpinellifolium. The alignment was performed using Multalign (Corpet, 1988). Conserved residues are colored in red (high consensus level 90%) and in blue (low consensus level 50%). A position with no conserved residue is represented by a dot in the consensus line. The consensus symbols are ! (I/V), and # (N/D/Q/E).

A BLAST-N search (https://solgenomics.net/tools/blast/) using as query the cDNA sequence of TCMP-2 against the "*S. pennellii* WGS chromosomes" revealed a certain degree of homology with the *Sopen07g024560* gene. The nucleotide sequence of *Sopen07g024560* was translated and subsequently aligned with the amino acid sequence of TCMP-2. The alignment shows a high percentage of homology with TCMP-2 only in the amino acid stretch 25 (Met) - 56 (Leu) (Figure 11).

Figure 11. Sequence alignment of TCMP-2 and S. pennelli Sopen07g024560. The alignment was performed using Multalign (Corpet, 1988). Conserved residues are colored in red (high consensus level 90%) and in blue (low consensus level 50%).

Since a functional TCMP-2 seems to be lacking in *S. pennelli* genome, in collaboration with Professor Alejandro Atarés of the Institute of Molecular and Cellular Biology of Plants of Valencia, we overexpressed the *Sl*TCMP-2 in *S. pennellii* (accessions LA716 and 20164) (see 3.1). The transgenic state of putative T0 transformants was evaluated by PCR using primers spanning from the TCMP-2 CDS to the *nos* terminator (Figure 12). Ploidy level analysis revealed a diploid state for all the PCR positive plants (data not shown). T0 transgenic plants are currently growing in greenhouse to obtain T1 seeds.

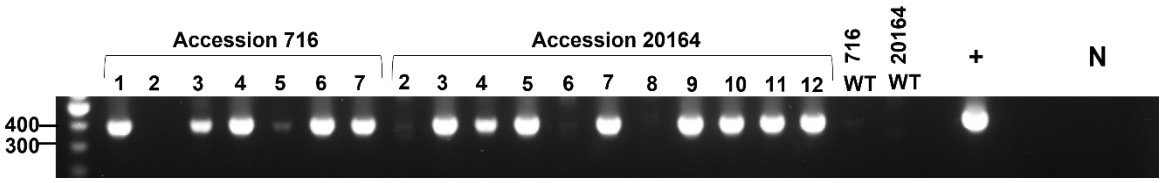

Figure 12. 2% agarose gel reports amplicons corresponding to the correct amplification of the transgene. The length of the amplicon is 367 bp. N: non template control. +: positive control.

4.5. TCMP-2 interacts with a member of the BBX family

4.5.1. Searching for TCMP interacting partners by Yeast two-hybrid (Y2H) screen

The analysis of *pTCMP-2::TCMP-1* and *35S::TCMP-2* plants supported a role for TCMP-2 in flowering and fruit development. To better define the role of TCMP-2, we decided to identify its interacting partners by performing a high-throughput Y2H screen. The mature TCMP-2 protein was used as a bait against an ovary/fruit cDNA library.

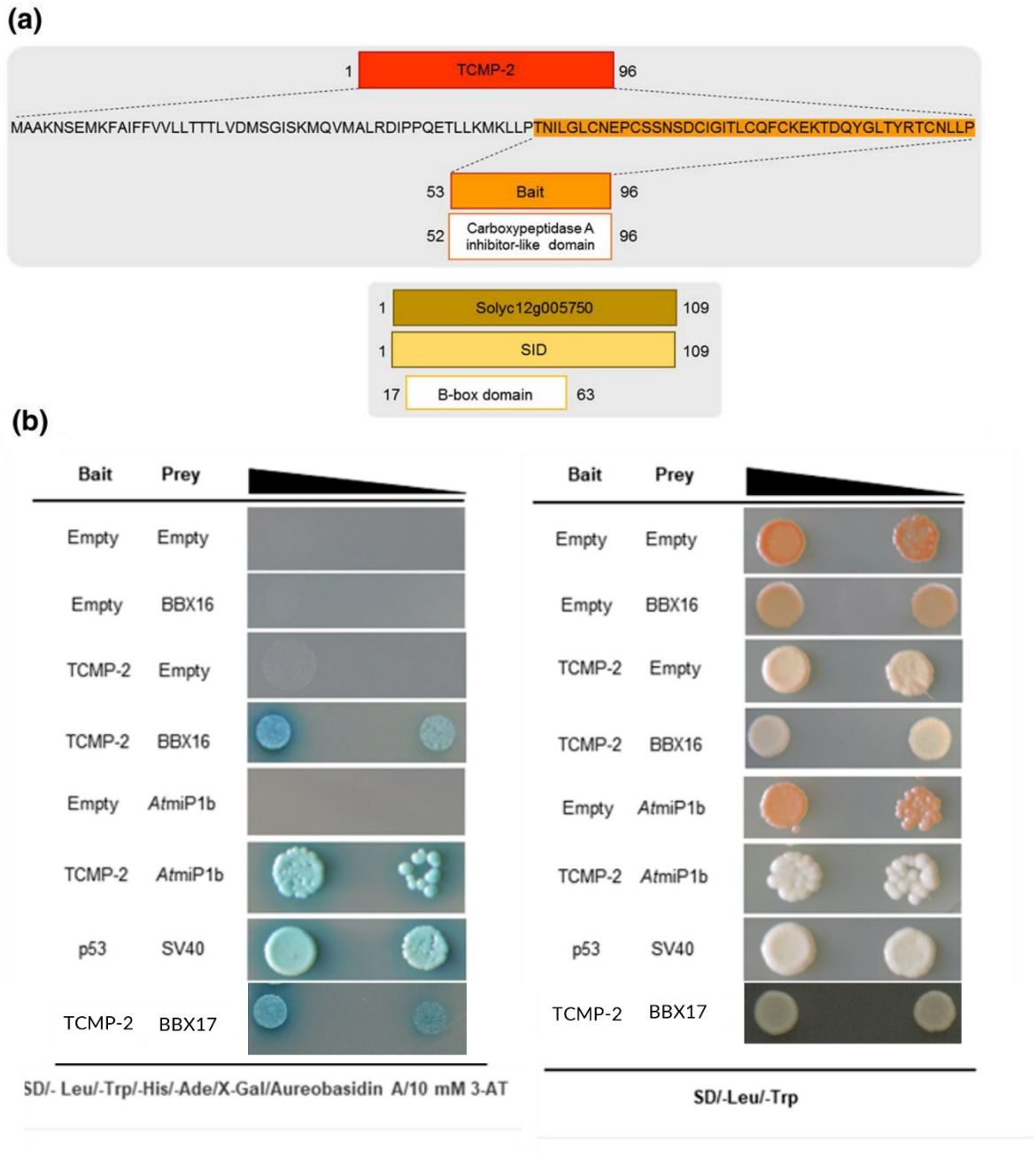

Figure 13. TCMP-2 interacts with SlBBX16. a) Schematic representation of the mature TCMP-2 protein portion used as bait in the Y2H library screen and of its interactor Solyc12g005750, which encodes for a B-box domain (BBX) containing protein. The selected interaction domain (SID) spans the entire 109 amino acid open reading frame of Solyc12g005750. b) Y2H analysis of TCMP-2 interaction with SlBBX16, SlBBX17 and AtmiP1b. Yeast cells transformed with different combinations of constructs containing TCMP-2 fused with the DNA binding domain

(BD; bait; TCMP-2); SlBBX16, SlBBX17 and AtmiP1b fused with the activation domain (AD; prey; BBX16, BBX17, AtmiP1b) were mated. For negative controls, pGBKT7 without insert (BD alone; Empty) and pGADT7 without insert (AD alone; Empty) were used. For each interaction, two increasing dilutions of the mated cultures were used (10^{-2} and 10^{-3}) and spotted on control medium (SD/-Leu/-Trp) and on selection medium plates (SD/-Leu/-Trp/-His/-Ade/X-Gal/Aureobasidin A/10 mM 3-AT). Interaction of p53 with SV40 was used as a positive control of the mating system.

Among the 47 potential interacting partners identified, which were categorized into C and D classes (Table S.8, Appendix A), we focused our attention on a "C" ranked interactor (*Solyc12g005750*) of 109 amino acids, annotated as a B-box Zinc finger CONSTANS-LIKE 4 protein (Figure 13a). Hereafter, the protein product encoded by *Solyc12g005750* is indicated as *Sl*BBX16 following the classification of Chu and collaborators (2016).

Two independent clones matching the *Sl*BBX16 were found to interact with the bait (Table S.8, Appendix A), with the "selected interacting domain" (SID) responsible for the interaction with TCMP-2, corresponding to the entire *Sl*BBX16 protein (Figure 13a).

The interaction between TCMP-2 and *Sl*BBX16 was also verified *in vivo* in yeast by performing an *ad hoc* Y2H analysis (Figure 13b).

*Sl*BBX16 is a member of the B-box (BBX) Zn finger protein family that is characterized by the presence of one or more B-box domains, predicted to mediate protein-protein interactions (Gangappa & Botto, 2014; Graeff et al., 2016; Khanna et al., 2009), and of a CCT domain, associated with a role in transcriptional regulation and nuclear transport (Gendron et al., 2012; Yan et al., 2011). Phylogenetic comparison carried out with tomato and Arabidopsis BBX members (Figure 14a and Table S.9, Appendix A), revealed that the closest homolog of *Sl*BBX16 in tomato is *Sl*BBX17 (*Solyc07g052620*; Figure 14b), whereas in Arabidopsis is miP1b (named also *At*BBX31; Graeff et al., 2016), which shows a 48% amino acid sequence identity (Figure 14b). A second BBX protein of Arabidopsis that presents high similarity to *Sl*BBX16 (45% identical) is *At*miP1a (referred to as *At*BBX30). Tomato BBX16 and BBX17 have in common with Arabidopsis miP1a and miP1b the presence of only one BBX domain in their amino acid sequence (CX2CX8CX7CX2CX4HX8H) and the lack of a CCT domain (Figure 14a). The principal function of these proteins is to interfere with the formation of protein complexes due to the lack of the CCT domain (Gangappa & Botto, 2014; Graeff et al., 2016). In a recent study, *At*miP1a/b microproteins were proved to engage CONSTANS (CO), a positive regulator of flowering time (Graeff et al., 2016), in a repressor complex with TOPLESS (TPL) determining the inhibition of *FLOWERING LOCUS T* (*FT*) expression (Graeff et al., 2016). The overexpression of either *At*miP1a or*At*miP1b causes late flowering due to a failure in the

induction of FT expression under inductive long day (LD) conditions (Tiwari et al., 2010; Valverde et al., 2004).

Considering the amino acid sequence homology between *Sl*BBX16 and the Arabidopsis miP1-b, we also demonstrated that TCMP-2 can interact with *At*miP1b. In addition, we proved that TCMP-2 can interact with *Sl*BBX17 (Figure 13b).

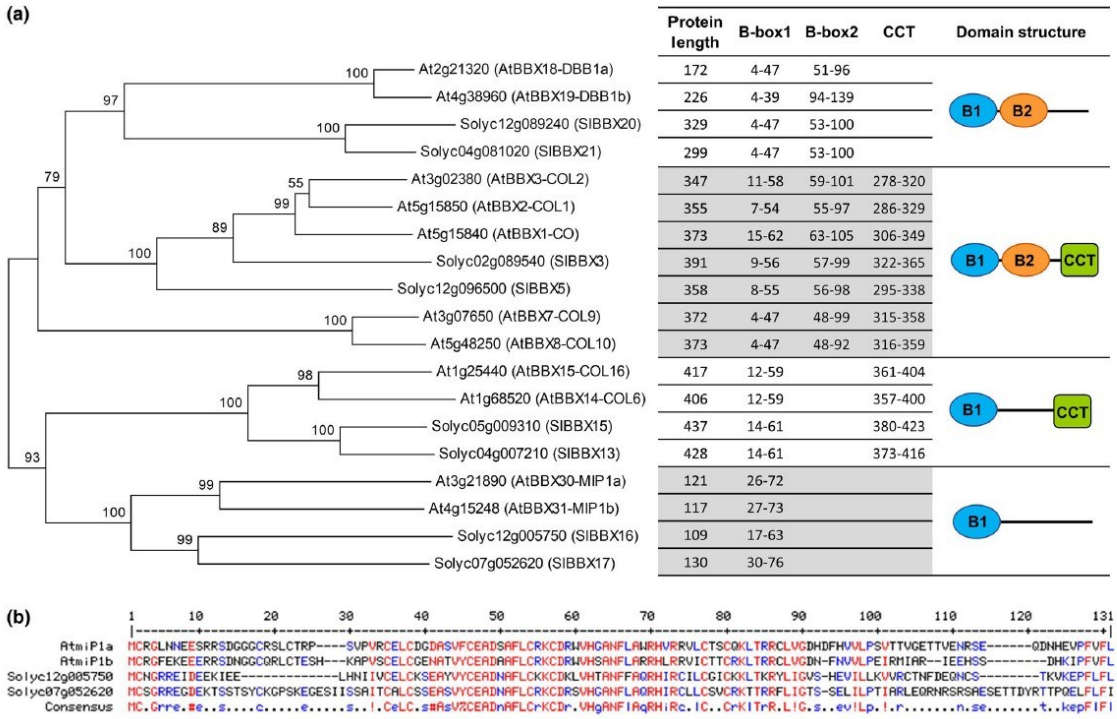

Figure 14. Sequence comparison of tomato and Arabidopsis BBX proteins. a) Phylogenetic tree of tomato and Arabidopsis BBX family members and structural domains of the BBX proteins. A total of nineteen protein sequences were aligned in MEGA 5 (Tamura et al., 2011), using the default ClustalW algorithm. The evolutionary history was inferred using the Minimum Evolution method (Rzhetsky & Nei, 1992). The optimal tree with the sum of branch length = 307.80664062 is shown. The percentage of replicate trees in which the associated taxa clustered together in the bootstrap test (500 replicates) are shown above the branches (Felsenstein, 1985). The tree is drawn to scale, with branch lengths in the same units as those of the evolutionary distances used to infer the phylogenetic tree. The evolutionary distances were computed using the number of differences method (Nei & Kumar, 2000) and are in the units of the number of amino acid differences per sequence. The ME tree was searched using the Close-Neighbor-Interchange (CNI) algorithm (Nei & Kumar, 2000) at a search level of 1. The Neighbor-joining algorithm (Saitou & Nei, 1987) was used to generate the initial tree. The analysis involved 19 amino acid sequences. All positions containing gaps and missing data were eliminated. There was a total of 86 positions in the final dataset. For each BBX protein in the phylogenetic tree, the corresponding amino acid length, the position of the conserved domain/s identified using the SMART (Simple Modular Architecture Research Tool) web resource (http://smart.embl.de; Letunic & Bork, 2018), and the schematic drawing of the domain structure are indicated. The SlBBX16, SlBBX17, AtmiP1a, and AtmiP1b proteins characterized by the presence of a single B-box domain cluster together. b) Alignment created by Multalign (Corpet, 1988) of the SlBBX16 (Solyc12g005750), SlBBX17 (Solyc07g052620), AtmiP1a(AtBBX30), and AtmiP1b (AtBBX31) proteins. Conserved residues are colored in red (high consensus level 90%) and in blue (low consensus level 50%). A position with no conserved residues is represented by a dot in the consensus line. The consensus symbols are ! (IV), % (FY), and# (NDE).

4.5.2. Bimolecular fluorescence complementation (BiFC) and Ratiometric BIFC (rBIFC)

To test the interaction between TCMP-2 and *Sl*BBX16 *in planta*, BiFC analysis (Walter et al., 2004) was performed via transient expression in *Nicotiana tabacum* epidermal cells. The reconstitution of the yellow fluorescent protein (YFP) showed by the confocal laser scanner microscopy confirmed that the TCMP-2 protein can physically interact with *Sl*BBX16 *in vivo* (Figure 15a). To demonstrate whether the B-box domain of *Sl*BBX16 was responsible for the interaction with the TCMP-2, we performed a ratiometric BIFC (rBIFC). With this strategy, the two putative interacting partners are simultaneously cloned into a single vector backbone also containing an internal fluorescent marker for constitutive expression control and ratiometric analysis (Grefen and Blatt, 2018).

rBIFC was carried out using a deleted version of the *Sl*BBX16 protein as negative control of the interaction (hereafter indicated as ΔBBX16), in which the first sixty amino acids (the protein region containing the characteristic residues of the B-box domain) were removed. Four different combinations of constructs for rBIFC were performed, considering two conformational alternatives differing in the position of TCMP-2 (cloned either downstream or upstream of the N-terminus of YFP, *i.e.,* nYFP::TCMP-2//BBX16::cYFP and TCMP-2::nYFP//BBX16::cYFP). *Sl*BBX16 is fused upstream to the C-terminus of YFP in both constructs. The controls (*i.e.*, nYFP::TCMP-2//ΔBBX16::cYFP and TCMP-2::nYFP//ΔBBX16::cYFP) contain the mutated *Sl*BBX16 (Figure 15b). The interactions appeared generally weak, indicating some uncharacterized limitations to the efficient interaction of protein partners but a significantly stronger signal was revealed for the combination nYFP::TCMP-2//BBX16::cYFP (Figure 15b). The signal for this combination was highly variable in different cells so that, even if higher, it was not significantly different from the signal of the conformational alternative TCMP-2::nYFP//BBX16::cYFP.

The differences with deletion controls were statistically significant, indicating that the removal of the B-box domain of *Sl*BBX16 restrains the interaction.

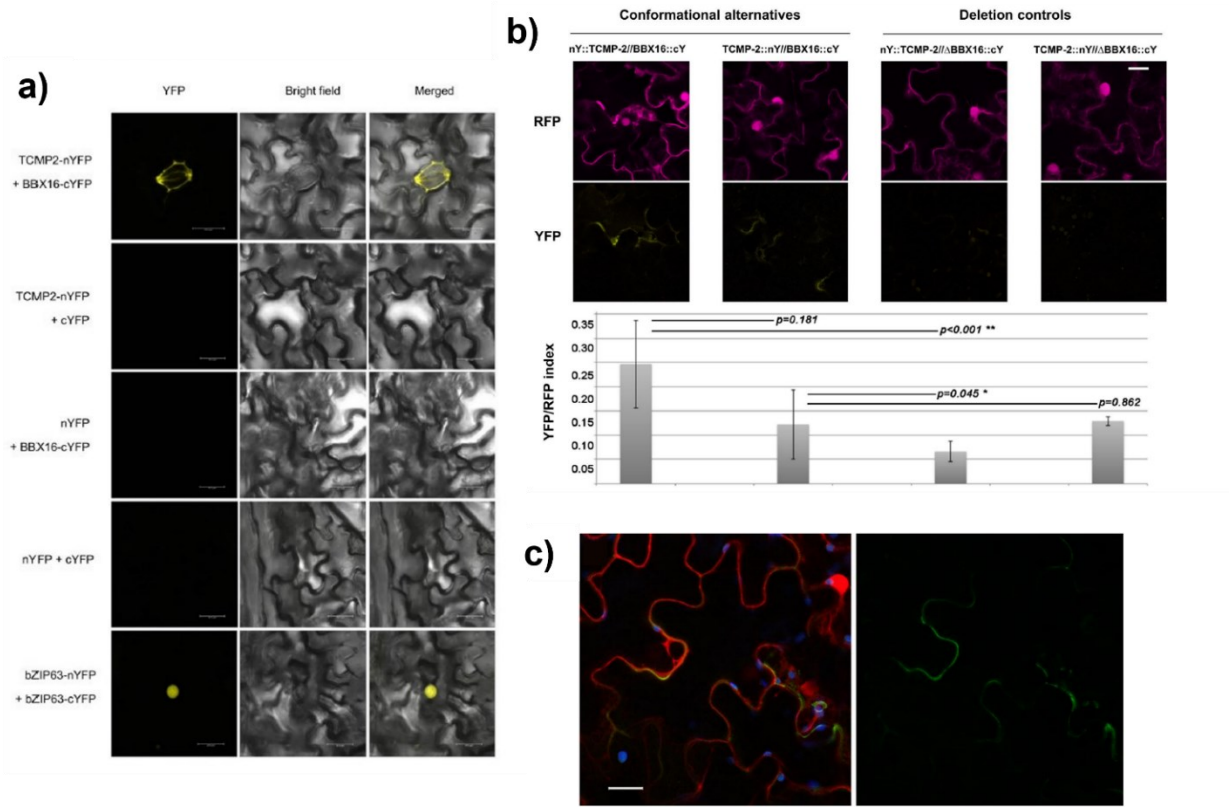

Figure 15. In vitro interaction between TCMP-2 and SlBBX16. a) Nicotiana tabacum epidermal cells showing the interaction between TCMP-2 and Sl*BBX16. A. tumefaciens cells harboring the mature TCMP-2 fused with the N-terminus of YFP (nYFP) and the* Sl*BBX16 fused with the C-terminus of YFP (cYFP) were co-infiltrated into tobacco leaves. nYFP and cYFP empty vectors were used as negative controls; the combination of bZIP63-nYFP and bZIP63-cYFP was used as a positive control. The cells were imaged by confocal microscopy 36-48 hr later. Scale bars indicate 25 µm. b) Quantitative rBIFC analysis of TCMP-2 interaction with* Sl*BBX16 with different control deletion constructs. The higher row of images shows representative tobacco epidermal cells transiently transformed and expressing the cytosolic reference RFP; below the YFP complemented signal, corresponding to the indicated construct combination is shown; scale bar = 20 µm. YFP/RFP fluorescence intensities from 7 different independent samples were calculated as the average YFP/RFP ratio. Independent samples Student's t-test was applied (*p < 0.05). c) Confocal images of tobacco epidermal cells agroinfiltrated with the vector containing the construct nYFP::TCMP-2//BBX16::cYFP. On the left, YFP complemented fluorescence (in green) can be distinguished in between cytosolic RFP (in red) and chlorophyll epifluorescence (in blue); on the right, after subtraction of overlapping signal, YFP fluorescence appears distributed on peripheral cellular membranes. Scale bars: 20 µm.*

Only in the case of the combination nYFP::TCMP-2//BBX16::cYFP, it was possible to observe fluorescent signals compatible with cellular membranes (Figure 15b and 15c), but signal weakness suggests that further investigations are required to define the localization of the interacting proteins.

4.6. *The ectopic overexpression of* TCMP-2 *in Arabidopsis affects the flowering time*

Considering that: i) overexpression of TCMP-2 in tomato flower buds determines an acceleration in the transition from the vegetative stage to the reproductive phase; ii) constitutive overexpression of TCMP-2 in MicroTom resulted in a tendency to an indeterminate habit and early flowering; iii) TCMP-2 can interact with *At*miP1b; we decided to ectopically express the TCMP-2 CDS (*35S::TCMP-2*) in Arabidopsis to study whether it can interfere with endogenous pathways controlling reproductive development. Two independent transgenic lines, named #B2 and #M3, expressing TCMP-2 were obtained (Figure 16).

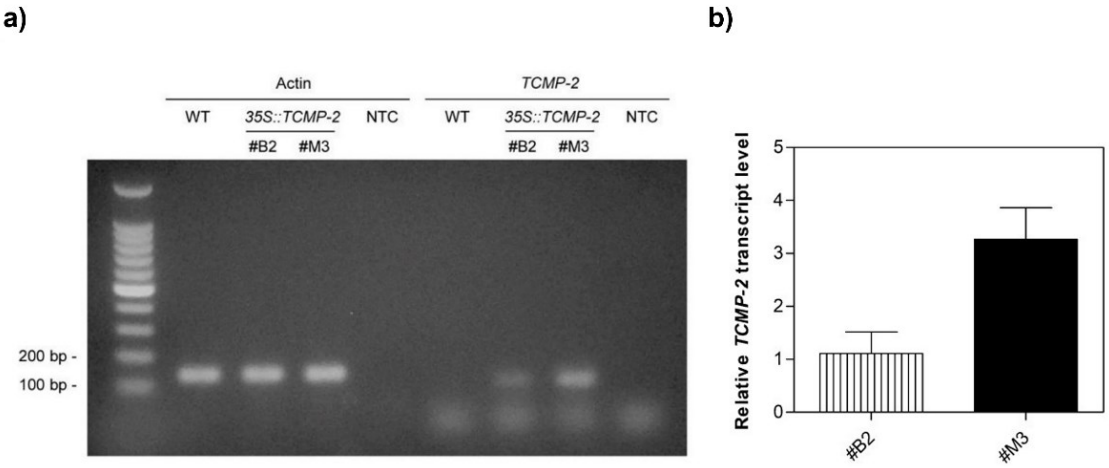

Figure 16. Expression analysis of 35S::TCMP-2 Arabidopsis plants. RT-PCR analysis was carried out on WT plants and transgenic #B2 and #M3 lines using primers pairs on actin and TCMP-2 coding sequence. a) Agarose gel showing RT-PCR products. NTC= not template control. b) qRT-PCR analysis reporting the expression level of the transgene in the two 35S::TCMP-2 lines. The values reported are means ± SE (n= 3).

WT, #B2 and #M3 plants were grown under LD light regimen and the phenotype was monitored from sowing to flowering, counting the days needed for reach the flower transition with the appearance of the flower stem (Figure 17). The transgenic lines showed an anticipate flowering time: on the average, they flowered 3-4 days earlier than WT plants (Figure 17d). At flower transition, the number of rosette leaves was counted showing a reduction for both the transgenic lines compared to the WT plants (Figure 17b). The early flowering phenotype observed in Arabidopsis plants over-expressing TCMP-2 resembles that detected when *At*miP1a/b were silenced (Graeff et al., 2016; Figure 17a). Since the transition from vegetative to reproductive growth is controlled in Arabidopsis by multiple molecular

pathways, which converge on the induction of florigen gene, the expression of *FT* (*At1g65480*) was evaluated in rosette leaves of WT and *35S::TCMP-2* plants.

The transcript level of *FT* was increased approximately 3- and 5-fold in #B2 and #M3 transgenic lines respectively, as compared with the WT (Figure 17c).

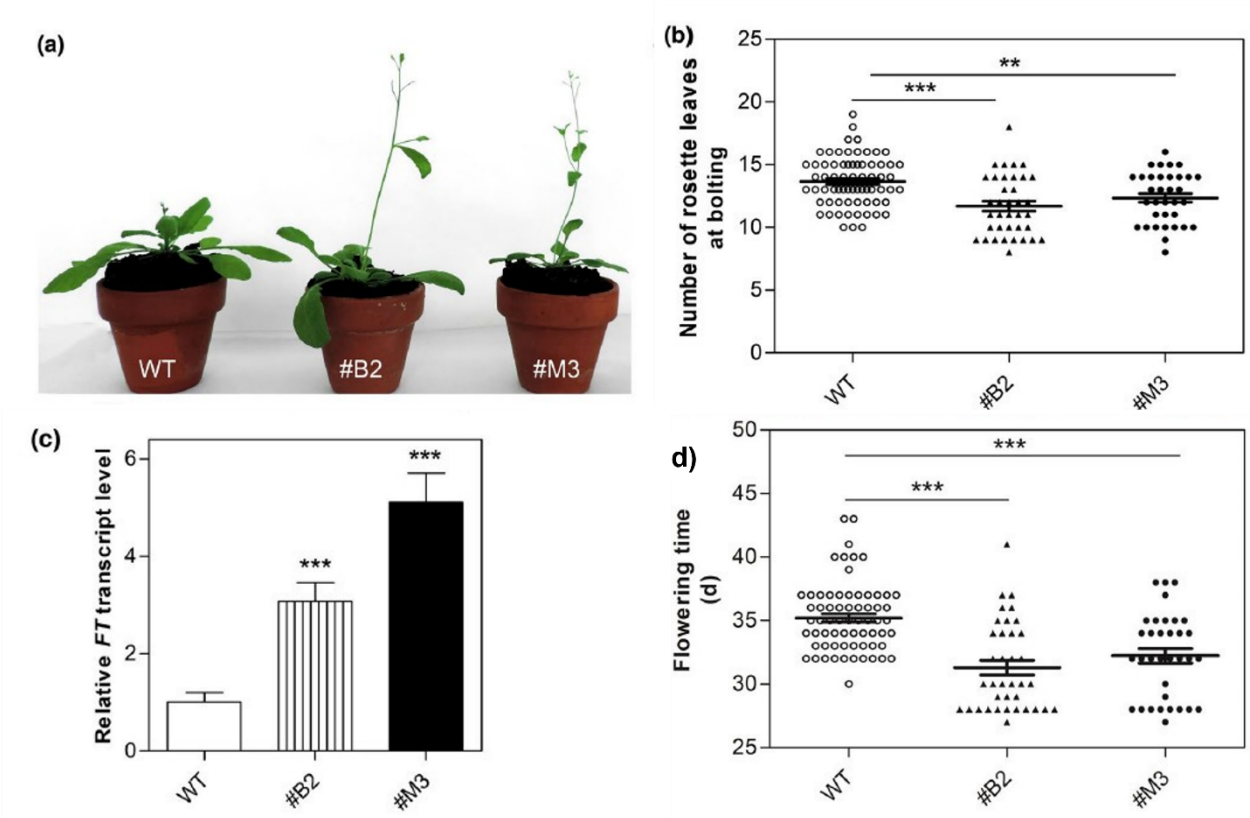

*Figure 17. Arabidopsis plants over-expressingTCMP-2 display early flowering time. a) Picture representative of the early flowering phenotype 35S::TCMP-2 lines (#B2 and #M3) compared to a WT plant at the same age. b) Number of rosette leaves produced at bolting.c) Expression level of FT evaluated in leaves of WT and #B2 and #M3 transgenic lines. The values reported in (c) are means ± SE (n = 3). d) Quantification of the flowering time by counting the day from germination at which each plant reaches bolting. The values reported in panels (a), (b) and (d) are means ± SE (n ≥ 34 plants). Student's t-test was used to compare differences between transgenic and WT plants (**p < 0.01; ***p < 0.001).*

5. DISCUSSION

In Angiosperms, fruit set is defined as the transition from a quiescent ovary to a rapidly growing young fruit, which is an important process in the sexual reproduction of flowering plants (de Jong et al., 2009). This crucial phase depends on successful fertilization and is subject to many genetic factors and environmental conditions, such as day length and temperature, as well as endogenous signals (Lifschitz et al., 2014). Classical hormones and transcription factors regulate this process, but various miniproteins and small peptides can also take part in this phase over short and long distances.

Secreted signaling peptides can be divided into two major categories: small post-translationally modified peptides and Cys-rich peptides (CRPs), typically containing 6-8 Cys residues forming intramolecular disulfide bonds (Matsubayashi & Sakagami, 2006). Plant peptides act at different levels during reproductive development; for instance, some CRPs specifically expressed in flowers, control the communication between male and female reproductive organs and gametic cells during fertilization (Dresselhaus & Franklin-Tong, 2013; Ingram& Gutierrez-Marcos, 2015).

TCMP-1 and TCMP-2 are tomato CRPs peptides/miniproteins that function as metallocarboxypeptidase inhibitors which have been extensively studied and characterized since their discovery (Hass & Hermodson, 1981b; Martineau et al., 1991). TCMP-1 is highly expressed in flower buds before anthesis and TCMP-2 shows its maximum expression at mature green and ripe fruit stage (Cavallini et al., 2011). In leaves TCMP-1 expression is induced by wounding and elicitors of biotic stress responses hinting at a role in plant defense (Díez-Díaz et al., 2004; Martineau et al., 1991). More recently, it was found that TCMP-1 is also responsive to abiotic stress (Manara et al., 2020). Functional data on TCMP-2 revealed that it is implicated in early fruit development (Molesini et al., 2018; Molesini et al., 2020 and this thesis). The availability of tomato genome sequence revealed that TCMP-1 and TCMP-2 belong to a larger gene family. From data retrieved from the KNOTTIN database (www.dsimb.inserm.fr/KNOTTIN), we identified ten tomato “uncharacterized cystine-knot proteins” (namely A-J), with putative function as metallocarboxypeptidase inhibitors. None of the other family members exhibited a peculiar expression pattern during early fruit development as that observed for TCMP-2 (Figure 3), which prompted us to focus our study on TCMP-2.

In this PhD thesis, we took advantage of already produced transgenic plants over-expressing TCMP-2 in flower buds (pTCMP-2::TCMP-1; Molesini et al., 2018), which displayed an earlier fruit production, to further investigate the role of TCMP-2 in reproductive development. Our phenotypic analysis aimed to establish whether the early fruit production was associated with a perturbation in flowering process.

Considering the appearance of the first inflorescence, no differences were observed between the transgenic and the WT plants; but changes in flowering pattern were evident in the sympodial units, indicating an accelerated shoot growth termination.

As known, the transition to flowering is synonymous with termination in tomato (Lifschitz et al., 2014). Tomato is a day-neutral plant in which the production of flowers is not correlated with the photoperiodic conditions, although other environmental factors such as light intensity and ambient temperature can affect flowering (Calvert, 1964). In tomato, flowering is induced by SFT (homolog to FLOWERING LOCUS T also known as Florigen), while sympodial cycling is controlled by the ratio between SFT and SP (antiflorigen) (Lifschitz et al., 2014). The SFT expression in the leaves of pTCMP-2::TCMP-1 transgenic plants was induced, whereas SP expression in the meristems remained unchanged. The increased expression of *SFT* in the leaves normally correlates with a higher amount of the protein transported to the meristem, where SFT antagonizes the *Sl*SP action. On the other hand, since *Sl*SP mRNA level in the meristem did not change in the transgenic plants, it is likely that SFT/SP protein ratio increases. This evidence is in accordance with the proposed dynamic SFT/SP ratio that depends on the imported florigen (SFT) in the meristem which causes the shift to shoot termination in tomato (Lifschitz et al., 2014).

To corroborate these results in a different tomato cultivar, we overexpressed TCMP-2 in MicroTom. The decreased number of leaves before the first inflorescence, accompanied by a reduction in the stem height in the majority of transgenic lines, may suggest that the overexpression of TCMP-2 determines an acceleration in the transition from the vegetative to the reproductive phase, also in the MicroTom genetic background (Figure 9). Despite this, no significant differences between transgenic lines and WT plants were recorded in either the number of flowers or in the number of fruits considering the first four trusses. The total productivity was no affected as well.

The phylogenetic analysis of the Solanaceae specific TCMPs in *Solanum pennelli* and *Solanum pimpinellifolium,* which are important donors of germplasm for the cultivated tomato,

revealed that homologs of all TCMP family members are present in both *S. pennelli* and *S. pimpinellifolium*, except for TCMP-2 homolog in *S. pennellii* (Figure 10). By bioinformatic analysis, we demonstrated that *S. pennelli* genome contains a truncated form of TCMP-2 protein that lacks the cystine-knot motif. In collaboration with IBMCP, we have overexpressed *Sl*TCMP-2 in two accessions of *S. pennellii* (LA716 and 20164).

We have already obtained several independent *S.pennellii* T0 transgenic lines; phenotypic analysis will be performed in the successive T1 generation.

The mode of action of TCMPs in plants remains largely unknown due to the absence of homologous genes in other model species, including Arabidopsis. In several cases, CRPs act as signaling molecules in plant development by modifying the activity of multimeric complexes (De Coninck & De Smet, 2016; Tavormina et al., 2015). To gain further insights into the role of TCMP-2 in reproductive development, we conducted a yeast two-hybrid (Y2H) screen to discover its potential cellular partners.

TCMP-2 was proved to interact *in vitro* and *in vivo* with *Sl*BBX16, which is a member of the BBX protein family. Additionally, an *ad hoc* Y2H showed that TCMP-2 can interact with *Sl*BBX17, the closest *Sl*BBX16 homolog (Figure 13). BBX proteins are known to participate in photomorphogenesis, UV-B protection, and photoperiodic flowering control (Graeff et al., 2016; Heng et al., 2019; Song et al., 2020;Yadav et al., 2019). In Arabidopsis, the closest homologs of *Sl*BBX16 and *Sl*BBX17 are *At*BBX30 and *At*BBX31 (also referred to as miP1a and miP1b; Figure 14), respectively. We demonstrated that TCMP-2 was able to interact with miP1b of Arabidopsis.

A severe delay in the flowering time was obtained in *A. thaliana* plants over-expressing *At*mip1b and *At*mip1a grown under LD conditions, as a result of flowering repression by the transcriptional inhibition of the florigen gene FLOWERING LOCUS T (Graeff et al., 2016). In contrast, the downregulation by RNA silencing of either *At*miP1b or both *At*miP1a/b determined an earlier flowering as compared with WT plants (Graeff et al., 2016). The Arabidopsis double mutant bbx30-2 bbx31-2 obtained by CRISPR/Cas also flowered earlier than the WT (Heng et al., 2019).

We have hypothesized that, thanks to the capacity of TCMP-2 to interact with *At*miP1b, TCMP-2 overexpression in Arabidopsis might mimic the effect of *At*miP1b silencing observed by Greff et al., 2016 and Heng et al., 2019. In accordance with this hypothesis, Arabidopsis plants ectopically over-expressing TCMP-2 showed an anticipated flowering transition and

an increased level of florigen (FT) expression. Thus, although TCMP-2 is a Solanaceous-specific gene, the altered flowering phenotype caused by its ectopic overexpression proved that the TCMP-2 protein is able to interact with components of the signaling pathway controlling flowering transition in Arabidopsis, most probably likely due to its capacity to bind BBX proteins.

Since *Solanum lycopersicum* differs from Arabidopsis in the photoperiodic control (i.e., day-neutral vs. long-day), TCMP-2 could represent an additional regulatory element which, through interaction with BBX microProteins, modulates the effects of environmental factors (*e.g.*, temperature) or endogenous signals on flowering regulation.

6. BIBLIOGRAPHY

Aliberti, A., Olivieri, F., Graci, S., Rigano, M. M., Barone, A., & Ruggieri, V. (2020). *Genomic Dissection of a Wild Region in a Superior Solanum pennellii Introgression Sub-Line with High Ascorbic Acid Accumulation in Tomato Fruit*. https://doi.org/10.3390/genes11080847

Atarés, A., Moyano, E., Morales, B., Schleicher, P., Osvaldo García-Abellán, J., Antón, T., García-Sogo, B., Perez-Martin, F., Lozano, R., Borja Flores, F., Moreno, V., del Carmen Bolarin, M., & Pineda, B. (2011). *An insertional mutagenesis programme with an enhancer trap for the identification and tagging of genes involved in abiotic stress tolerance in the tomato wild-related species Solanum pennellii*. https://doi.org/10.1007/s00299-011-1094-y

Barozzi, F., Papadia, P., Stefano, G., Renna, L., Brandizzi, F., Migoni, D., Fanizzi, F. P., Piro, G., & di Sansebastiano, G. pietro. (2019). Variation in membrane trafficking linked to SNARE AtSYP51 interaction with aquaporin NIP1;1. *Frontiers in Plant Science*, *9*, 1949. https://doi.org/10.3389/FPLS.2018.01949/BIBTEX

Bayés, A., de la Vega, M. R., Vendrell, J., Aviles, F. X., Jongsma, M. A., & Beekwilder, J. (2006). Response of the digestive system of Helicoverpa zea to ingestion of potato carboxypeptidase inhibitor and characterization of an uninhibited carboxypeptidase B. *Insect Biochemistry and Molecular Biology*, *36*(8), 654–664. https://doi.org/10.1016/J.IBMB.2006.05.010

Calafiore, R., Aliberti, A., Ruggieri, V., Olivieri, F., Rigano, M. M., & Barone, A. (2019). Phenotypic and molecular selection of a superior solanum pennellii introgression sub-line suitable for improving quality traits of cultivated tomatoes. *Frontiers in Plant Science*, *10*, 190. https://doi.org/10.3389/FPLS.2019.00190/BIBTEX

Calafiore, R., Ruggieri, V., Raiola, A., Rigano, M. M., Sacco, A., Hassan, M. I., Frusciante, L., & Barone, A. (2016). Exploiting genomics resources to identify candidate genes underlying antioxidants content in tomato fruit. *Frontiers in Plant Science*, *7*(APR2016), 397. https://doi.org/10.3389/FPLS.2016.00397/BIBTEX

Calvert, A. (2015). Gkowth and Flowering of the Tomato in Relation to Natural Light Conditions. *Http://Dx.Doi.Org/10.1080/00221589.1964.11514104*, *39*(3), 182–193. https://doi.org/10.1080/00221589.1964.11514104

Cavallini, C., Trettene, M., Degan, M., Delva, P., Molesini, B., Minuz, P., Pandolfini, T., & Pandolfini, T. (2011). Anti-angiogenic effects of two cystine-knot miniproteins from tomato fruit Keywords cystine-knot miniproteins; angiogenesis; MAPK pathway; tomato fruit. *British Journal of Pharmacology*, *162*, 1261. https://doi.org/10.1111/j.1476-5381.2010.01154.x

Chu, Z., Wang, X., Li, Y., Yu, H., Li, J., Lu, Y., Li, H., & Ouyang, B. (2016). Genomic organization, phylogenetic and expression analysis of the B-Box gene family in tomato. *Frontiers in Plant Science*, *7*(OCTOBER2016), 1552. https://doi.org/10.3389/FPLS.2016.01552/BIBTEX

Cotabarren, J., Tellechea, M. E., Avilés, F. X., Lorenzo Rivera, J., & Obregón, W. D. (2018). Biochemical characterization of the YBPCI miniprotein, the first carboxypeptidase inhibitor isolated from Yellow Bell Pepper (Capsicum annuum L). A novel contribution to the knowledge of miniproteins stability. *Protein Expression and Purification*, *144*, 55–61. https://doi.org/10.1016/J.PEP.2017.12.003

Daly, N. L., & Craik, D. J. (2011). Bioactive cystine knot proteins. *Current Opinion in Chemical Biology*, *15*(3), 362–368. https://doi.org/10.1016/J.CBPA.2011.02.008

Davuluri, G. R., van Tuinen, A., Fraser, P. D., Manfredonia, A., Newman, R., Burgess, D., Brummell, D. A., King, S. R., Palys, J., Uhlig, J., Bramley, P. M., Pennings, H. M. J., & Bowler, C. (2005). Fruit-specific RNAi-mediated suppression of DET1 enhances carotenoid and flavonoid content in tomatoes. *Nature Biotechnology 2005 23:7*, *23*(7), 890–895. https://doi.org/10.1038/nbt1108

de Abreu-Neto, J. B., Turchetto-Zolet, A. C., de Oliveira, L. F. V., Bodanese Zanettini, M. H., & Margis-Pinheiro, M. (2013). Heavy metal-associated isoprenylated plant protein (HIPP): characterization of a family of proteins exclusive to plants. *The FEBS Journal*, *280*(7), 1604–1616. https://doi.org/10.1111/FEBS.12159

de Caroli, M., Manno, E., Perrotta, C., de Lorenzo, G., di Sansebastiano, G. pietro, & Piro, G. (2020). CesA6 and PGIP2 Endocytosis Involves Different Subpopulations of TGN-Related Endosomes. *Frontiers in Plant Science*, *11*, 350. https://doi.org/10.3389/FPLS.2020.00350/BIBTEX

de Jong, M., Mariani, C., & Vriezen, W. H. (2009). The role of auxin and gibberellin in tomato fruit set. *Journal of Experimental Botany*, *60*(5), 1523–1532. https://doi.org/10.1093/JXB/ERP094

Díez-Díaz, M., Conejero, V., Rodrigo, I., Pearce, G., & Ryan, C. A. (2004). Isolation and characterization of wound-inducible carboxypeptidase inhibitor from tomato leaves. *Phytochemistry*, *65*(13), 1919–1924. https://doi.org/10.1016/J.PHYTOCHEM.2004.06.007

Dresselhaus, T., & Franklin-Tong, N. (2013). Male–Female Crosstalk during Pollen Germination, Tube Growth and Guidance, and Double Fertilization. *Molecular Plant*, *6*(4), 1018–1036. https://doi.org/10.1093/MP/SST061

Eshed, Y., & Zamir, D. (1994). A genomic library of Lycopersicon pennellii in L. esculentum: A tool for fine mapping of genes. In *Euphytica* (Vol. 79).

Fan, Y., Yang, W., Yan, Q., Chen, C., & Li, J. (2019). *Genome-Wide Identification and Expression Analysis of the Protease Inhibitor Gene Families in Tomato*. https://doi.org/10.3390/genes11010001

Formstecher, E., Aresta, S., Collura, V., Hamburger, A., Meil, A., Trehin, A., Reverdy, C., Betin, V., Maire, S., Brun, C., Jacq, B., Arpin, M., Bellaiche, Y., Bellusci, S., Benaroch, P., Bornens, M., Chanet, R., Chavrier, P., Delattre, O., … Daviet, L. (2005). Protein interaction mapping: A Drosophila case study. *Genome Research*, *15*(3), 376. https://doi.org/10.1101/GR.2659105

Gangappa, S. N., & Botto, J. F. (2014). The BBX family of plant transcription factors. *Trends in Plant Science*, *19*(7), 460–470. https://doi.org/10.1016/J.TPLANTS.2014.01.010

Gisbert, C., Arrillaga, I., Roig, L. A., & Moreno, V. (1999). Acquisition of a collection of Lycopersicon pennellii (Corr. D'Arcy) transgenic plants with uidA and nptII marker genes. *Journal of Horticultural Science and Biotechnology*, *74*(1), 105–109. https://doi.org/10.1080/14620316.1999.11511081

Graeff, M., Straub, D., Eguen, T., Dolde, U., Rodrigues, V., Brandt, R., & Wenkel, S. (2016). MicroProtein-Mediated Recruitment of CONSTANS into a TOPLESS Trimeric Complex Represses Flowering in Arabidopsis. *PLoS Genetics*, *12*(3). https://doi.org/10.1371/journal.pgen.1005959

Graham, J. S., & Ryan, C. A. (1981). Accumulation of a metallo-carboxypeptidase inhibitor in leaves of wounded potato plants. *Biochemical and Biophysical Research Communications*, *101*(4), 1164–1170. https://doi.org/10.1016/0006-291X(81)91570-9

Grefen, C., & Blatt, M. R. (2012). A 2in1 cloning system enables ratiometric bimolecular fluorescence complementation (rBiFC). *BioTechniques*, *53*(5), 311–314. https://doi.org/10.2144/000113941/FORMAT/EPUB

Hartl, M., Giri, A. P., Kaur, H., & Baldwin, I. T. (2010). Serine protease inhibitors specifically defend Solanum nigrum against generalist herbivores but do not influence plant growth and development. *The Plant Cell*, *22*(12), 4158–4175. https://doi.org/10.1105/tpc.109.073395

Hass, G. M., & Hermodson, M. A. (1981a). Amino acid sequence of a carboxypeptidase inhibitor from tomato fruit. *Biochemistry*, *20*(8), 2256–2260. https://doi.org/10.1021/BI00511A029

Heng, Y., Lin, F., Jiang, Y., Ding, M., Yan, T., Lan, H., Zhou, H., Zhao, X., Xu, D., & Deng, X. W. (2019). B-box containing proteins bbx30 and bbx31, acting downstream of hy5, negatively regulate photomorphogenesis in arabidopsis. *Plant Physiology*, *180*(1), 497–508. https://doi.org/10.1104/pp.18.01244

Ingram, G., & Gutierrez-Marcos, J. (2015). *Peptide signalling during angiosperm seed development*. https://doi.org/10.1093/jxb/erv336

Ireland, D. C., Colgrave, M. L., & Craik, D. J. (2006). A novel suite of cyclotides from Viola odorata: sequence variation and the implications for structure, function and stability. *The Biochemical Journal*, *400*(1), 1–12. https://doi.org/10.1042/BJ20060627

Iyer, S., & Acharya, K. R. (2011). Tying the knot: the cystine signature and molecular-recognition processes of the vascular endothelial growth factor family of angiogenic cytokines. *The FEBS Journal*, *278*(22), 4304–4322. https://doi.org/10.1111/J.1742-4658.2011.08350.X

Jones, C. M., Rick, C. M., Adams, D., Jernstedt, J., & Chetelat, R. T. (2007). GENEALOGY AND FINE MAPPING OF OBSCURAVENOSA, A GENE AFFECTING THE DISTRIBUTION OF CHLOROPLASTS IN LEAF VEINS, AND EVIDENCE OF SELECTION DURING BREEDING OF TOMATOES (LYCOPERSICON ESCULENTUM; SOLANACEAE) 1. *American Journal of Botany*, *94*(6), 935–947. https://doi.org/10.3732/ajb.94.6.935

Kobayashi, M., Nagasaki, H., Garcia, V., Just, D., Bres, C., Mauxion, J. P., le Paslier, M. C., Brunel, D., Suda, K., Minakuchi, Y., Toyoda, A., Fujiyama, A., Toyoshima, H., Suzuki, T., Igarashi, K., Rothan, C., Kaminuma, E., Nakamura, Y., Yano, K., & Aoki, K. (2014). Genome-Wide Analysis of Intraspecific DNA Polymorphism in 'Micro-Tom', a Model Cultivar of Tomato (Solanum lycopersicum). Plant and Cell Physiology, 55(2), 445–454. https://doi.org/10.1093/PCP/PCT181

Kolmar, H. (2010). Engineered cystine-knot miniproteins for diagnostic applications. *Expert Review of Molecular Diagnostics*, *10*(3), 361–369. https://doi.org/10.1586/ERM.10.15

le Nguyen, D., Heitz, A., Chiche, L., Castro, B., Boigegrain, R. A., Favel, A., & Coletti-Previero, M. A. (1990). Molecular recognition between serine proteases and new bioactive microproteins with a knotted structure. *Biochimie*, *72*(6–7), 431–435. https://doi.org/10.1016/0300-9084(90)90067-Q

Lifschitz, E., Ayre, B. G., Eshed, Y., Coupland, G., Mount, S. M., & Sharma, R. (2014). *Florigen and anti-florigen – a systemic mechanism for coordinating growth and termination in flowering plants*. https://doi.org/10.3389/fpls.2014.00465

Lippman, Z. B., Semel, Y., Zamir, D., Susan Wessler, by, Dawe, K., & Leebens-Mack, J. (2007). *An integrated view of quantitative trait variation using tomato interspecific introgression lines This review comes from a themed issue on Genomes and evolution Edited*. https://doi.org/10.1016/j.gde.2007.07.007

Livak, K. J., & Schmittgen, T. D. (2001). Analysis of Relative Gene Expression Data Using Real-Time Quantitative PCR and the 2−ΔΔCT Method. *Methods*, *25*(4), 402–408. https://doi.org/10.1006/METH.2001.1262

Lufrano, D., Cotabarren, J., Garcia-Pardo, J., Fernandez-Alvarez, R., Tort, O., Tanco, S., Avilés, F. X., Lorenzo, J., & Obregón, W. D. (2015). Biochemical characterization of a novel carboxypeptidase inhibitor from a variety of Andean potatoes. *Phytochemistry*, *120*, 36–45. https://doi.org/10.1016/J.PHYTOCHEM.2015.09.010

Manara, A., Fasani, E., Molesini, B., DalCorso, G., Pennisi, F., Pandolfini, T., & Furini, A. (2020). The tomato metallocarboxypeptidase inhibitor I, which interacts with a heavy metal-associated isoprenylated protein, is implicated in plant response to cadmium. *Molecules*, *25*(3). https://doi.org/10.3390/MOLECULES25030700

Martineau, B., McBride, K. E., & Houck, C. M. (1991). Regulation of metallocarboxypeptidase inhibitor gene expression in tomato. *Molecular & General Genetics : MGG*, *228*(1–2), 281–286. https://doi.org/10.1007/BF00282477

Matsubayashi, Y., & Sakagami, Y. (2006). Peptide hormones in plants. *Annual Review of Plant Biology*, *57*, 649–674. https://doi.org/10.1146/ANNUREV.ARPLANT.56.032604.144204

Menda, N., Strickler, S. R., & Mueller, L. A. (2013). Advances in tomato research in the post-genome era. *Plant Biotechnology*, *30*, 243–256. https://doi.org/10.5511/plantbiotechnology.13.0904a

Molesini, B., Dusi, V., Pennisi, F., & Pandolfini, T. (2020). How Hormones and MADS-Box Transcription Factors Are Involved in Controlling Fruit Set and Parthenocarpy in Tomato. *Genes*, *11*(12), 1–17. https://doi.org/10.3390/GENES11121441

Molesini, B., Rotino, G. L., Dusi, V., Chignola, R., Sala, T., Mennella, G., Francese, G., & Pandolfini, T. (2018a). Two metallocarboxypeptidase inhibitors are implicated in tomato fruit development and regulated by the Inner No Outer transcription factor. *Plant Science*, *266*, 19–26. https://doi.org/10.1016/J.PLANTSCI.2017.10.011

Molesini, B., Rotino, G. L., Dusi, V., Chignola, R., Sala, T., Mennella, G., Francese, G., & Pandolfini, T. (2018b). Two metallocarboxypeptidase inhibitors are implicated in tomato fruit development and regulated by the Inner No Outer transcription factor. *Plant Science*, *266*, 19–26. https://doi.org/10.1016/J.PLANTSCI.2017.10.011

Molesini, B., Treggiari, D., Dalbeni, A., Minuz, P., & Pandolfini, T. (2017). Plant cystine-knot peptides: pharmacological perspectives. *British Journal of Clinical Pharmacology*, *83*(1), 63–70. https://doi.org/10.1111/BCP.12932

Norton, R. S., & Pallaghy, P. K. (1998). The cystine knot structure of ion channel toxins and related polypeptides. *Toxicon : Official Journal of the International Society on Toxinology*, *36*(11), 1573–1583. https://doi.org/10.1016/S0041-0101(98)00149-4

Pallaghy, P. K., Norton, R. S., Nielsen, K. J., & Craik, D. J. (1994). A common structural motif incorporating a cystine knot and a triple-stranded β-sheet in toxic and inhibitory polypeptides. *Protein Science*, *3*(10), 1833–1839. https://doi.org/10.1002/PRO.5560031022

Paris, N., Saint-Jean, B., Faraco, M., Krzeszowiec, W., Dalessandro, G., Neuhaus, J. M., & di Sansebastiano, G. pietro. (2010). Expression of a glycosylated GFP as a bivalent reporter in exocytosis. *Plant Cell Reports*, *29*(1), 79–86. https://doi.org/10.1007/S00299-009-0799-7

Pear, J. R., Ridge, N., Rasmussen, R., Rose, R. E., & Houck, C. M. (1989). Isolation and characterization of a fruit-specific cDNA and the corresponding genomic clone from tomato. In *Plant Molecular Biology* (Vol. 13).

Quilis, J., En L Opez-Garc Ia, B., Meynard, D., Guiderdoni, E., & Segundo, B. S. (1989). *Inducible expression of a fusion gene encoding two proteinase inhibitors leads to insect and pathogen resistance in transgenic rice*. https://doi.org/10.1111/pbi.12143

Quilis, J., Meynard, D., Vila, L., Avilés, F. X., Guiderdoni, E., & San Segundo, B. (2007). A potato carboxypeptidase inhibitor gene provides pathogen resistance in transgenic rice. *Plant Biotechnology Journal*, *5*(4), 537–553. https://doi.org/10.1111/J.1467-7652.2007.00264.X

Rain, J. C., Selig, L., de Reuse, H., Battaglia, V., Reverdy, C., Simon, S., Lenzen, G., Petel, F., Wojcik, J., Schächter, V., Chemama, Y., Labigne, A., & Legrain, P. (2001). The protein-protein interaction map of Helicobacter pylori. *Nature*, *409*(6817), 211–215. https://doi.org/10.1038/35051615

Rees, D. C., & Lipscomb, W. N. (1980). Structure of potato inhibitor complex of carboxypeptidase A at 5.5-A resolution. *Proceedings of the National Academy of Sciences of the United States of America*, *77*(1), 277–280. https://doi.org/10.1073/PNAS.77.1.277

Ryan, C. A. (1980). Wound-Regulated Synthesis and Vacuolar Compartmentation of Proteinase Inhibitors in Plant Leaves. *Current Topics in Cellular Regulation*, *17*(C), 1–23. https://doi.org/10.1016/B978-0-12-152817-1.50005-5

Ryan, C. A., Hass, G. M., & Kuhn, R. W. (1974). Purification and Properties of a Carboxypeptidase Inhibitor from Potatoes. *Journal of Biological Chemistry*, *249*(17), 5495–5499. https://doi.org/10.1016/S0021-9258(20)79755-3

Song, Z., Bian, Y., Liu, J., Sun, Y., & Xu, D. (2020). B-box proteins: Pivotal players in light-mediated development in plants FA. *JIPB Journal of Integrative Plant Biology*. https://doi.org/10.1111/jipb.12935

Tavormina, P., de Coninck, B., Nikonorova, N., de Smet, I., & Cammue, B. P. A. (2015). *The Plant Peptidome: An Expanding Repertoire of Structural Features and Biological Functions OPEN*. https://doi.org/10.1105/tpc.15.00440

Tiwari, S. B., Shen, Y., Chang, H. C., Hou, Y., Harris, A., Ma, S. F., McPartland, M., Hymus, G. J., Adam, L., Marion, C., Belachew, A., Repetti, P. P., Reuber, T. L., & Ratcliffe, O. J. (2010). The flowering time regulator CONSTANS is recruited to the FLOWERING LOCUS T promoter via a unique cis-element. *New Phytologist*, *187*(1), 57–66. https://doi.org/10.1111/J.1469-8137.2010.03251.X

Valverde, F., Mouradov, A., Soppe, W., Ravenscroft, D., Samach, A., & Coupland, G. (2004). Photoreceptor regulation of CONSTANS protein in photoperiodic flowering. *Science (New York, N.Y.)*, *303*(5660), 1003–1006. https://doi.org/10.1126/SCIENCE.1091761

Vicente, M. H., Zsögön, A., Lopo De Sá, A. F., Ribeiro, R. v, & Peres, L. E. P. (2015). Physiology Semi-determinate growth habit adjusts the vegetative-to-reproductive balance and increases productivity and water-use efficiency in tomato (Solanum lycopersicum). *Journal of Plant Physiology*, *177*, 11–19. https://doi.org/10.1016/j.jplph.2015.01.003

Villanueva, J., Canals, F., Prat, S., Ludevid, D., Querol, E., & Avilés, F. X. (1998). Characterization of the wound-induced metallocarboxypeptidase inhibitor from potato 1. *FEBS Letters*, *440*(1–2), 175–182. https://doi.org/10.1016/S0014-5793(98)01447-1

Vitt, U. A., Hsu, S. Y., & Hsueh, A. J. W. (2001). *Evolution and Classification of Cystine Knot-Containing Hormones and Related Extracellular Signaling Molecules*. http://hormone.

Walter, M., Chaban, C., Schü Tze, K., Batistic, O., Weckermann, K., Nä Ke, C., Blazevic, D., Grefen, C., Schumacher, K., Oecking, C., Harter, K., & Rg Kudla, J. (2004). *Visualization of protein interactions in living plant cells using bimolecular fluorescence complementation*. https://doi.org/10.1111/j.1365-313X.2004.02219.x

Werle, M., Schmitz, T., Huang, H. L., Wentzel, A., Kolmar, H., & Bernkop-Schnürch, A. (2006). The potential of cystine-knot microproteins as novel pharmacophoric scaffolds in oral peptide drug delivery. *Journal of Drug Targeting*, *14*(3), 137–146. https://doi.org/10.1080/10611860600648254

Wojcik, J., Boneca, I. G., & Legrain, P. (2002). Prediction, Assessment and Validation of Protein Interaction Maps in Bacteria. *Journal of Molecular Biology*, *323*(4), 763–770. https://doi.org/10.1016/S0022-2836(02)01009-4

Yadav, A., Ravindran, N., Singh, D., Puthan, •, Rahul, V., & Datta, S. (2020). *Role of Arabidopsis BBX proteins in light signaling*. https://doi.org/10.1007/s13562-020-00597-2

Zhang, X., Henriques, R., Lin, S. S., Niu, Q. W., & Chua, N. H. (2006). Agrobacterium-mediated transformation of Arabidopsis thaliana using the floral dip method. *Nature Protocols*, *1*(2), 641–646. https://doi.org/10.1038/NPROT.2006.97

Chapter 2 | Tomato BBX16 and BBX17 microproteins

1. INTRODUCTION

Transcription factors (TFs) play a pivotal role in signal transduction pathways and can establish crosstalks between different signaling pathways regulating processes related to plant development. B-Box (BBX) family represents a group of zinc-finger TFs and regulators that plays a decisive role in plant growth and development acting on different processes during the plant life cycle (Gangappa & Botto, 2014; Yadav et al., 2020). These TFs contain a characteristic zinc-finger domain, stabilized by metal ions including zinc, which permits the interaction with DNA, RNA, and proteins (Khanna et al., 2009).

The availability of sequenced plant genomes has enabled the identification of BBX genes in a large number of model species and crops (Talar & Kiełbowicz-matuk, 2021): for example, in apple there are 64 BBX representatives (Liu et al., 2018), 37 in pear (Cao et al., 2017), 32 in Arabidopsis (Khanna et al., 2009) , 30 in rice and potato (Huang et al., 2012; Talar et al., 2017), 29 in tomato (Chu et al., 2016), and 24 in grapevine (Wei et al., 2020). A phylogenetic analysis also revealed the presence of BBX proteins in algae like *Volvox carteri, Chlamydomonas reinhardtii, Ostreococcus tauris* and *O. lucimarinus*, suggesting that the earliest BBX proteins in photosynthetic organisms originated about one billion years ago (Crocco & Botto, 2013; Peers & Niyogi, 2008).

The BBX family is characterized by the presence of one or two zinc-finger-containing BBX domains in the N-terminal region. Depending on their consensus sequence and distance between the zinc-binding residues, the BBX domains are classified into two types, known as B-box1 (B1) and B-box2 (B2), and play a crucial role in protein–protein interaction (Gangappa & Botto, 2014; Graeff et al., 2016; Khanna et al., 2009). Some BBX proteins also possess a CCT domain (CONSTANS, CO-like, and TIMING OF CAB: TOC1), which is associated with a role in transcriptional regulation and nuclear transport, and several other conserved motifs localized outside the domains mentioned above (Crocco & Botto, 2013).

1.1. Origin, evolution and structure of BBX genes

The first evidence related to the presence of a BBX domain in a protein sequence was reported by Reddy and collaborators (1991). Their findings were relative to an “unusual” novel zinc finger-like region, found in the cDNA sequence of *xnf7* (Maternally Expressed Novel Zinc Finger Nuclear Phosphoprotein in *Xenopus levis*) thought to be responsible for association of the protein with DNA. The zinc finger domain of the XNF7 protein was very

similar to a class of Cys-His structures found in a small family of genes (Freemont et al., 1991). In particular, Reddy & Etkin (1991) reported that in addition to a RING finger (firstly called A-box; nowadays known as Really Interesting New Gene finger domain, which is a protein structural domain of zinc finger type which contains a C_3HC_4), XNF7 also possessed a second zinc binding domain, termed the B-box (CHC_3H_2), followed closely by a predicted α-helical coiled-coil domain. This tripartite domain was then found in other genes maintaining the spacing between the domains found in XNF7 (Reddy & Etkin, 1991; Torok & Etkin, 2001). These genes are: RET protooncogene (Takahashi et al., 1988); RPT-1, a down regulator of the interleukin 2 receptor gene (Patarca et al., 1988); HIV LTR, SS-A/Ro, an RNA binding autoantigen (Chan et al., 1991); PML gene, which is a myeloid specific transcription factor found fused to the retinoic acid receptor gene in Promyelocytic Leukemia (de Thé et al., 1991; Kakizuka et al., 1991).

The peculiar association of the B-box with RING finger and coiled-coil domains characterizes the tripartite motif proteins, named RBCC/TRIM (RING, B-box, coiled-coil/TRIPARTITE motif). In animals, the RBCC/TRIM family includes proteins involved in diverse cellular processes like apoptosis, cell cycle regulation and viral response (Meroni & Diez-Roux, 2005). In these proteins, the BBX domains are present in the N-terminus as a single B-box or tandem repeats designated as B-box1 (B1) and B-box2 (B2) (Massiah et al., 2006). Despite the functional importance of RBCC/TRIM proteins in animals, this type of proteins is absent in plants (R. Khanna et al., 2009; Crocco & Botto, 2013).

Comprehensive phylogenetic and structural analyses of 214 BBX proteins from twelve representative plant species, including four green algae, a moss, a lycophyte, three monocotyledons and three dicotyledons, were presented in the work of Crocco and Botto (2013; Figure 1), suggesting their ancient origin (Peers & Niyogi, 2008). In most green algae BBX proteins have a single B-box motif, nonetheless the presence of two B-box motifs in the unicellular green alga *Chlamydomonas* hints that the B-box duplication event has taken place much before land colonization of plants, at least 450 million years ago (Gangappa & Botto, 2014). The rapid expansion of BBX proteins during the course of evolution and the highly conserved domain topology across the plant kingdom, evoke that this multi-protein family may have important physiological roles during adaptation of land plants.

Regardless of the plant species, all BBX family members possess a common structure that consist of one single B-box domain or two arranged in tandem. These B-Box domains consist

of around 40 amino acids and the two types, B1 and B2, differ in the consensus sequence and the spacing of the seven or eight Zn (II)-binding residues (Kluska et al., 2018). Khanna et al. (2009) grouped the 32 members of *A. thaliana* BBX family in five classes (Figure 1). Members of group I (*At*BBX1 through *At*BBX6) contain B1, B2 and CCT domain. Members of group II (*At*BBX7 through *At*BBX13) possess the same structure of group I with some differences at the consensus sequences of the B2 domain (Chang et al., 2008; Crocco & Botto, 2013). Group III members (*At*BBX14 through *At*BBX17) contain B1 and CCT. Group IV (*At*BBX18 through *At*BBX25) comprises B1 and B2, and no CCT domains. Lastly, group V (*At*BBX26 through *At*BBX32) is made up of members with just a single B1 domain (Khanna et al., 2009; Gangappa & Botto, 2014; Figure 1). Following the same criteria, BBX genes of other species such as tomato, potato, rice, and maize were grouped in subfamilies (respectively: Chu et al., 2016; Huang et al., 2012; Talar et al., 2017; Li et al., 2017), maintaining the subdivision into the five clades.

As mentioned before, some BBX proteins possess a CCT domain which was firstly found in proteins involved in flowering regulation such as CONSTANS (CO), CO-LIKE and TIMING OF CAB1 (TOC1) proteins in *Arabidopsis*. This domain, 42–43 amino acid-long, is localized at the C-terminus and part of this sequence is dedicated to the nuclear localization signal (NLS) (Gangappa & Botto, 2014). In addition to the BBX and the CCT domains, a binding sequence motif for protein–protein interaction, called the VP (VALINE-PROLINE) motif, consisting in six amino acids consensus sequence (G-I/VV-P-S/T-F), was identified by Holm and collaborators (2001). VP is located at the C-terminus and separated by 16–20 amino acids from the CCT domain. Seven novel motifs, M1 -M7, were identified at conserved positions in the BBX protein sequence; these motifs were specific to different sub-groups (Crocco & Botto, 2013). M1 and M2 are specific to the BBX members of group I, M3 to those of group II, M4 and M5 to those of group III and M6 and M7 to those of group IV. Their role has not yet been defined, except for the M6 motif. M6 is present in *At*BBX24 and *At*BBX21, two homologous BBX proteins that negatively and positively regulate photomorphogenic development, respectively. The conversion from M6 of *At*BBX21 to M6 of *At*BBX24 has abolished the photomorphogenesis promoting effect of *At*BBX21 leading to the hypothesis that M6 may determine the function of the C-terminal domain in light signaling (Job et al., 2018).

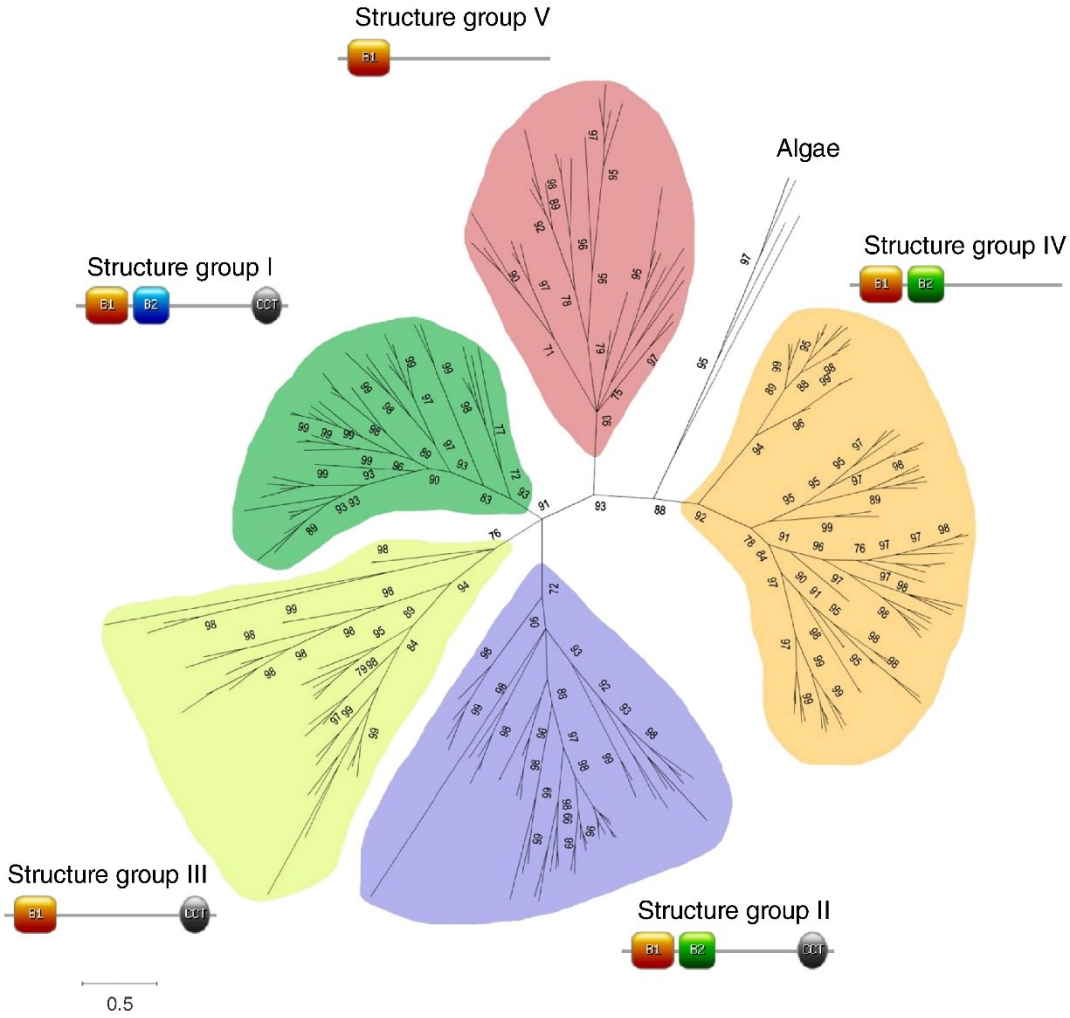

Figure 1. Unrooted Bayesian inference phylogenetic tree for 214 BBX proteins. Full-length proteins of the 214 BBX members were aligned using ClustalW (Thompson et al., 1997). The best-scoring model for the BBX full-length protein alignment was the Dayhoff probability model, with a rate variation among sites calculated as a gamma distribution (+ G). MrBayes (Ronquist and Huelsenbeck, 2003) was used to construct a Bayesian inference phylogenetic tree with 2,000,000 generations. Bootstrap values (> 50%) for this tree are shown on respective branches. The 214 BBX full-length proteins were grouped into five different structure groups (I to IV). A similar tree was obtained with MEGA 5.01 (Tamura et al., 2011) using the neighbor-joining (NJ) method. Schematic diagram of protein domain structures is indicated for each structure group. B1, B-box domain type 1; B2, B-box domain type 2; CCT domain (Crocco & Botto, 2013).

1.2. Function of BBX genes

BBX proteins cover different functions in plant growth and development ranging from the involvement in seedling photomorphogenesis (Fan et al., 2012; Holtan et al., 2011), anthocyanin accumulation, seed germination, carotenoid biosynthesis, hormonal signaling pathways, photoperiodic regulation of flowering (Graeff et al., 2016; Wenkel et al., 2006), shade avoidance (Crocco et al., 2010, 2011) and responses to biotic and abiotic stresses (Kiełbowicz-Matuk et al., 2014; Q. Wang et al., 2013; Vaishak et al., 2019).

Due to their structure characterized by the BBX and the CCT domains, they can play several molecular actions. The BBX domain is involved in protein–protein interaction (Khanna et al., 2009; Qi et al., 2012;Talar & Kiełbowicz-matuk, 2021) and the CCT domain in nuclear localization, DNA binding and protein–protein interaction. It was demonstrated that Arabidopsis BBX protein TOC1 binds DNA via CCT domain (Gendron et al., 2012). Moreover, it was reported that CO can physically interact with the promoter of Flowering Locus T (FT) through the CCT domain (Tiwari et al., 2010; Song et al., 2012; Wenkel et al., 2006; Graeff et al., 2016; Vaishak et al., 2019).

Numerous studies have shown that BBX proteins act as transcription factors or transcriptional regulators, working in parallel and coordinating with other factors in light-controlled seedling development. ELONGATED HYPOCOTYL 5 (HY5) is a member of the bZIP transcription factor family that inhibits hypocotyl growth and lateral root development and promotes pigment accumulation in a light-dependent manner (Gangappa & Botto, 2016). HY5 has been shown to functionally interact with B-box proteins such as *At*BBX21 and *At*BBX22 enhancing its function in promoting photomorphogenesis through a direct physical interaction (Datta, Hettiarachchi, et al., 2007; Datta, Johansson, et al., 2008). On the other hand, *At*BBX24 and *At*BBX25 were found to suppress the same function interacting with HYPOCOTYL 5 HOMOLOG (HYH) (Gangappa et al., 2013).

BBXs and HY5 also play critical roles in flavonoid accumulation. HY5 is induced by light and acts not only directly upregulating the expression of PRODUCTION OF ANTHOCYANIN PIGMENT 1 (PAP1/MYB75) and PRODUCTION OF FLAVONOL GLYCOSIDES 1 and 3 (PFG1/MYB12 and PGF3/MYB111), which activate flavonoid biosynthesis genes, but also directly associating with different promoters of flavonoid biosynthesis genes, such as CHALCONE SYNTHASE (CHS), CHALCONE ISOMERASE (CHI) and LEUCOANTHOCYANIDIN DIOXYGENASE (LDOX), to promote their expression (Gangappa & Botto, 2016). It was shown that *At*BBX21 enhances HY5 expression, with a consequent induction of flavonoid biosynthesis genes and accumulation of anthocyanin (Datta, Hettiarachchi, et al., 2007).

*At*BBX23 associates with the promoter region of CHS through HY5, thus activating the transcription of CHS and EARLY LIGHT INDUCIBLE 2 (ELIP2, a positive regulator of the chlorophyll biosynthesis), suggesting that *At*BBX23 plays a positive role in the control of anthocyanin and chlorophyll accumulation (X. Zhang et al., 2017).

Recently, a study was conducted on a pear homolog of *At*BBX22, *Pirus pirifolia* BBX16 that controls light-induced anthocyanin production activating *Pp*MYB10, a crucial transcription factor for the expression of structural genes in the anthocyanin pathway. *Pp*BBX16 cannot directly bind the promoter of *Pp*MYB10 and requires the presence of *Pp*HY5 to achieve complete functionality. Moreover, *Pp*BBX16 can promote the expression level of anthocyanin-related genes, such as *Pp*CHI and *Pp*CHS as shown in the dual luciferase assay (Bai et al., 2019). *Pp*BBX16 ectopic expression in Arabidopsis determined an increased anthocyanin biosynthesis in the hypocotyls and at the top of the floral stems. Additionally, its overexpression in pear calli increased the anthocyanin biosynthesis only under light conditions, and its transient overexpression in pear fruit resulted in increased anthocyanin accumulation in the peel (Bai et al., 2019).

*At*BBX19 was identified as a negative regulator of flowering time and a suppressor of photomorphogenesis (C. Q. Wang et al., 2014). In addition, a new function as suppressor of germination has recently been proved (M. Bai et al., 2019). Seed germination is governed by two major endogenous hormonal cues that are abscisic acid (ABA) and gibberellic acid (GA), an inhibitor and a promoter of germination, respectively. It was shown that *At*BBX19 binds to GT1, a light-responsive motif presents in the promoter of *ABI5* gene, that codes for a protein implicated in the ABA-dependent arrest of germination. As a consequence of BBX19 binding to GT1, *ABI5* expression is induced with negative effects on seed germination (M. Bai et al., 2019).

BBX proteins have been found to be involved also in shade avoidance. The shade-avoidance syndrome (SAS) includes elongation of vegetative structures, reduction of branching and acceleration of flowering, a consequence of perception of light changes in the environment. Reduction of red to far-red ratio (R:FR) occurring in the environment of plant growing in the shade of neighboring plants are sensed by the phytochrome system triggering changes in plant growth and development. Crocco et al. (2015) demonstrated that PIF4, a key transcription factor in the shade signaling network, is regulated by the interplay between the *At*BBX24 transcriptional regulator and DELLA proteins, which are negative regulators of the gibberellin (GA) signaling.

*At*BBX18 was found to be an essential determinant involved in heat stress (HS) response in higher plants besides promoting hypocotyl elongation under blue light condition through an increase in bioactive GA levels (Wang et al., 2013). In particular, downregulation of *BBX18*

obtained by gene silencing enhanced HS tolerance in Arabidopsis, whereas its over-expression decreased HS tolerance. Indeed, the expression of Hsp101, a heat shock protein playing a crucial role in inducing thermotolerance, was enhanced in BBX18 silenced lines and reduced in BBX18 over-expressing lines compared to that in WT plants (Q. Wang et al., 2013).

A recent study revealed that *Sl*BBX17, the tomato homolog of *At*BBX31, acts as a positive regulator of heat tolerance in tomato (Xu et al., 2022) by reducing ROS accumulation and modulating the expressions of several heat shock proteins under heat stress. Moreover, *Sl*BBX17 overexpression resulted in multiple phenotypes including dwarfism and reduced accumulation of chlorophylls in leaves, indicating that this protein might negatively affect plant growth and development. Even though the expression levels of *Sl*GA20ox1, *Sl*GA20ox2 and *Sl*GA3ox1, which encode key enzymes in the biosynthesis of bioactive GAs, were downregulated in *Sl*BBX17 over-expressing plants, the endogenous contents of GA1 showed no differences between *Sl*BBX17 over-expressing and WT plants. However, exogenous application of bioactive GA3 was able to partially restore the dwarf phenotype (Xu et al., 2022).

The role of the tomato *Sl*BBX20 was recently investigated by producing over-expressing tomato plants (Xiong et al., 2019). *Sl*BBX20-over-expressing plants exhibited elevated carotenoid levels in fruits indicating that *Sl*BBX20 may be a critical regulator of carotenoid biosynthesis and could be a new target for the genetic improvement of the nutritional quality of tomato fruit (Xiong et al., *2019). Sl*BBX20 regulates the expression of phytoene synthase (*PSY1*), which catalyzes the first step of the carotenoid biosynthetic pathway, by directly binding the G-box motif in *PSY1* promoter (Xiong et al., 2019).

One of the most studied physiological processes involving BBX proteins is flowering, so the following section is dedicated to this topic.

1.2.1 Flowering process

In *Arabidopsis thaliana* about 180 genes have been found to be involved in the control of flowering-time based on isolation of loss-of-function mutations or analysis of transgenic plants (Fornara et al., 2010). Many of the genes implicated in the flowering networks act in more than one tissue and in more than one mechanism during floral induction. Four major flowering pathways have been identified in plants, namely photoperiod, autonomous, gibberellin and vernalization pathways (Robertson Mcclung, 2021; Z. Wu et al., 2020;

Mutasa-Göttgens & Hedden, 2009; Kim et al., 2009). Moreover, several additional pathways have recently been integrated such as sugar-, hormone-, and ambient temperature-dependent pathways (Bolouri Moghaddam & van den Ende, 2013; Izawa, 2020; Susila et al., 2018).

The most important aspect of the day-length measurement system is the circadian regulation of *CONSTANS* (*CO*; *At*B*BX1*) transcript level and the light-regulation of CO protein stability and activity (Hayama & Coupland, 2004). *A. thaliana* CONSTANS (*At*CO) was the first BBX gene to be identified and characterized, which belongs to subgroup I and contains two B-box domains and a CCT domain (Putterill et al., 1995). In Arabidopsis, flowering is controlled by photoperiod and is promoted during LD conditions characteristic of spring and early summer. The Arabidopsis *constans* mutant was characterized as defective in flowering response to photoperiod. The mutant lost the capacity to distinguish the photophase, showing a late flowering under LD, but not under short day (SD) conditions (Valverde, 2011). It was successively demonstrated that *At*CO links the circadian clock activity with the regulation of genes controlling shoot meristem identity (Suárez-López et al., 2001).

Under LD conditions, CO mRNA normally accumulates at the end of the light period, and in SD, during the night. The coincidence of CO mRNA expression and exposure of plants to light under LDs stabilizes the CO protein in the nucleus, causing activation of FLOWERING LOCUS T (FT) transcription (Valverde et al., 2004), which is a potent activator of flowering (Kobayashi et al., 1999). CO binds FT promoter through CCT domain (Tiwari et al., 2010), thus inducing FT transcription in the companion cells. FT protein then moves through the vascular tissue to the shoot apex (Turck et al., 2008). After reaching the shoot apex, FT interacts with the bZIP transcription factor FD (FLOWERING LOCUS D) inducing the transition from vegetative to floral meristem (Abe et al., 2005).

A severe delay in the flowering time was obtained in *A. thaliana* plants over-expressing *At*BBX30 and *At*BBX31 (also referred respectively as miP1b and miP1a) grown under LD light regimen (Graeff et al., 2016). miP1a/b have a circadian expression profile and are co-expressed with CO and FT in leaf vasculature system. These miPs belong to the V group of BBX, characterized by the presence of only B1 and a PFVFL motif that allows the interaction with TOPLESS (TPL), a co-repressor protein. Graeff et al. (2016) demonstrated that miPs are able to interact with CO and TPL and suggested that the formation of the trimeric complex

(miP1a/b-CO-TPL) suppresses the CO-mediated induction of FT expression causing the late flowering phenotype observed in miP1a/b over-expressing plants (Graeff et al., 2016).

The relevant role of CO *(i.e., At*BBX1) in photoperiodic induction of flowering prompted to search for BBX1 homologs in other species, including cereals. Homologs of *At*CO have been found in sorghum (*Sorghum bicolor*) and barley (*Hordeum vulgare*) which are LD cereal crops (Campoli et al., 2012; S. Yang et al., 2014; Kikuchi et al., 2012). Under LD conditions, the CO homolog *Sb*Hd1 activates flowering by inducing *Sb*CN8 and *Sb*CN12, two FT-like genes. In barley, *Hv*CO1 and *Hv*CO9 are involved in the activation of FT-like genes required for flowering induction.

In rice, floral transition is promoted under SD condition. Flowering time (also known as ''heading date'' in rice) is determined both by photoperiod and by duration of vegetative growth. Rice possesses two florigen genes, HEADING DATE 3A (Hd3a) and RICE FLOWERING LOCUS T 1 (RFT1), and at least two flowering pathways to regulate the expression of florigens, the Heading date 1 (Hd1) pathway which is conserved between rice and Arabidopsis, and the Early heading date 1 (Ehd1) pathway which is unique to rice (Doi et al., 2004). Hd3a and RFT1, regulate flowering under SD and LD, respectively. In the Hd1 conserved pathway, Hd1 (*Os*BBX18) is homolog of *At*CO and, acts upstream of Hd3a.

Zea mais is another typical SD plant where the BBX gene corresponding to the Arabidopsis CO (Conz1) activates the FT-like ZCN8, which acts as a flowering inducer (Meng et al., 2011; Miller et al., 2008).

In chrysanthemum, three B-box proteins were identified that regulate flowering time in a positive or negative manner. *Cm*BBX8 stimulates flowering in summer-flowering chrysanthemum grown under LD conditions (L. Wang et al., 2019), while *Cm*BBX13 and *Cm*BBX24 proteins cause late flowering under LD and/or SD conditions (Ping et al., 2019; Yang et al., 2014).

The control of flowering in *Solanum lycopersicum* is different from that described in *A. thaliana* and cereals. Tomato is a day-neutral plant, with sympodial architecture in which the branching occurs when the terminal bud ceases to grow (usually because a terminal flower has formed) and an axillary bud or buds become new leader shoots producing many vegetative sympodial/axillary shoots with multi-flowered inflorescences (Figure 2).

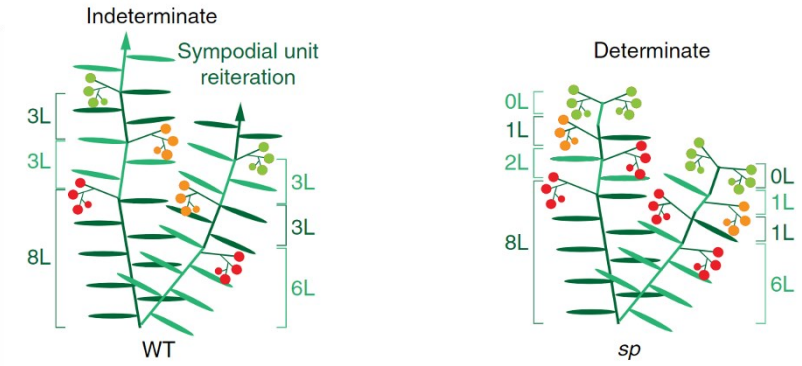

Figure 2. Schematic representation of indeterminate and determinate habitus of tomato (modified from Choon-Tak Kwon et al., 2020)

The upright growth of tomato is manifested by an apparent linear shoot consisting of a reiteration of consecutive sympodial units (SU), each forming three leaves before terminating in a compound inflorescence. In tomato, "indeterminate" growth indicates that plants grow indefinitely by repeating SUs in which flowering and fruiting occurs sequentially, from bottom to top. On the contrary, "determinate" tomato plants progressively reduce the number of leaves in each SUs until terminated in two consecutive inflorescences. The formation of more distal axillary meristems allow growth to continue, with the development of further terminal inflorescences, leading to a bushy, compact plant (Zsögön et al., 2017). Sympodial cycling is mainly controlled by a balance between the activity of two antagonistic genes: flower-promoting (the FT homologue encoding florigen named SINGLE FLOWER TRUSS; SFT) and flower-repressing (SELF-PRUNING; *Sl*SP) (Lifschitz & Eshed, 2014). The maintenance of a proper SFT/SP is essential for sympodial cycling activation, regulating shoot architecture in a quantitative manner (Jiang et al., 2013; Lifschitz & Eshed, 2014) although many other repressive and inducing determinants of flowering have been described in tomato (Silva et al., 2019). *Sl*CO1 and *Sl*CO- like genes have been identified in tomato and an *in-silico* analyses predicted their interaction with some key flowering genes (T. Yang et al., 2020). Nevertheless, till now there is no evidence of an inhibitory flowering complex in tomato similar to that described in Arabidopsis (i.e., the trimeric complex miPs/CO/TPL; Graef et al., 2016).

Interestingly, an acceleration in the formation of SUs was observed in tomato transgenic plants overexpressing TCMP-2, in flower buds before anthesis (this thesis and Molesini et al., 2020) (Appendix B). No differences in the number of leaves below the first inflorescence

were observed between transgenic and WT plants. However, in approximately 70% of the transgenic plants, changes in flowering pattern were noted. For instance, some plants did not show activation of the sympodial cycle in the main shoot but after the primary inflorescence, the shoot terminated with a second inflorescence. This phenotype was associated with an increased expression of SFT on the average doubled in the transgenic lines as compared with WT. In addition, TCMP-2 was proven to physically interact with *Sl*BBX16, the closest homolog of miP1b in Arabidopsis.

2. AIM OF THE WORK

A detailed study of two *Arabidopsis thaliana* microProteins, miP1a and miP1b (respectively *At*BBX30 and *At*BBX31), revealed that these proteins interact with CONSTANS and additionally engage in a larger protein complex involving the co-repressor protein TOPLESS through the PFVFL motif, thus causing a delay in flowering time (Graeff et al., 2016): *A. thaliana* over-expressing miP1a and miP1b showed delayed flowering, whereas an early flowering phenotype was reported in *A. thaliana* *At*BBX30/31 double knock-out mutants (Heng et al., 2019).

In *S. lycopersicum* *Sl*BBX16 and *Sl*BBX17 are the closest homologs of *At*BBX30 and *At*BBX31, respectively. *Sl*BBX16, *Sl*BBX17, *At*BBX30 and *At*BBX31 are members of BBX group V characterized by the presence of only one B-box domain predicted to mediate protein-protein interactions (Gangappa & Botto, 2014; Graeff et al., 2016; Khanna et al., 2009) and by the lack of a CCT domain, which is associated with a role in transcriptional regulation and nuclear transport (Gendron et al., 2012).

Hence, in this section of my thesis we focused on *Sl*BBX17 with the aim to investigate its functional role in reproductive development. We ectopically overexpressed *Sl*BBX17 and its homolog *Sl*BBX16 in *A. thaliana* WT and *At*BBX30/31 double knockout mutant. We also overexpressed *Sl*BBX17 in MicroTom. We use the strong and constitutive CaMV 35S promoter to drive the expression of BBX coding regions to obtain a general and potentially strong effect on the whole plant. The obtainment of these transgenic plants permits us to identify morphological changes in reproductive development. We also studied by Y2H the possible interaction between *Sl*BBX17 and CO and TPL of *A. thaliana* and tomato.

3. MATERIALS AND METHODS

3.1. Preparation of the genetic construct for SlBBX16 and SlBBX17 overexpression

The tomato DNA sequences corresponding to the coding regions of *Sl*BBX17 (*Solyc07g052620*) and of *Sl*BBX16 (*Solyc12g005750*) were amplified by PCR using cDNAs as template. The upstream and downstream primers were designed to introduce at the 5′-terminal end the restriction site for *Kpn*I and at the 3′-terminal end the restriction site for *BamH*I. The primer sequences used are listed in Table S.7 – Appendix A. Amplification products were purified and subsequently subcloned in the pGEM®-T Easy Vector (Promega GmbH, Mannheim, Germany) and checked by sequencing. The recombinant vectors were double digested with *Kpn*I-*BamH*I and the resulting fragments were ligated in a derivative of pBin19 vector, under the control of CaMV35S promoter.

Agrobacterium tumefaciens cells (strain GV2260) were transformed by electroporation with resulting genetic constructs (*35S::SlBBX16; 35S::SlBBX17*) (Figure 3).

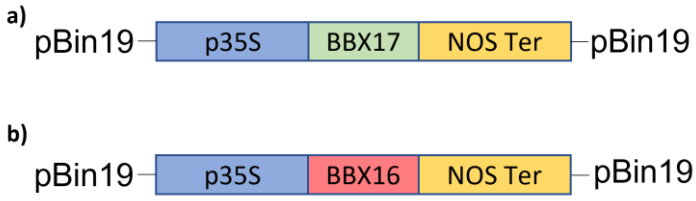

Figure 3. Schematic representation of the genetic cassettes used for plant transformation.

3.2. Floral dip transformation of Arabidopsis plants for the overexpression of SlBBX17 and SlBBX16 and phenotypic analysis

Arabidopsis thaliana WT (ecotype Col-0) and double knock-out mutant *At*bbx30 bbx31 (ecotype Col-0; kindly provided by the Department of Plant and Environmental Sciences University of Copenhagen, Denmark) plants were transformed with the genetic constructs of interest (Figure 3) through the floral dip method (Zhang et al., 2006). The transgenic plants were selected using Kanamycin (50 µg mL^{-1}) in the germination medium (Table S1, Appendix

A). The transgenic state was confirmed by PCR using primers spanning from the CaMV 35S promoter to the *nos* terminator; and the expression of the transgene was evaluated by RT-PCR. Homozygous plants at the T3 generation were used for subsequent phenotypic evaluation. Plants were germinated in pots and maintained in a growth chamber at a constant temperature of 25°C under long-day conditions (16 hr/8 hr light/dark cycle, photosynthetic photon fluence rate of 150 µmol m^{-2} s^{-1} over the waveband 400-700 nm). Number of rosette leaves at bolting and flowering time were measured.

3.3. Yeast Two-Hybrid screen

The Matchmaker Gold Yeast Two-Hybrid System (Clontech) was used to test the interaction between *Sl*BBX17 or a mutated version of *Sl*BBX17 (PFVFL at C-terminal; also referred to as *Sl*BBX16* and *Sl*BBX17*) and *At*CO, *At*TPL, *Sl*CO1 and *Sl*TPL following the manufacturer's instruction with minor modifications. The entire protein coding sequence of *Sl*BBX17 was used as bait and expressed as a fusion to the GAL4 DNA-binding domain in the pGBKT7 vector, and then the recombinant plasmid was introduced into Y2H Gold yeast strain.

Full-length ORFs of *At*CO (*At5g15840*), *At*TPL (*At1g15750*), *Sl*CO1 (*Solyc02g089540*), and *Sl*TPL1 (*Solyc03g117360*), representing the prays, were cloned into pGADT7vector in frame with the GAL4 Activation domain and the resulting recombinant vectors introduced into Y187 yeast strain. For negative controls, pGBKT7 without insert (BD alone; Empty) and pGADT7 without insert (AD alone; Empty) were used. After mating the yeast cells, the cultures were spread on agar plates and then incubated at 30°C for 3 days. Growth of yeast on SD/-Leu/-Trp medium was used as a control for the presence of both recombinant plasmids, and growth of yeast cells on selective medium (SD/-Leu/-Trp/-His/-Ade/X-Gal/Aureobasidin A) plus 10 mM 3-aminotriazole (3-AT) was used to determine positive interactions.

3.4. Agrobacterium-mediated MicroTom genetic transformation and phenotypic analysis

Following the same protocol described in the Chapter 1, paragraph 3.2, T0 transformed plants over-expressing *Sl*BBX17 were obtained. The transgenic state of T0 plants was evaluated by PCR amplifying the entire genetic cassette from the CaMV35S promoter and the *nos t*erminator. *Sl*BBX17 gene expression was evaluated by RT-PCR. The phenotypic analyses were conducted on plants at T1 generation, grown in pots under the greenhouse during autumn 2021. The following parameters were recorded: height of the plants (stem

length up to the first inflorescence), number of leaves before the first inflorescence, number of flowers of the first 4 inflorescences, total number of flowers at anthesis, fruit set and total productivity.

3.5. Genomic DNA extraction

Genomic DNA isolation from Arabidopsis tissues was performed using the "Thermo Scientific™ Phire™ Plant Direct PCR Kit" following the manufacturer's instructions.

For the isolation of genomic DNA from tomato plants, the CTAB buffer was used (2% w/v CTAB, 1.4 M NaCl, 0.2% (v/v) β-mercaptoethanol, 20mM EDTA, 100 mM Tris-HCl pH 8.0, 1% (w/v) polyvinylpyrrolidone) starting from 1 g of fresh tissue.

3.6. RNA extraction and quantitative RT-PCR analysis

Total RNA extraction and qRT-PCR analyses were performed as previously described (Chapter1, paragraph 3.8).

3.7. Phenotypic evaluation

Microtom and Arabidopsis phenotypic analyses were conducted as described in Chapter 1, paragraph 3.9.

3.8 Statistical analysis

Statistical analysis was performed as described in Chapter 1, paragraph 3.13.

4. RESULTS

4.1. Molecular and phenotypic analysis of Arabidopsis over-expressing SlBBX16 or SlBBX17

Considering the phenotype observed in Arabidopsis plants over-expressing *At*BBX30 or *At*BBX31, consisting in a marked delay in flowering time evaluated in terms of number of leaves at bolting (Graeff et al., 2016), we overexpressed *Sl*BBX16 and *Sl*BBX17 in Arabidopsis Col-0 WT and *At*BBX30/31 double knock-out mutant and evaluated the effects on flowering. About 25 plants per line were grown under LD condition and their transgenic state was confirmed by PCR (an example is reported in figure 4a).

*Sl*BBX16 and *Sl*BBX17 expression was checked by RT-PCR using primers covering a portion of the CDS (Figure 4b).

Two *35S::SlBBX17* transgenic lines (#1 and #4) and three *35S::SlBBX16* transgenic lines (#3, #4 and #5) obtained in Col-0 background, and two transgenic lines (#1 and #5) for *35S::SlBBX17* and two (#2 and #3) for *35S::BBX16* obtained in the *At*BBX30/BBX31 double knock-out mutant background (*At*BBX30/31 KO), were selected for subsequent phenotypic analyses.

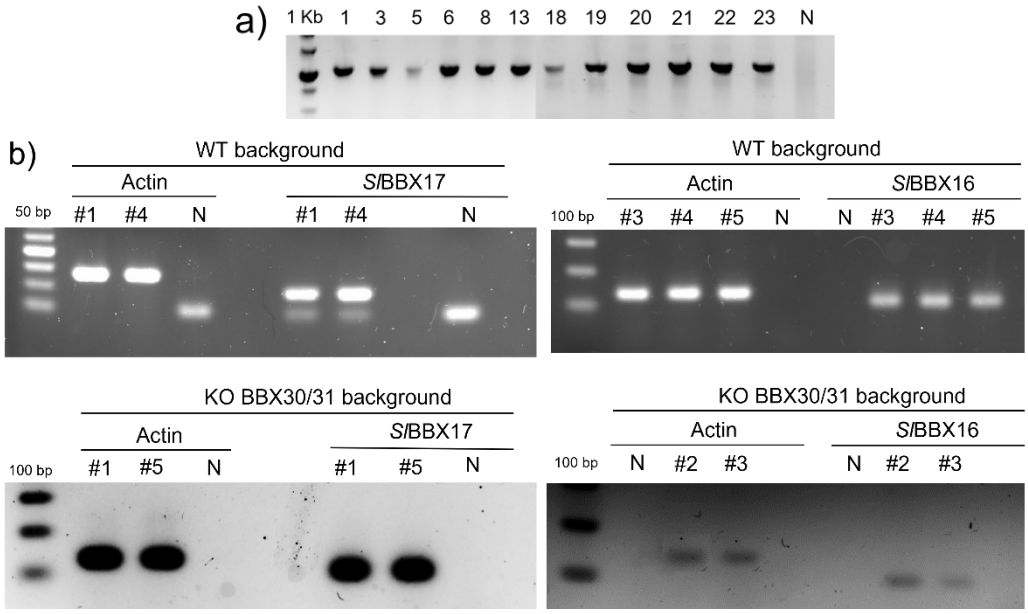

Figure 4. Molecular analysis of SlBBX17 over-expressing Arabidopsis plants. a) A representative 1% agarose gel displaying amplicons corresponding to the correct amplification of the transgenes. The length of the amplicon is 1143 bp. N= not template control. b) 2 % agarose gel showing RT-PCR analysis carried out on 35S::SlBBX16-17 in WT and AtBBX30-31KO genetic background, using primers pairs on actin and BBX16-17 coding sequence. The length of the amplicons is 95 bp for SlBBX17 and 110 bp for SlBBX16. N= not template control.
The molecular ladders used are: 1 kb Promega, 50 bp EuroClone.

The independent *35S::SlBBX17/16* lines were phenotypically characterized comparing them with WT or *At*BBX30/31 KO under LD conditions. Number of rosette leaves at bolting and flowering time, in terms of days between sowing and bolting, were recorded (Figure 5).

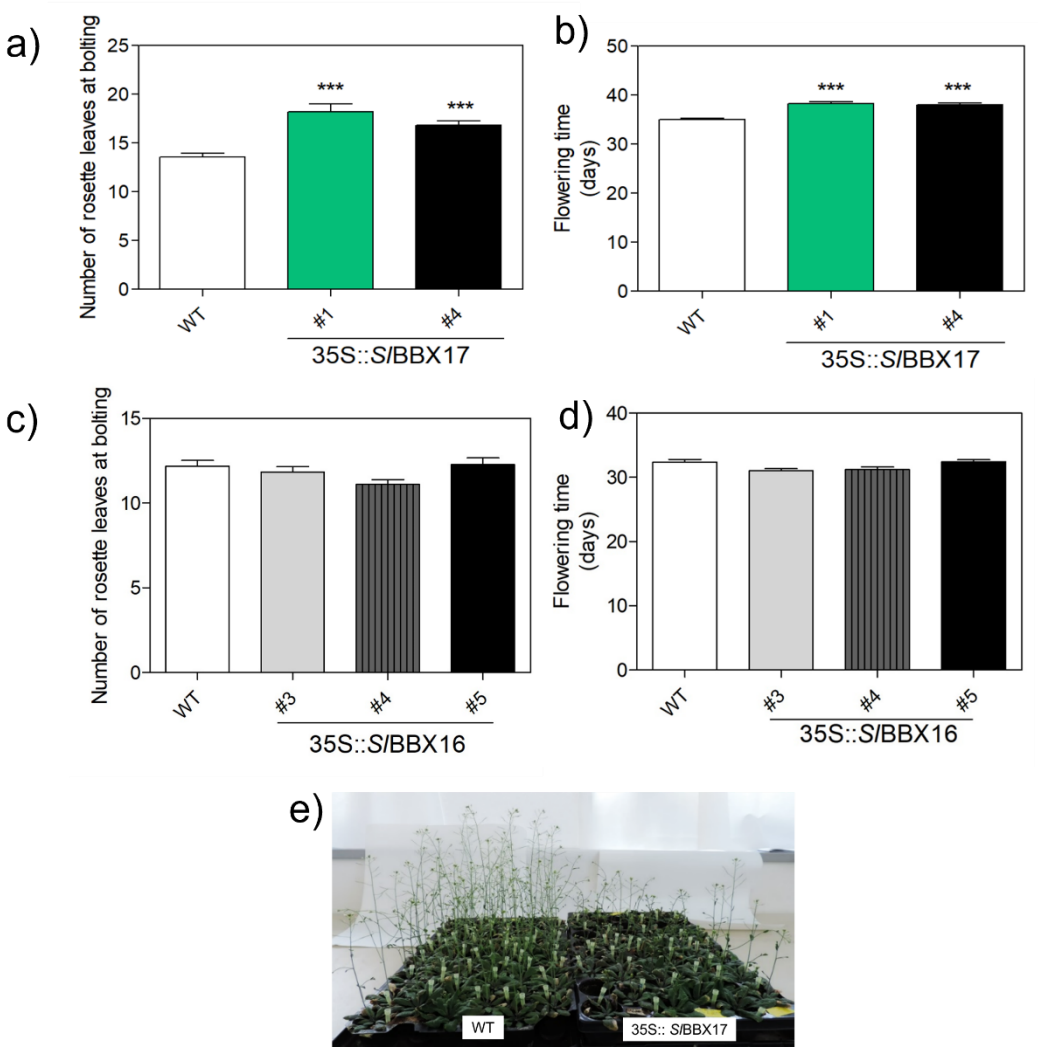

*Figure 5. Phenotypic analysis of Arabidopsis plants over-expressing SlBBX16-17 in Col-0 background. a) and c) Number of rosette leaves produced at bolting. b) and d) Flowering time expressed as time needed to reach bolting starting from germination. e) Picture representative of the delayed flowering phenotype displayed by the 35S::SlBBX17 lines (#1 and #4) compared to WT plant. The values reported in panels (a;b;c;d) are means ± SE (n ≥ 25 plants). Student's t-test was used to compare differences between transgenic and WT plants (***p < 0.001).*

Both the over-expressing *Sl*BBX17 lines in Col-0 background displayed a statistically significant increase in the number of rosette leaves at bolting and in the time to reach flowering (Figure 5a and 5b); on the other hand, none of the *35S::SlBBX16* transgenic lines exhibited alterations in flowering parameters (Figure 5c and 5d). The inhibitory effects on flowering observed in Arabidopsis over-expressing *Sl*BBX17 was less pronounced than that

produced by overexpression of *At*BBX30/31 *in A. thaliana* (Graeff et al., 2016). The *Sl*BBX16 over-expressing plants did not differ from WT ones.

To investigate whether *Sl*BBX16 and *Sl*BBX17 could complement *At*BBX30 and *At*BBX31 function we overexpressed the two genes in the *At*BBX30/31 KO double mutant. Both the over-expressing *Sl*BBX17 transgenic lines displayed a very slight increase in the number of days to reach the flowering transition (Figure 6b), and only one transgenic line (#5) showed an increased number of leaves at bolting.

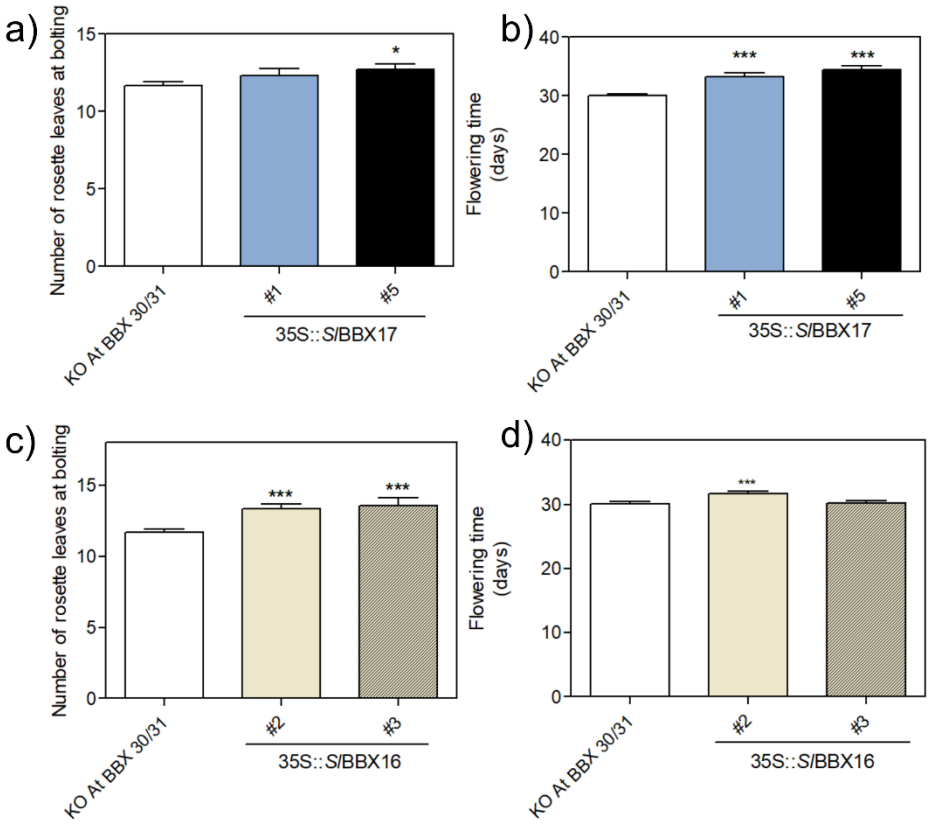

*Figure 6. Phenotypic analysis of Arabidopsis plants over-expressing SlBBX16-17 in AtBBX30-31 KO genetic background. a) and c) Number of rosette leaves produced at bolting in 35S::SlBBX17 or SlBBX16, respectively. b) and d) Flowering time expressed as time needed to reach bolting starting from germination. The values reported in all panels are means ± SE (n ≥ 20 plants). Student's t-test was used to compare differences between transgenic and WT plants (*p < 0.05; ***p < 0.001).*

The two *Sl*BBX16 transgenic lines displayed a slight increase in rosette leaves number at bolting (Figure 6c) but only in line #2 this increase was associated with the augmented number of days needed to reach the flower transition (Figure 6d). These data hint that the tomato *Sl*BBX16 and *Sl*BBX17 can have an influence on the transition to flowering but cannot fully replace the function of *At*BBX30/31.

4.2. Analysis of BBX16 and BBX17 interaction with components of the Arabidopsis flowering repressor complex

The phenotype exhibited by *35S::SlBBX17* resembles, in an attenuated form, the phenotype shown by over-expressing *At*BBX30/31 plants (Graeff et al.,2016).

Thus, we have investigated by Y2H whether *Sl*BBX16 and *Sl*BBX17 could interact with *At*CO and *At*TPL to test whether *Sl*BBX16/17 could participate in the formation of a trimeric complex, similar to that described by Graeff et al., 2016 (Figure 7a). *Ad hoc* Y2H using *Sl*BBX16 and *Sl*BBX17 as a bait and *At*CO and/or *At*TPL as preys, was performed. No interaction was detected after mating the transformed yeast cells (Figure 7c and d). The interaction between *At*BBX30-31 with *At*CO and *At*TPL of Arabidopsis is mediated by the presence of the aa motif PFVLF at the C terminus of *At*BBXs proteins (Graef et al., 2016). Since in *Sl*BBX16 and *Sl*BBX17, the PFVLF motif is replaced by PFLFL and LFLFI, respectively, we performed the Y2H also using mutated versions of *Sl*BBXs obtained by changing the PFLFL and LFLFI motives in PFVLF (Figure 7b, e and f). No interaction between the mutated *Sl*BBXs and *At*CO and *At*TPL seems to occur (Figure 7e and f).

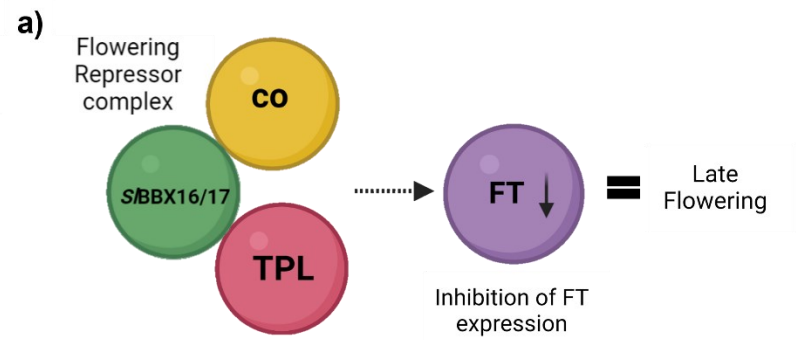

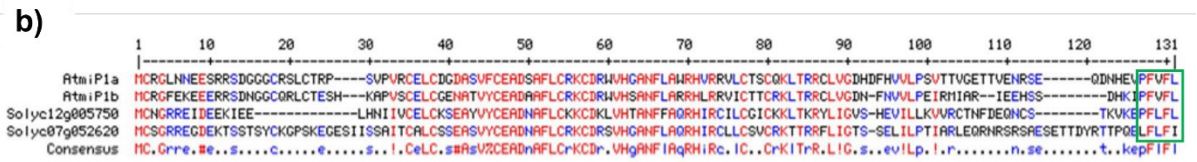

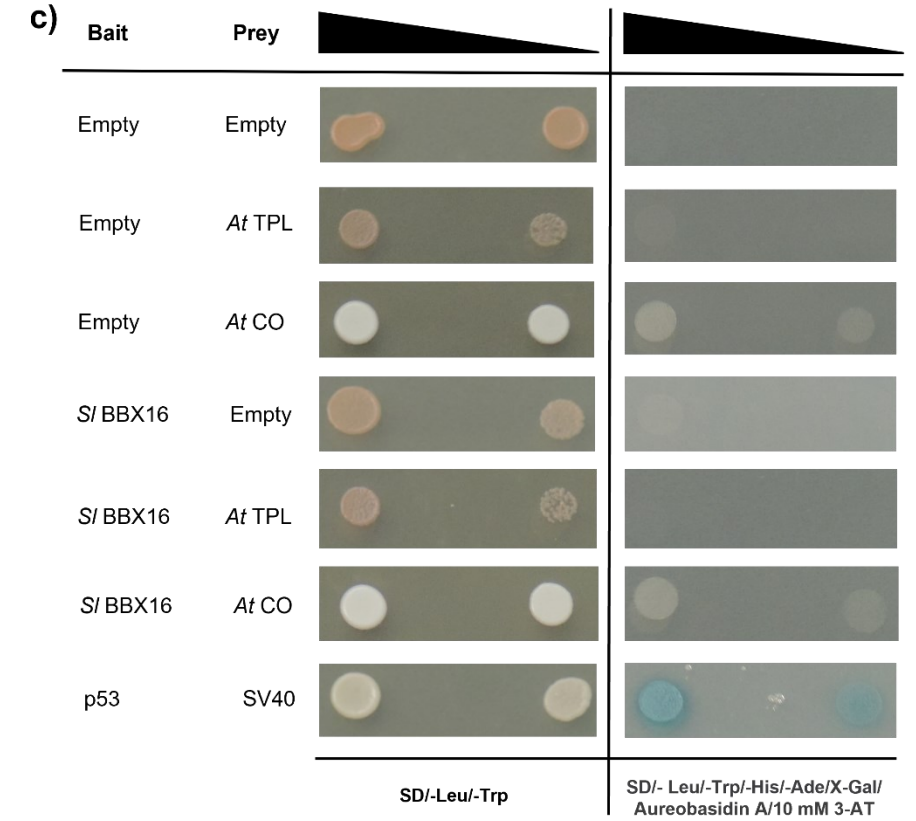
c)
Bait
Prey
Empty
Empty
Empty
At TPL
Empty
At CO
Sl BBX16
Empty
Sl BBX16
At TPL
Sl BBX16
At CO
p53
SV40
SD/-Leu/-Trp
SD/- Leu/-Trp/-His/-Ade/X-Gal/
Aureobasidin A/10 mM 3-AT

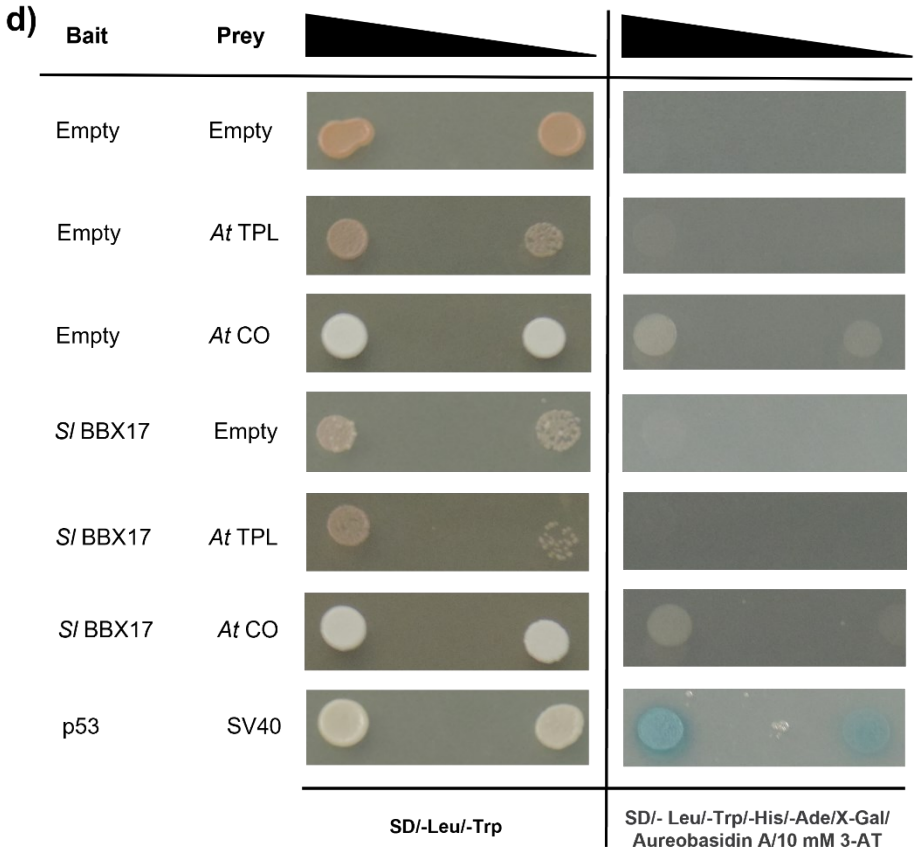
d)
Bait
Prey
Empty
Empty
Empty
At TPL
Empty
At CO
Sl BBX17
Empty
Sl BBX17
At TPL
Sl BBX17
At CO
p53
SV40
SD/-Leu/-Trp
SD/- Leu/-Trp/-His/-Ade/X-Gal/
Aureobasidin A/10 mM 3-AT

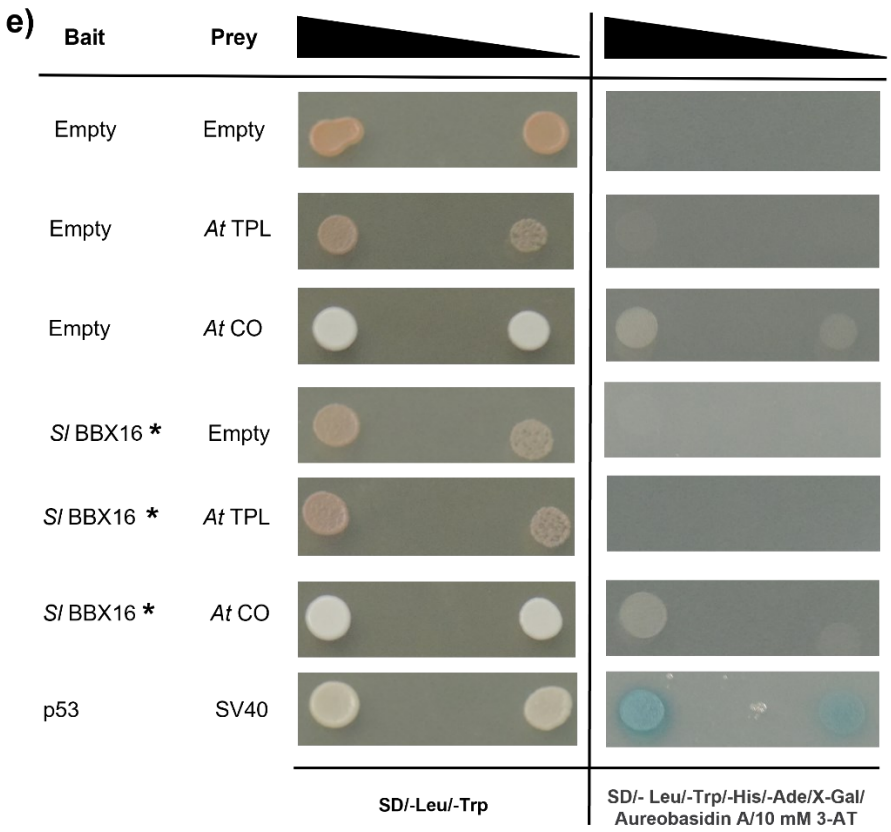
e)
Bait
Prey
Empty
Empty
Empty
At TPL
Empty
At CO
Sl BBX16 *
Empty
Sl BBX16 *
At TPL
Sl BBX16 *
At CO
p53
SV40
SD/-Leu/-Trp
SD/- Leu/-Trp/-His/-Ade/X-Gal/
Aureobasidin A/10 mM 3-AT

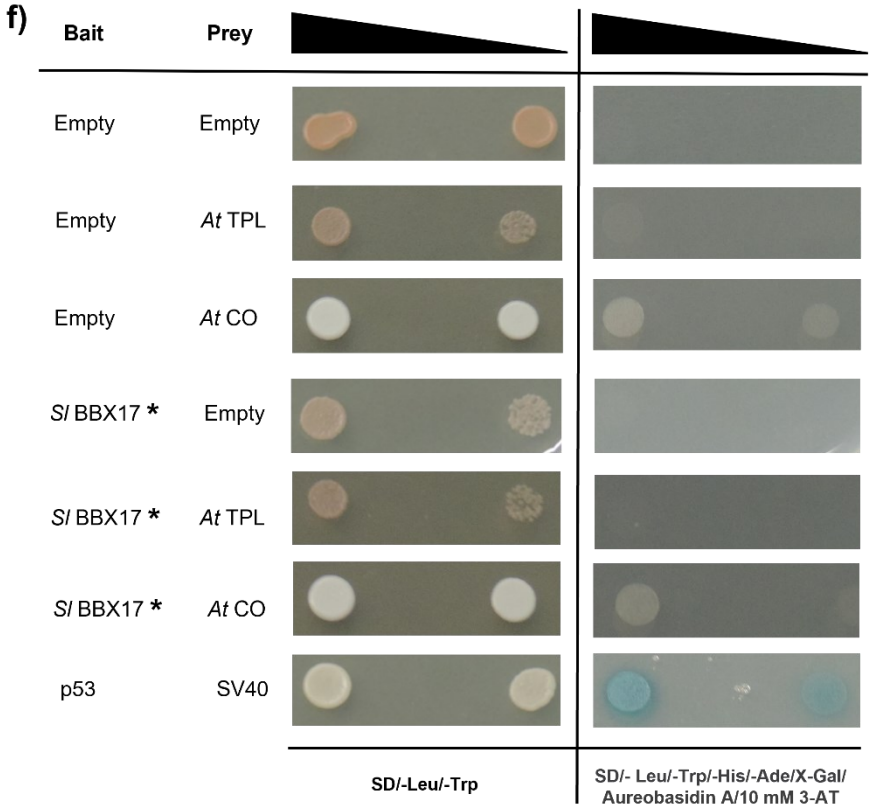
f)
Bait
Prey
Empty
Empty
Empty
At TPL
Empty
At CO
Sl BBX17 *
Empty
Sl BBX17 *
At TPL
Sl BBX17 *
At CO
p53
SV40
SD/-Leu/-Trp
SD/- Leu/-Trp/-His/-Ade/X-Gal/
Aureobasidin A/10 mM 3-AT

Figure 7. Y2H analysis of the interaction between SlBBX16-17 and AtCO and AtTPL. a) representative model of protein interaction between AtBBX30/31, CO and TPL based on the findings proposed by Graeff et al.2016. b) Alignment created by Multalign (Corpet, 1988) of the SlBBX16 (Solyc12g005750), SlBBX17 (Solyc07g052620), AtmiP1a (AtBBX30), and AtmiP1b (AtBBX31) proteins. Conserved residues are coloured in red (high consensus level 90%) and in blue (low consensus level 50%). A position with no conserved residues is represented by a dot in the consensus line. The consensus symbols are ! (I/V), % (F/Y), and # (N/D/E). c) Y2H interaction assay between SlBBX16 and AtCO and AtTPL. d) Y2H interaction assay between AtBBX17 and AtCO and AtTPL. e) Y2H interaction assay between mutated SlBBX16 and AtCO1 and AtTPL. f) Y2H interaction assay between mutated SlBBX17 and AtCO and AtTPL1. For negative controls, pGBKT7 without insert (BD alone; Empty), pGADT7 without insert (AD alone; Empty), were used. For each protein-protein interaction, two increasing dilutions of the mated cultures were used (10^{-2} and 10^{-3}) and spotted on control medium (SD/-Leu/-Trp) and on selection medium plates (SD/-Leu/-Trp/-His/-Ade/X-Gal/Aureobasidin A/10 mM 3-AT). Interaction of p53 with SV40 was used as a positive control of the mating system.

4.3. *Functional analysis of SlBBX17 in tomato*

4.3.1 SlBBX17 expression pattern analysis in MicroTom

To improve our knowledge of the possible involvement of *Sl*BBX17 in the flower/fruit development of tomato, we at first carried out the expression analysis of *Sl*BBX17 in different organs of MicroTom plants (Figure 8). *Sl*BBX17 is expressed in all the floral organs (i.e., young fruit, ovary, and petals) and leaves. Concerning the floral organs, a high expression level was recorded in the anthers (i.e., 200 folds higher than that in the other organs) (Figure 8).

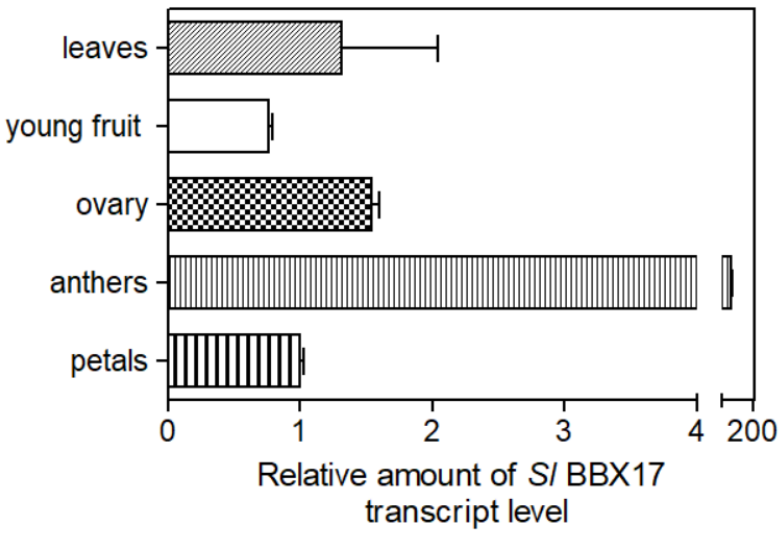

Figure 8. Expression analysis of SlBBX17 in WT MicroTom organs. The values reported are means ± SE (n = 3). Each biological sample represents a pool of organs collected from three different plants. The floral organs were dissected from flowers at anthesis, young fruit was sampled at the 0.5 cm diameter. The expression level in petals was used as calibrator.

4.3.2. Overexpression of SlBBX17 in MicroTom plants

From the genetic transformation of the MicroTom plants with the *35S::SlBBX17* construct (Figure 3.1), we obtained 19 putatively transformed plants that were acclimatized in the greenhouse and molecularly analyzed for the determination of the transgenic state. By PCR analysis we confirmed that 15 independent transgenic plants contain the entire cassette. In figure 9a, a representative agarose gel image of several transgenic lines is reported. The expression of *Sl*BBX17 was evaluated in the PCR positive plants by RT-PCR (data do not show). Three independent lines (#11, # 15 and #18) were selected for the subsequent phenotypic and molecular analysis (Figure 9b).

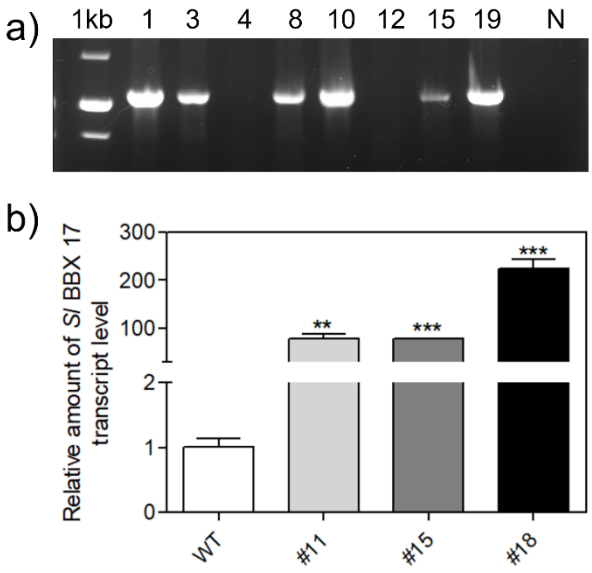

*Figure 9. Molecular analysis of SlBBX17 in WT and 35S::BBX17 MicroTom plants. a) Evaluation of transgenic state. A representative 1% agarose gel displaying amplicons corresponding to the correct amplification of the transgene.b) qRT-PCR analysis of SlBBX17 expression in WT and transgenic plant. The values reported are means ± SE (n = 3). Each biological represents a pool of leaves collected from 5-8 plants. The SlBBX17 transcript level in WT was used as calibrator. Student's t-test was used for the statistical analysis (**P < 0.01; ***P < 0.001).*

The phenotypic analysis was carried out in T1 on about 5-8 individuals per transgenic line and WT (cv MicroTom TOMJPF00001). Height of the plants (stem length up to the first inflorescence), number of leaves before the first inflorescence, number of flowers at anthesis, number of flowers in the first 4 inflorescences, fruit set, total productivity and ripening were recorded (Figure 10).

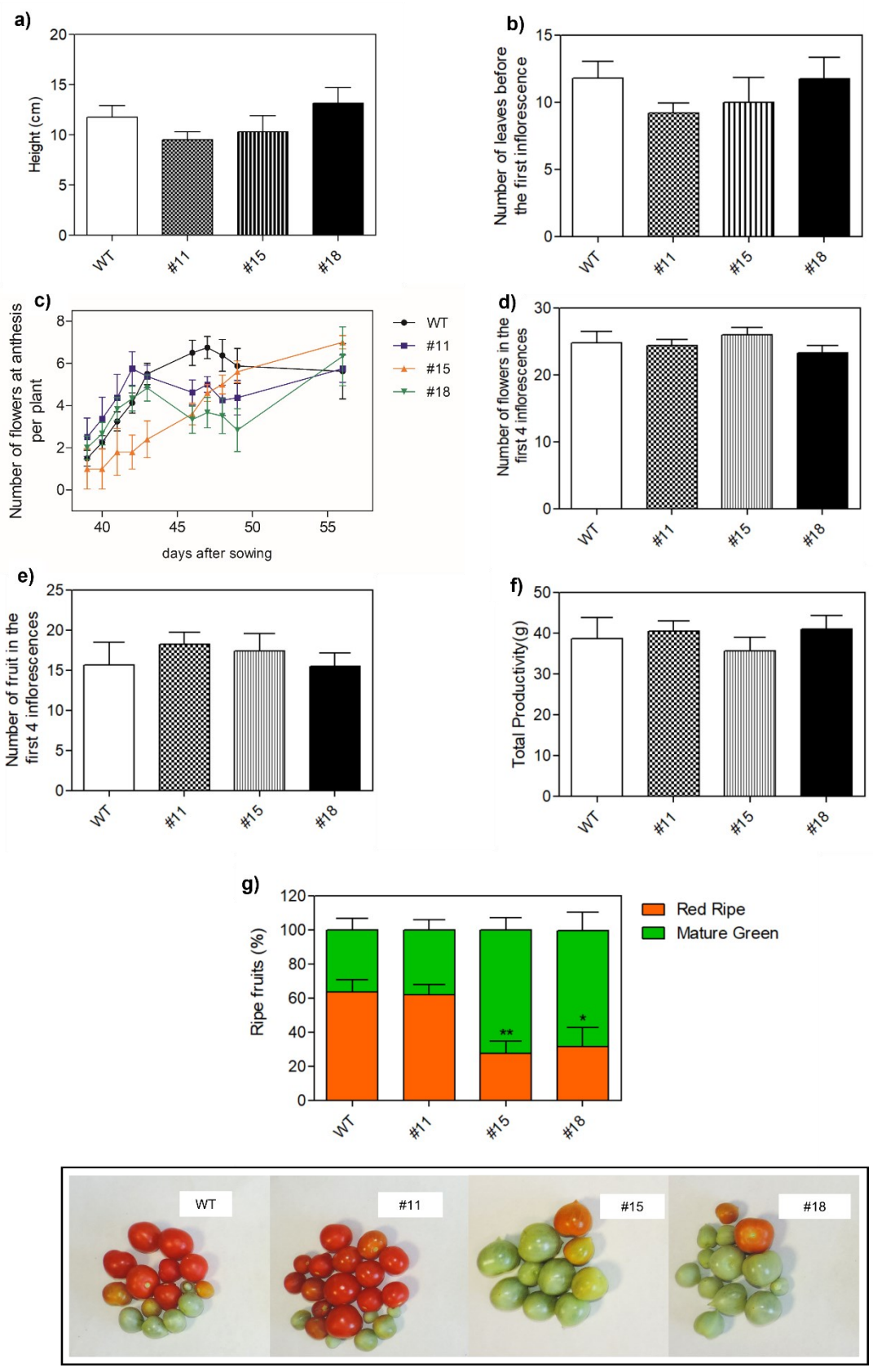

Figure 10. Phenotypic analysis of T1 MicroTom over-expressing SlBBX17. a) shoot height (cm) measured 48 days fter sowing; b) number of leaves before the first inflorescence; c) number of flowers per plant from 39 to 56 days after sowing; d) number of flowers in the first 4 inflorescences per plant; e) number of fruits in the first 4 inflorescences per plant; f) total productivity; g) percentage of ripe fruits collected 4 months after sowing. The

*values reported are means ± SEM (n= 5-7). Student's t-test was used for the statistical analysis (*P < 0.05; **P < 0.01).*

The height and number of leaves before the first inflorescence showed no significant differences in transgenic plants compared with WT (Figure 10a and b). More interestingly, the total number of flowers counted at the anthesis denoted similar initial flower production for WT and over-expressing plants, but in the transgenic lines, a subsequent decline in flower development was noticed between 46 and 48 days after sowing (Figure 10c). Nevertheless, no statically significant results were appreciable in the total number of flowers considering the first four inflorescences and the number of fruits derived from the same inflorescences (Figure 10d and e). The total fruit productivity seems unaffected by the transgene overexpression (Figure 10f). However, a marked delay in fruit development, manifested by the reduced number of ripe fruits collected 4 months after sowing, was observed in two (i.e., #15, and #18) out of three over-expressing lines compared to the WT (Figure 10g).

4.4. Functional analysis of SlBBX17 in tomato

As mentioned before (Chapter 1, this thesis) transgenic plants (pTCMP-2::TCMP-1) with an increased TCMP-2 expression in flower buds before anthesis displayed anticipated shoot termination, which is synonymous with early flowering. In addition, we proved (Chapter 1, this thesis) that TCMP-2 was able to interact with *At*BBX30, *Sl*BBX16 and *Sl*BBX17 (Molesini et., 2020, Chapter 1 this thesis) and that its overexpression in Arabidopsis caused early flowering. We can hypothesize that TCMP-2 can favor FT expression by sequestering *At*BBX30, thus inhibiting the formation of the trimeric repressor complex with TPL (Figure 11a).

We have analyzed by Y2H the possible interaction between TCMP-2 and *Sl*CO1 and *Sl*TPL (Figure 11b) as well as the interaction between *Sl*BBX17 and *Sl*CO1 and *Sl*TPL (Figure 11c) with the purpose of verifying the formation in tomato of a trimeric complex similar to that described in Arabidopsis (Graeff et al., 2016).

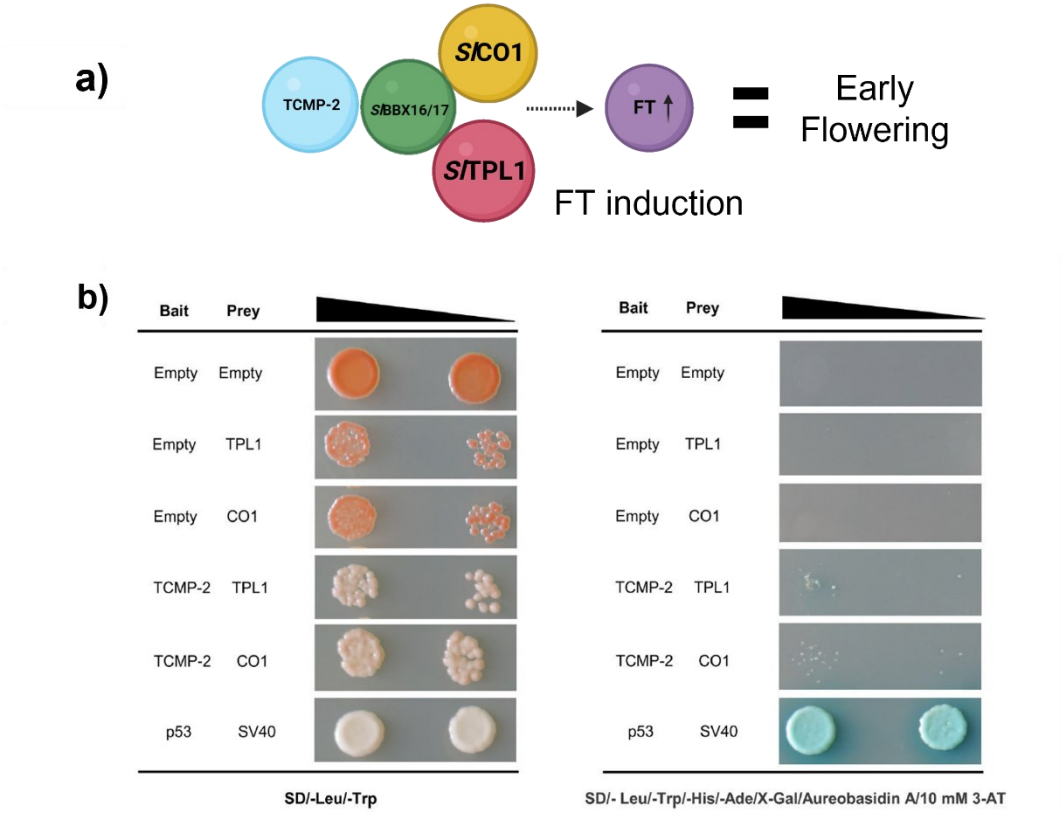
a)
TCMP-2
SlBBX16/17
SlCO1
SlTPL1
FT
Early Flowering
FT induction
b)
Bait
Prey
Empty Empty
Empty TPL1
Empty CO1
TCMP-2 TPL1
TCMP-2 CO1
p53 SV40
SD/-Leu/-Trp
SD/- Leu/-Trp/-His/-Ade/X-Gal/Aureobasidin A/10 mM 3-AT
c)
Bait
Prey
Empty Empty
Empty Sl TPL1
Empty Sl CO1
Sl BBX17 Empty
Sl BBX17 Sl TPL1
Sl BBX17 Sl CO1
p53 SV40
SD/-Leu/-Trp
SD/- Leu/-Trp/-His/-Ade/X-Gal/
Aureobasidin A/10 mM 3-AT

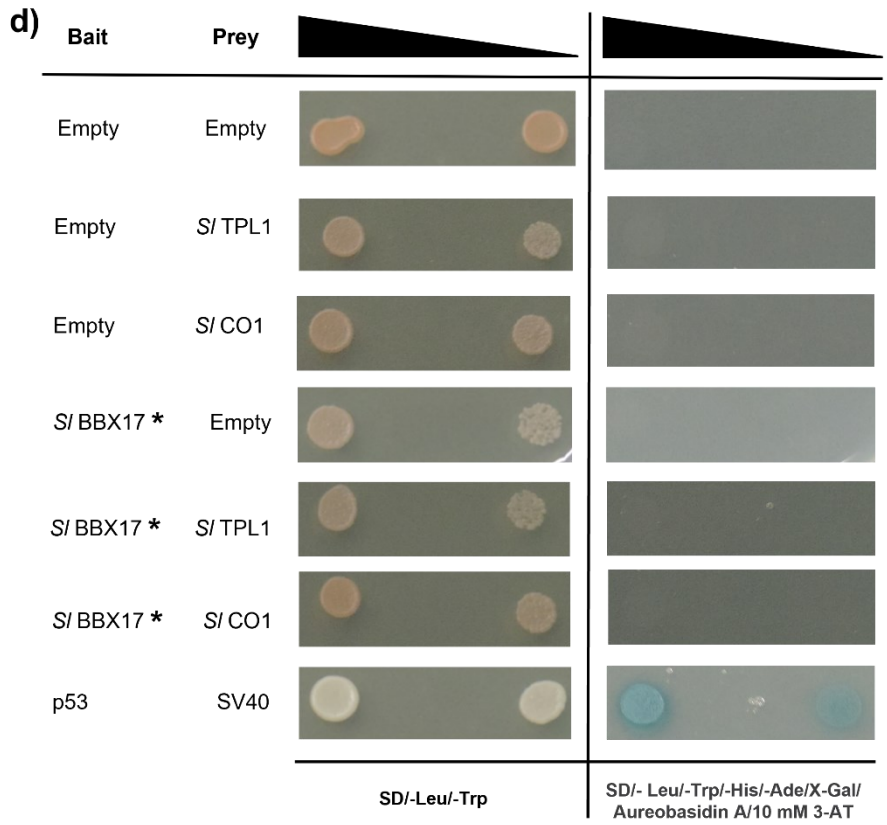

Figure 11. Y2H analysis of the interaction between SlBBX16-17 and SlCO1 and SlTPL1. a) Hypothetical model of proteins interactions in tomato. b) Y2H interaction assay between TCMP-2 and SlCO1 and SlTPL1. c) Y2H interaction assay between SlBBX17 and SlCO1 and SlTPL1. d) Y2H interaction assay between mutated SlBBX17 and SlCO1 and SlTPL1. For negative controls, pGBKT7 without insert (BD alone; Empty), pGADT7 without insert (AD alone; Empty), were used. For each protein-protein interaction, two increasing dilutions of the mated cultures were used (10^{-2} and 10^{-3}) and spotted on control medium (SD/-Leu/-Trp) and on selection medium plates (SD/-Leu/-Trp/-His/-Ade/X-Gal/Aureobasidin A/10 mM 3-AT). Interaction of p53 with SV40 was used as a positive control of the mating system.

TCMP-2 and *SlBBX*17 were fused in frame with the binding domain (BD) of the GAL4 transcription factor and *Sl*CO1 and *Sl*TPL1 were fused to the activation domain (AD). The results indicate that neither TCMP-2 nor *Sl*BBX17 can directly bind neither *Sl*CO1 nor *Sl*TPL1 (Figure 11b and 11c).

The interaction between *At*BBX30-31 with *At*CO and *At*TPL of Arabidopsis is mediated by the presence of the aa motif PFVLF at the C terminal amino of *At*BBXs (Graeff et al., 2016). Since *Sl*BBX17 contains a LFLFI motif instead of PFVLF, we generated a mutated version of *Sl*BBX17 protein, where the LFLFI motif is replaced by PFVLF (Figure 7b). We performed the Y2H also using this mutated version as bait; nevertheless, our results reveal that not even the mutated form of *Sl*BBX17 is able to interact with *Sl*CO1 and *Sl*TPL1 (Figure 11d).

5. DISCUSSION

BBX proteins are a class of zinc-coordinated transcription factors or regulators that not only directly mediate the transcription of target genes but also interact with various other factors to create a complex regulatory network involved in the control of plant growth and development (Graeff et al., 2016; Yadav et al., 2019). BBX genes are evolutionarily conserved in various plant species and fulfill distinct functions in regulating plant developmental processes including seedling photomorphogenesis, anthocyanins biosynthesis, photoperiodic regulation of flowering, and hormonal pathways (Crocco & Botto, 2013). Several BBX proteins are involved in biotic and abiotic stress responses (Q. Wang et al., 2013; Xu et al., 2022). A unique domain structure identifies BBX proteins, which is defined by the presence of one or two B-Box motif, predicted to mediate protein-protein interaction; an additional CCT motif, which is associated with a role in transcriptional regulation and nuclear transport, can be present (Gendron et al., 2012). Based on the presence of these specific domains, BBX proteins are classified into five structural groups.

Arabidopsis is the plant model system for LD flowering plants and numerous studies were conducted to elucidate the transition from the vegetative phase to the reproductive stage, identifying at least four major pathways, which regulate this intricate process. Flowering time is controlled by the photoperiodic regulation of the BBX protein CONSTANS (CO; *At*BBX1), whose mRNA level accumulates at the end of the light period under LD and during the night in SD. CO protein is stabilized in the nucleus by the light during LDs, causing the subsequent activation of FLOWERING LOCUS T (FT) transcription (Valverde et al., 2004), which is a potent activator of flowering (Kobayashi et al., 1999).

Recently, two BBX microproteins, named *At*BBX31 and *At*BBX30 (also referred to as *At*mip1a and *At*mip1b, respectively have been shown to interfere in the Arabidopsis flowering process under LD conditions (Graeff et al., 2016). These *At*miPs belong to the fifth group in the BBX classification proposed by Khanna et al., (2009) which is characterized by proteins that possess only one B-Box domain in their sequence. The B-Box motif is responsible for protein-protein interaction: indeed, it permits the binding between *At*CO and *At*miP1a/b. Moreover, the PFVFL motif present at the C-terminus of the amino acid sequence of *At*miP1a permits its interaction with TOPLESS (TPL), a co-repressor flowering protein. Thus, a trimeric repressor complex is formed which results in a decrease in the transcription of FT, causing

an extreme delayed phenotype in Arabidopsis plants over-expressing miPs under inductive LD conditions (Figure 7a).

Solanum lycopersicum is a day neutral plant and the mechanism controlling the flowering process in this species is not completely elucidated. The closest homologs of *At*BBX30 and *At*BBX31 in tomato are *Sl*BBX16 and *Sl*BBX17, respectively.

In this thesis, to gain further insight into tomato BBX, we constitutively overexpress *Sl*BBX16 and *Sl*BBX17 in *Arabidopsis* Col-0 WT and in the double *At*BBX30/31 KO mutant backgrounds. In both backgrounds, the overexpression of *Sl*BBX17 influences the flower transition, leading to a slight delay in the flowering time and an increased number of leaves before the first inflorescence (Figure 5a and b), although much less marked if compared with the phenotype displayed by Arabidopsis plants over-expressing the endogenous *At*BBX30 (miP1a). On the other hand, no significant differences were detected in the over-expressing *Sl*BBX16 plants in WT background (Figure 5c and d) while a slight increase in the number of rosette leaves at bolting was observed when *Sl*BBX16 was overexpressed in the double *At*BBX30/31 KO mutant background (Figure 6c and d). It is possible that the tomato BBX16/17 cannot efficiently interact with *At*CO and *At*TPL. Indeed, this hypothesis was strengthened by the results obtained by Y2H (Figure 7c). Additional Y2H assays using mutated versions of *Sl*BBX16/17, suggested that the lack of interaction was not due to the absence of the 5 amino-acid long PFVFL motif present in C-terminal region of the endogenous *At*BBX30/31 protein (Figure 7d). Further analyses will be necessary to corroborate the absence of interactions between *Sl*BBX16/17 and *At*CO/*At*TPL using independent *in vitro* or *in vivo* techniques.

The functional role of *Sl*BBX17 was studied by its overexpression in MicroTom, focusing on reproductive development on the basis of its interaction with TCMP-2 and its pattern of expression in the floral organs. The overexpression of *Sl*BBX17 in MicroTom resulted in some alterations in the flower/fruit development (Figure 10). The formation of the first inflorescence was not delayed as proved by the unchanged number of leaves below the first flower truss in comparison to WT. However, the development of the successive inflorescences was successively slowed, and a delay was also observed in fruit development since a lower percentage of ripe fruits was detected in the transgenic plants (Figure 10g). These results are in accordance with the observation reported in an indeterminate tomato

cultivar, where over-expression of *Sl*BBX17 caused a delay in the formation of the first visible flower buds (Xu et al., 2022).

The effects of *Sl*BBX17 overexpression on flowering in tomato are opposite to the precious termination observed when the *Sl*BBX-interacting partner, i.e., TCMP-2, was overexpressed in flower buds. This suggests that the interaction of these two proteins can be related to the control of flowering pattern in tomato. Our Y2H analysis seems to exclude that TCMP-2 and *Sl*BBX17 can form a complex with *Sl*CO1 and *Sl*TPL1 (Figure 11). In this regard, since the function of CO1 and CO-like in tomato has been poorly investigated (T. Yang et al., 2020), it will be interesting to explore the activity of other members of this family in tomato reproductive development and their possible interaction with TCMP-2 and *Sl*BBX17.

In addition, further investigations on the role in flowering and fruiting of *Sl*BBX16, the closet homolog of *Sl*BBX17, may allow us to draw a clear picture of the function of BBXs belonging to the group V in tomato.

6. BIBLIOGRAFY

Abe, M., Kobayashi, Y., Yamamoto, S., Daimon, Y., Yamaguchi, A., Ikeda, Y., Ichinoki, H., Notaguchi, M., Goto, K., & Araki, T. (2005). FD, a bZIP protein mediating signals from the floral pathway integrator FT at the shoot apex. *Science (New York, N.Y.)*, *309*(5737), 1052–1056. https://doi.org/10.1126/SCIENCE.1115983

Bai, M., Sun, J., Liu, J., Ren, H., Wang, K., Wang, Y., Wang, C., & Dehesh, K. (2019). *The B-box protein BBX19 suppresses seed germination via induction of ABI5*. https://doi.org/10.1111/tpj.14415

Bai, S., Tao, R., Tang, Y., Yin, L., Ma, Y., Ni, J., Yan, X., Yang, Q., Wu, Z., Zeng, Y., & Teng, Y. (2019). *BBX16, a B-box protein, positively regulates light-induced anthocyanin accumulation by activating MYB10 in red pear*. https://doi.org/10.1111/pbi.13114

Bolouri Moghaddam, M. R., & van den Ende, W. (2013). Sugars, the clock and transition to flowering. *Frontiers in Plant Science*, *4*(FEB), 22. https://doi.org/10.3389/FPLS.2013.00022/BIBTEX

Campoli, C., Drosse, B., Searle, I., Coupland, G., & von Korff, M. (2012). Functional characterisation of HvCO1, the barley (Hordeum vulgare) flowering time ortholog of CONSTANS. *The Plant Journal : For Cell and Molecular Biology*, *69*(5), 868–880. https://doi.org/10.1111/J.1365-313X.2011.04839.X

Cao, Y., Han, Y., Meng, D., Li, D., Jiao, C., Jin, Q., Lin, Y., & Cai, Y. (2017). B-BOX genes: Genome-wide identification, evolution and their contribution to pollen growth in pear (Pyrus bretschneideri Rehd.). *BMC Plant Biology*, *17*(1), 1–12. https://doi.org/10.1186/S12870-017-1105-4/FIGURES/7

Chan, E. K. L., Hamel, J. C., Buyon, J. P., & Tan, E. M. (1991). Molecular definition and sequence motifs of the 52-kD component of human SS-A/Ro autoantigen. *The Journal of Clinical Investigation*, *87*(1), 68–76. https://doi.org/10.1172/JCI115003

Chang, C. S. J., Li, Y. H., Chen, L. T., Chen, W. C., Hsieh, W. P., Shin, J., Jane, W. N., Chou, S. J., Choi, G., Hu, J. M., Somerville, S., & Wu, S. H. (2008). LZF1, a HY5-regulated transcriptional factor, functions in Arabidopsis de-etiolation. *The Plant Journal : For Cell and Molecular Biology*, *54*(2), 205–219. https://doi.org/10.1111/J.1365-313X.2008.03401.X

Chu, Z., Wang, X., Li, Y., Yu, H., Li, J., Lu, Y., Li, H., & Ouyang, B. (2016). Genomic organization, phylogenetic and expression analysis of the B-Box gene family in tomato. *Frontiers in Plant Science*, *7*(OCTOBER2016), 1552. https://doi.org/10.3389/FPLS.2016.01552/BIBTEX

Crocco, C. D., & Botto, J. F. (2013a). BBX proteins in green plants: insights into their evolution, structure, feature and functional diversification. *Gene*, *531*(1), 44–52. https://doi.org/10.1016/J.GENE.2013.08.037

Crocco, C. D., Holm, M., Yanovsky, M. J., & Botto, J. F. (2011). Function of B-BOX under shade. *Plant Signaling & Behavior*, *6*(1), 101–104. https://doi.org/10.4161/psb.6.1.14185

Datta, S., Hettiarachchi, C., Johansson, H., & Holm, M. (2007). *SALT TOLERANCE HOMOLOG2, a B-Box Protein in Arabidopsis That Activates Transcription and Positively Regulates Light-Mediated Development W*. https://doi.org/10.1105/tpc.107.054791

Datta, S., Johansson, H., Hettiarachchi, C., Irigoyen, M. L., Desai, M., Rubio, V., & Holm, M. (2008). *LZF1/SALT TOLERANCE HOMOLOG3, an Arabidopsis B-Box Protein Involved in Light-Dependent Development and Gene Expression, Undergoes COP1-Mediated Ubiquitination W*. https://doi.org/10.1105/tpc.108.061747

de Thé, H., Lavau, C., Marchio, A., Chomienne, C., Degos, L., & Dejean, A. (1991). The PML-RARα fusion mRNA generated by the t(15;17) translocation in acute promyelocytic leukemia encodes a functionally altered RAR. *Cell*, *66*(4), 675–684. https://doi.org/10.1016/0092-8674(91)90113-D

Doi, K., Izawa, T., Fuse, T., Yamanouchi, U., Kubo, T., Shimatani, Z., Yano, M., & Yoshimura, A. (2004). Ehd1, a B-type response regulator in rice, confers short-day promotion of flowering and controls FT-like gene expression independently of Hd1. *Genes & Development*, *18*(8), 926. https://doi.org/10.1101/GAD.1189604

Fan, X. Y., Sun, Y., Cao, D. M., Bai, M. Y., Luo, X. M., Yang, H. J., Wei, C. Q., Zhu, S. W., Sun, Y., Chong, K., & Wang, Z. Y. (2012). BZS1, a B-box protein, promotes photomorphogenesis downstream of both brassinosteroid and light signaling pathways. *Molecular Plant*, *5*(3), 591–600. https://doi.org/10.1093/MP/SSS041

Fornara, F., de Montaigu, A., & Coupland, G. (2010). SnapShot: Control of flowering in arabidopsis. *Cell*, *141*(3). https://doi.org/10.1016/J.CELL.2010.04.024

Freemont, P. S., Hanson, I. M., & Trowsdale, J. (1991). A novel gysteine-rich sequence motif. *Cell*, *64*(3), 483–484. https://doi.org/10.1016/0092-8674(91)90229-R

Gangappa, S. N., & Botto, J. F. (2014). The BBX family of plant transcription factors. *Trends in Plant Science*, *19*(7), 460–470. https://doi.org/10.1016/J.TPLANTS.2014.01.010

Gangappa, S. N., & Botto, J. F. (2016). The Multifaceted Roles of HY5 in Plant Growth and Development. *Molecular Plant*, *9*(10), 1353–1365. https://doi.org/10.1016/J.MOLP.2016.07.002

Gangappa, S. N., Holm, M., & Botto, J. F. (2013). *Plant Signaling & Behavior Molecular interactions of BBX24 and BBX25 with HYH, HY5 HOMOLOG, to modulate Arabidopsis seedling development*. https://doi.org/10.4161/psb.25208

Gendron, J. M., Pruneda-Paz, J. L., Doherty, C. J., Gross, A. M., Kang, S. E., & Kay, S. A. (2012). Arabidopsis circadian clock protein, TOC1,is a DNA-binding transcription factor. *Proceedings of the National Academy of Sciences of the United States of America*, *109*(8), 3167–3172. https://doi.org/10.1073/PNAS.1200355109/SUPPL_FILE/SD01.XLSX

Graeff, M., Straub, D., Eguen, T., Dolde, U., Rodrigues, V., Brandt, R., & Wenkel, S. (2016). MicroProtein-Mediated Recruitment of CONSTANS into a TOPLESS Trimeric Complex Represses Flowering in Arabidopsis. *PLoS Genetics*, *12*(3). https://doi.org/10.1371/journal.pgen.1005959

Heng, Y., Lin, F., Jiang, Y., Ding, M., Yan, T., Lan, H., Zhou, H., Zhao, X., Xu, D., & Deng, X. W. (2019). *B-Box Containing Proteins BBX30 and BBX31, Acting Downstream of HY5, Negatively Regulate Photomorphogenesis in Arabidopsis 1*. https://doi.org/10.1104/pp.18.01244

Holm, M., Hardtke, C. S., Gaudet, R., & Deng, X. W. (2001). Identification of a structural motif that confers specific interaction with the WD40 repeat domain of Arabidopsis COP1. *EMBO Journal*, *20*(1–2), 118–127. https://doi.org/10.1093/EMBOJ/20.1.118

Holtan, H. E., Bandong, S., Marion, C. M., Adam, L., Tiwari, S., Shen, Y., Maloof, J. N., Maszle, D. R., Ohto, M. aki, Preuss, S., Meister, R., Petracek, M., Repetti, P. P., Reuber, T. L., Ratcliffe, O. J., & Khanna, R. (2011). BBX32, an Arabidopsis B-Box Protein, Functions in Light Signaling by Suppressing HY5-Regulated Gene

Expression and Interacting with STH2/BBX21. *Plant Physiology*, *156*(4), 2109. https://doi.org/10.1104/PP.111.177139

Huang, J., Zhao, X., Weng, X., Wang, L., & Xie, W. (2012). The Rice B-Box Zinc Finger Gene Family: Genomic Identification, Characterization, Expression Profiling and Diurnal Analysis. *PLOS ONE*, *7*(10), e48242. https://doi.org/10.1371/JOURNAL.PONE.0048242

Izawa, T. (2020). *What is going on with the hormonal control of flowering in plants?* https://doi.org/10.1111/tpj.15036

Jiang, K., Liberatore, K. L., Park, S. J., Alvarez, J. P., & Lippman, Z. B. (2013). Tomato Yield Heterosis Is Triggered by a Dosage Sensitivity of the Florigen Pathway That Fine-Tunes Shoot Architecture. *PLOS Genetics*, *9*(12), e1004043. https://doi.org/10.1371/JOURNAL.PGEN.1004043

Job, N., Yadukrishnan, P., Bursch, K., Datta, S., & Johansson, H. (2018). *Two B-Box Proteins Regulate Photomorphogenesis by Oppositely Modulating HY5 through their Diverse C-Terminal Domains 1[OPEN]*. https://doi.org/10.1104/pp.17.00856

Kakizuka, A., Miller, W. H., Umesono, K., Warrell, R. P., Frankel, S. R., Murty, V. V. V. S., Dmitrovsky, E., & Evans, R. M. (1991). Chromosomal translocation t(15;17) in human acute promyelocytic leukemia fuses RARα with a novel putative transcription factor, PML. *Cell*, *66*(4), 663–674. https://doi.org/10.1016/0092-8674(91)90112-C

Khanna, R., Kronmiller, B., Maszle, D. R., Coupland, G., Holm, M., Mizuno, T., & Wu, S. H. (2009). The Arabidopsis B-Box Zinc Finger Family. *The Plant Cell*, *21*(11), 3416. https://doi.org/10.1105/TPC.109.069088

Kiełbowicz-Matuk, A., Rey, P., & Rorat, T. (2014). Interplay between circadian rhythm, time of the day and osmotic stress constraints in the regulation of the expression of a Solanum Double B-box gene. *Annals of Botany*, *113*(5), 831–842. https://doi.org/10.1093/AOB/MCT303

Kikuchi, R., Kawahigashi, H., Oshima, M., Ando, T., & Handa, H. (2012). (No Title). *Journal of Experimental Botany*, *63*(2), 773–784. https://doi.org/10.1093/jxb/err299

Kim, D. H., Doyle, M. R., Sung, S., & Amasino, R. M. (2009). Vernalization: Winter and the Timing of Flowering in Plants. *Http://Dx.Doi.Org/10.1146/Annurev.Cellbio.042308.113411*, *25*, 277–299. https://doi.org/10.1146/ANNUREV.CELLBIO.042308.113411

Kluska, K., Adamczyk, J., & Krężel, A. (2018). Metal binding properties, stability and reactivity of zinc fingers. *Coordination Chemistry Reviews*, *367*, 18–64. https://doi.org/10.1016/J.CCR.2018.04.009

Kobayashi, M., Nagasaki, H., Garcia, V., Just, D., Bres, C., Mauxion, J. P., le Paslier, M. C., Brunel, D., Suda, K., Minakuchi, Y., Toyoda, A., Fujiyama, A., Toyoshima, H., Suzuki, T., Igarashi, K., Rothan, C., Kaminuma, E., Nakamura, Y., Yano, K., & Aoki, K. (2014). Genome-Wide Analysis of Intraspecific DNA Polymorphism in 'Micro-Tom', a Model Cultivar of Tomato (Solanum lycopersicum). *Plant and Cell Physiology*, *55*(2), 445–454. https://doi.org/10.1093/PCP/PCT181

Kobayashi, Y., Kaya, H., Goto, K., Iwabuchi, M., & Araki, T. (1999). A pair of related genes with antagonistic roles in mediating flowering signals. *Science*, *286*(5446), 1960–1962. https://doi.org/10.1126/SCIENCE.286.5446.1960/SUPPL_FILE/1044707S2_THUMB.GIF

Kwon, C.-T., Heo, J., Lemmon, Z. H., Capua, Y., Hutton, S. F., van Eck, J., Ju Park, S., & Lippman, Z. B. (2020). *Rapid customization of Solanaceae fruit crops for urban agriculture*. https://doi.org/10.1038/s41587-019-0361-2

Li, W., Wang, J., Sun, Q., Li, W., Yu, Y., Zhao, M., & Meng, Z. (2017). *Expression analysis of genes encoding double B-box zinc finger proteins in maize*. https://doi.org/10.1007/s10142-017-0562-z

Lifschitz, E., & Eshed, Y. (2006). *Universal florigenic signals triggered by FT homologues regulate growth and flowering cycles in perennial day-neutral tomato*. https://doi.org/10.1093/jxb/erl106

Liu, X., Li, R., Dai, Y., Chen, X., & Wang, X. (2018). Genome-wide identification and expression analysis of the B-box gene family in the Apple (Malus domestica Borkh.) genome. *Molecular Genetics and Genomics : MGG*, *293*(2), 303–315. https://doi.org/10.1007/S00438-017-1386-1

Massiah, M. A., Simmons, B. N., Short, K. M., & Cox, T. C. (2006). Solution Structure of the RBCC/TRIM B-box1 Domain of Human MID1: B-box with a RING. *Journal of Molecular Biology*, *358*(2), 532–545. https://doi.org/10.1016/J.JMB.2006.02.009

Meng, X., Muszynski, M. G., & Danilevskaya, O. N. (2011). The FT-Like ZCN8 Gene Functions as a Floral Activator and Is Involved in Photoperiod Sensitivity in Maize. *The Plant Cell*, *23*(3), 942–960. https://doi.org/10.1105/TPC.110.081406

Meroni, G., & Diez-Roux, G. (2005). TRIM/RBCC, a novel class of "single protein RING finger" E3 ubiquitin ligases. *BioEssays*, *27*(11), 1147–1157. https://doi.org/10.1002/BIES.20304

Miller, T. A., Muslin, E. H., & Dorweiler, J. E. (2008). A maize CONSTANS-like gene, conz1, exhibits distinct diurnal expression patterns in varied photoperiods. *Planta*, *227*(6), 1377–1388. https://doi.org/10.1007/S00425-008-0709-1

Molesini, B., Dusi, V., Pennisi, F., di Sansebastiano, G. pietro, Zanzoni, S., Manara, A., Furini, A., Martini, F., Rotino, G. L., & Pandolfini, T. (2020). TCMP-2 affects tomato flowering and interacts with BBX16, a homolog of the arabidopsis B-box MiP1b. *Plant Direct*, *4*(11), e00283. https://doi.org/10.1002/PLD3.283

Mutasa-Göttgens, E., & Hedden, P. (2009). Gibberellin as a factor in floral regulatory networks. *Journal of Experimental Botany*, *60*(7), 1979–1989. https://doi.org/10.1093/JXB/ERP040

Patarca, R., Freeman, G. J., Schwartz, J., Singh, R. P., Kong, Q. T., Murphy, E., Anderson, Y., Sheng, F. Y., Singh, P., & Johnson, K. A. (1988). rpt-1, an intracellular protein from helper/inducer T cells that regulates gene expression of interleukin 2 receptor and human immunodeficiency virus type 1. *Proceedings of the National Academy of Sciences of the United States of America*, *85*(8), 2733–2737. https://doi.org/10.1073/PNAS.85.8.2733

Peers, G., & Niyogi, K. K. (2008a). Pond Scum Genomics: The Genomes of Chlamydomonas and Ostreococcus. *The Plant Cell*, *20*(3), 502–507. https://doi.org/10.1105/TPC.107.056556

Ping, Q., Cheng, P., Huang, F., Ren, L., Cheng, H., Guan, Z., Fang, W., Chen, S., Chen, F., & Jiang, J. (2019). The heterologous expression in Arabidopsis thaliana of a chrysanthemum gene encoding the BBX family transcription factor CmBBX13 delays flowering. *Plant Physiology and Biochemistry : PPB*, *144*, 480–487. https://doi.org/10.1016/J.PLAPHY.2019.10.019

Putterill, J., Robson, F., Lee, K., Simon, R., & Coupland, G. (1995). The CONSTANS gene of arabidopsis promotes flowering and encodes a protein showing similarities to zinc finger transcription factors. *Cell*, *80*(6), 847–857. https://doi.org/10.1016/0092-8674(95)90288-0

Qi, Q., Gibson, A., Fu, X., Zheng, M., Kuehn, R., Wang, Y., Wang, Y., Navarro, S., Morrell, J. A., Jiang, D., Simmons, G., Bell, E., Ivleva, N. B., McClerren, A. L., Loida, P., Ruff, T. G., Petracek, M. E., & Preuss, S. B. (2012). Involvement of the N-terminal B-box domain of arabidopsis BBX32 protein in interaction with soybean BBX62 protein. *Journal of Biological Chemistry*, *287*(37), 31482–31493. https://doi.org/10.1074/JBC.M112.346940

Reddy, B. A., & Etkin, L. D. (1991a). A unique bipartite cysteine-histidine motif defines a subfamily of potential zinc-finger proteins. *Nucleic Acids Research*, *19*(22), 6330. https://doi.org/10.1093/NAR/19.22.6330

Reddy, B. A., Kloc, M., & Etkin, L. (1991). The cloning and characterization of a maternally expressed novel zinc finger nuclear phosphoprotein (xnf7) in Xenopus laevis. *Developmental Biology*, *148*(1), 107–116. https://doi.org/10.1016/0012-1606(91)90321-S

Robertson Mcclung, C. (2021). *Circadian Clock Components Offer Targets for Crop Domestication and Improvement Clock Components Offer Targets for Crop Domestication and*. https://doi.org/10.3390/genes1203

Silva, G. F. F., Silva, E. M., Correa, J. P. O., Vicente, M. H., Jiang, N., Notini, M. M., Junior, A. C., de Jesus, F. A., Castilho, P., Carrera, E., L Opez-D Iaz, I., Grotewold, E., Peres, L. E. P., & Nogueira, F. T. S. (2019). Tomato floral induction and flower development are orchestrated by the interplay between gibberellin and two unrelated microRNA-controlled modules. *New Phytologist*, *221*, 1328–1344. https://doi.org/10.1111/nph.15492

Song, Y. H., Smith, R. W., To, B. J., Millar, A. J., & Imaizumi, T. (2012). FKF1 conveys timing information for CONSTANS stabilization in photoperiodic flowering. *Science*, *336*(6084), 1045–1049. https://doi.org/10.1126/SCIENCE.1219644/SUPPL_FILE/SONG.SOM.PDF

Suárez-López, P., Wheatley, K., Robson, F., Onouchi, H., Valverde, F., & Coupland, G. (2001). CONSTANS mediates between the circadian clock and the control of flowering in Arabidopsis. *Nature 2001 410:6832*, *410*(6832), 1116–1120. https://doi.org/10.1038/35074138

Susila, H., Nasim, Z., & Ahn, J. H. (2018). Ambient Temperature-Responsive Mechanisms Coordinate Regulation of Flowering Time. *International Journal of Molecular Sciences 2018, Vol. 19, Page 3196*, *19*(10), 3196. https://doi.org/10.3390/IJMS19103196

Takahashi, M., Inaguma, Y., Hiai, H., & Hirose, F. (1988). Developmentally regulated expression of a human "finger"-containing gene encoded by the 5' half of the ret transforming gene. *Molecular and Cellular Biology*, *8*(4), 1853–1856. https://doi.org/10.1128/MCB.8.4.1853-1856.1988

Talar, U., & Kiełbowicz-matuk, A. (2021b). Beyond Arabidopsis: BBX Regulators in Crop Plants. *International Journal of Molecular Sciences 2021, Vol. 22, Page 2906*, *22*(6), 2906. https://doi.org/10.3390/IJMS22062906

Talar, U., Kieøbowicz-Matuk, A., Czarnecka, J., & Rorat, T. (2017a). Genome-wide survey of B-box proteins in potato (Solanum tuberosum)—Identification, characterization and expression patterns during diurnal

cycle, etiolation and de-etiolation. *PLOS ONE*, *12*(5), e0177471. https://doi.org/10.1371/JOURNAL.PONE.0177471

Tiwari, S. B., Shen, Y., Chang, H. C., Hou, Y., Harris, A., Ma, S. F., McPartland, M., Hymus, G. J., Adam, L., Marion, C., Belachew, A., Repetti, P. P., Reuber, T. L., & Ratcliffe, O. J. (2010). The flowering time regulator CONSTANS is recruited to the FLOWERING LOCUS T promoter via a unique cis-element. *New Phytologist*, *187*(1), 57–66. https://doi.org/10.1111/J.1469-8137.2010.03251.X

Torok, M., & Etkin, L. D. (2001). Two B or not two B? Overview of the rapidly expanding B-box family of proteins. *Differentiation*, *67*(3), 63–71. https://doi.org/10.1046/J.1432-0436.2001.067003063.X

Turck, F., Fornara, F., & Coupland, G. (2008). Regulation and identity of florigen: FLOWERING LOCUS T moves center stage. *Annual Review of Plant Biology*, *59*, 573–594. https://doi.org/10.1146/ANNUREV.ARPLANT.59.032607.092755

Vaishak, K. P., Yadukrishnan, P., Bakshi, S., Kushwaha, A. K., Ramachandran, H., Job, N., Babu, D., & Datta, S. (2019). The B-box bridge between light and hormones in plants. In *Journal of Photochemistry and Photobiology B: Biology* (Vol. 191, pp. 164–174). Elsevier B.V. https://doi.org/10.1016/j.jphotobiol.2018.12.021

Valverde, F. (2011). CONSTANS and the evolutionary origin of photoperiodic timing of flowering. *Journal of Experimental Botany*, *62*(8), 2453–2463. https://doi.org/10.1093/jxb/erq449

Valverde, F., Mouradov, A., Soppe, W., Ravenscroft, D., Samach, A., & Coupland, G. (2004). Photoreceptor regulation of CONSTANS protein in photoperiodic flowering. *Science (New York, N.Y.)*, *303*(5660), 1003–1006. https://doi.org/10.1126/SCIENCE.1091761

Vicente, M. H., Zsögön, A., Lopo De Sá, A. F., Ribeiro, R. v, & Peres, L. E. P. (2015). Physiology Semi-determinate growth habit adjusts the vegetative-to-reproductive balance and increases productivity and water-use efficiency in tomato (Solanum lycopersicum). *Journal of Plant Physiology*, *177*, 11–19. https://doi.org/10.1016/j.jplph.2015.01.003

Wang, C.-Q., Guthrie, C., Sarmast, K., & Dehesh, K. (2014) *(BBX19 Interacts with CONSTANS to Repress FLOWERING LOCUS T Transcription, Defining a Flowering Time Checkpoint in Arabidopsis)*. https://doi.org/10.1105/tpc.114.130252

Wang, L., Sun, J., Ren, L., Zhou, M., Han, X., Ding, L., Zhang, F., Guan, Z., Fang, W., Chen, S., Chen, F., & Jiang, J. (2019). *CmBBX8 accelerates flowering by targeting CmFTL1 directly in summer chrysanthemum*. https://doi.org/10.1111/pbi.13322

Wang, Q., Tu, X., Zhang, J., Chen, X., & Rao, L. (2013). *Heat stress-induced BBX18 negatively regulates the thermotolerance in Arabidopsis*. https://doi.org/10.1007/s11033-012-2354-9

Wei, H., Wang, P., Chen, J., Li, C., Wang, Y., Yuan, Y., Fang, J., & Leng, X. (2020). Genome-wide identification and analysis of B-BOX gene family in grapevine reveal its potential functions in berry development. *BMC Plant Biology*, *20*(1), 1–19. https://doi.org/10.1186/S12870-020-2239-3/FIGURES/8

Wenkel, S., Turck, F., Singer, K., Gissot, L., le Gourrierec, J., Samach, A., & Coupland, G. (2006). CONSTANS and the CCAAT Box Binding Complex Share a Functionally Important Domain and Interact to Regulate Flowering of Arabidopsis. *The Plant Cell*, *18*(11), 2971–2984. https://doi.org/10.1105/TPC.106.043299

Wu, Z., Fang, X., Zhu, D., & Dean, C. (2020). Autonomous Pathway: FLOWERING LOCUS C Repression through an Antisense-Mediated Chromatin-Silencing Mechanism. *Plant Physiology*, *182*(1), 27–37. https://doi.org/10.1104/PP.19.01009

Xiong, C., Luo, D., Lin, A., Zhang, C., Shan, L., He, P., Li, B., Zhang, Q., Hua, B., Yuan, Z., Li, H., Zhang, J., Yang, C., Lu, Y., Ye, Z., & Wang, T. (2019). A tomato B-box protein SlBBX20 modulates carotenoid biosynthesis by directly activating PHYTOENE SYNTHASE 1, and is targeted for 26S proteasome-mediated degradation. *New Phytologist*, *221*, 279–294. https://doi.org/10.1111/nph.15373

Xu, X., Wang, Q., Li, W., Hu, T., Wang, Q., Yin, Y., Liu, X., He, S., Zhang, M., Liang, Y., Zhu, J., & Zhan, X. (2022). Overexpression of SlBBX17 affects plant growth and enhances heat tolerance in tomato. *International Journal of Biological Macromolecules*, *206*, 799–811. https://doi.org/10.1016/J.IJBIOMAC.2022.03.080

Yadav, A., Bakshi, S., Yadukrishnan, P., Lingwan, M., Dolde, U., Wenkel, S., Masakapalli, S. K., & Datta, S. (2019). The B-Box-Containing MicroProtein miP1a/BBX31 Regulates Photomorphogenesis and UV-B Protection. *Plant Physiology*, *179*(4), 1876–1892. https://doi.org/10.1104/PP.18.01258

Yadav, A., Ravindran, N., Singh, D., Puthan, •, Rahul, V., & Datta, S. (2020). *Role of Arabidopsis BBX proteins in light signaling*. https://doi.org/10.1007/s13562-020-00597-2

Yang, S., Weers, B. D., Morishige, D. T., & Mullet, J. E. (2014). CONSTANS is a photoperiod regulated activator of flowering in sorghum. *BMC Plant Biology*, *14*(1), 1–15. https://doi.org/10.1186/1471-2229-14-148/FIGURES/6

Yang, T., He, Y., Niu, S., Yan, S., & Zhang, Y. (2020). Identification and characterization of the CONSTANS (CO)/CONSTANS-like (COL) genes related to photoperiodic signaling and flowering in tomato. *Plant Science*, *301*, 110653. https://doi.org/10.1016/j.plantsci.2020.110653

Yang, Y., Ma, C., Xu, Y., Wei, Q., Imtiaz, M., Lan, H., Gao, S., Cheng, L., Wang, M., Fei, Z., Hong, B., & Gao, J. (2014). *A Zinc Finger Protein Regulates Flowering Time and Abiotic Stress Tolerance in Chrysanthemum by Modulating Gibberellin Biosynthesis C W OPEN*. https://doi.org/10.1105/tpc.114.124867

Zhang, X., Henriques, R., Lin, S. S., Niu, Q. W., & Chua, N. H. (2006). Agrobacterium-mediated transformation of Arabidopsis thaliana using the floral dip method. *Nature Protocols*, *1*(2), 641–646. https://doi.org/10.1038/NPROT.2006.97

Zhang, X., Huai, J., Shang, F., Xu, G., Tang, W., Jing, Y., & Lin, R. (2017). *A PIF1/PIF3-HY5-BBX23 Transcription Factor Cascade Affects Photomorphogenesis 1[OPEN]*. https://doi.org/10.1104/pp.17.00418

Zou, Z., Wang, R., Wang, R., Yang, S., & Yang, Y. (2017). Genome-wide identification, phylogenetic analysis, and expression profiling of the BBX family genes in pear. *Https://Doi.Org/10.1080/14620316.2017.1338927*, *93*(1), 37–50. https://doi.org/10.1080/14620316.2017.1338927

Zsögön, A., Cermak, T., Voytas, D., & Peres, L. E. P. (2017). Genome editing as a tool to achieve the crop ideotype and de novo domestication of wild relatives: Case study in tomato. *Plant Science*, *256*, 120–130. https://doi.org/10.1016/J.PLANTSCI.2016.12.012

7. APPENDIX A

Table S.1: Mourashige and Skoog medium composition (pH 5.7).

Components	Concentration
Sucrose	10 g/L
Agar	8 g/L
$CaCl_2$	332.02 mg/L
KH_2PO_4	170.00 mg/L
KNO_3	1900.00 mg/L
$MgSO_4$	180.54 mg/L
NH_4NO_3	1650.00 mg/L
$CoCl_2 \cdot 6H_2O$	0.025 mg/L
$CuSO_4 \cdot 5H_2O$	0.025 mg/L
FeNaEDTA	36.70 mg/L
H_3BO_3	6.20 mg/L
$MnSO_4 \cdot H_2O$	16.90 mg/L
Na_2MoO_4	0.25 mg/L
$ZnSO_4 \cdot 7H_2O$	8.60 mg/L

Table S.2: KCMS solid composition (pH 5.8).

Components	Concentration
Sucrose	20 g/L
MS powder mix	4,4 g/L
Thiamine	0,9 mg/L
KH_2PO_4	200mg/L
Acetosyringone	40 mg/L
2,4-D	0.2 mg/L
Kinetin	0.1 mg/L
Agar	7.5 mg/L

Table S.3: KCMS liquid composition (pH 5.7).

Components	Concentration
Sucrose	20 g/L
MS powder mix	4,4 g/L
Thiamine	0,9 mg/L
KH_2PO_4	200mg/L
Acetosyringone	0.2 mg/L

Table S.4: ***Regeneration medium-1 (pH 5.8).***

Components	Concentration
Sucrose	30 g/L
Agar	8 g/L
MS powder mix	4.4 g/L
Zeatin riboside	2 mg/L
Naftaleneacetic acid	0.01 mg/L
Nitsch Vitamins*	
Augmentin **	9 ml/L
Kanamycin	100 mg/L

*: Nitsch Vitamins composition**:** biotin 0.05 mg/L, folic acid 0.5 mg /L, glycine 2.0 mg/L, myo-inositol 100 mg/L, nicotinic acid 5 mg/L, pyridoxin 0.5 mg/L, thiamine 0.5 mg/L.
** Augmentin composition: dissolve 1g of amoxicillin and 200 mg of clavulanic acid in 10 ml of H_2O.

Table S.5: ***Regeneration medium-2 (pH 5.8).***

Components	Concentration
Sucrose	30 g/L
Agar	8 g/L
MS powder mix	4.4 g/L
Zeatin riboside	2 mg/L
Naftaleneacetic acid	0.01 mg/L
Nitsch Vitamins*	
Augmentin **	5 ml/L
Kanamycin	100 mg/L

Table S.6: ***Rooting medium (pH 5.8).***

Components	Concentration
Sucrose	10 g/L
Agar	4 g/L
Phytagel	3 g/L
MS powder mix	2.2 g/L
Nitsch Vitamins*	
Augmentin **	2.5 ml/L
Kanamycin	75 mg/L

Table S.7: Primers

Name	Experiment	Forward Sequence (5‘ → 3‘)	Reverse Sequence (5‘ → 3‘)
*Sl*SP Solyc06g074350	qRT-PCR	TTAGTGCGTGGACGGACTACTACT	GAGGGTGAACAACCATTAACCCCC
*Sl*SFT Solyc03g063100	qRT-PCR	AAACAGTGTATGCTCCAGGATGGC	AGATCTTCTACGTCCACCACTGCC
*Sl*CO1 Solyc02g089540	qRT-PCR	AAGATCAACCACAAGCCCCTA	TCCTCTGTGGAAAGCTGCTGTAG
*Sl*Actin Solyc11g005330	qRT-PCR	TTCAAAGGGCGAGTACGACGAG	CAGCAGACCCGAGTTCACTTTT
*Sl*BBX16 Solyc12g005750	qRT-PCR	TGTGAACTTTGTAAATCAGAAGCCT	TGCCTTTGAGCAAAGAAATTAGC
*Sl*TCMP-2 Solyc07g049140	qRT-PCR	ACGAACCTTGCAGCTCAAAC	GCAACAGGTTGCATGTACGG
*At*FT At1g65480	qRT-PCR	ACTGCAGGAATTCATCGTGTCGTG	GCAGCCACTCTCCCTCTGACAATT
*At*Actin At3g18780	qRT-PCR	TGTTCTCTCCTTGTACGCCAGT	CAGCAAGGTCAAGACGGAGGA
*Sl*BBX16 Solyc12g005750	Y2H	GGAGGCCAGTGAATTCTGCAATGGAAGAAGAGAAATTGA	CGAGCTCGATGGATCCGAGAAACAAAAAAGGTTCTTTC
*Sl*TCMP-2 Solyc07g049140	Y2H	CATGGAGGCCGAATTCACAAATATTTTGGGACTTTGTAACG	GCAGGTCGACGGATCCAGGCAACAGGTTGCATGTACG
*At*miP1b At4g15248	Y2H	GGAGGCCAGTGAATTCTGTAGAGGGTTTGAGAAAGAAGAAG	CGAGCTCGATGGATCCGAGAAACACAAAGGGAATTTTGTG
*Sl*CO1 Solyc02g089540	Y2H	GGAGGCCAGTGAATTCTTGAAAAAAGAGAACAGTAACAATTGGG	CGAGCTCGATGGATCCGAATGAAGGGACAATTCCATAATTGC
*Sl*TPL1 Solyc03g117360	Y2H	GGAGGCCAGTGAATTCTCATCTCTCAGTAGAGAGCTTG	CGAGCTCGATGGATCCTCTTGGTGCTTGATCGGAGC
P35S::TCMP2::tNOS	Transgenic state of 35S::TCMP -2 A. th. plants	CTTCGTCAACATGGTGGAGCACGACA	GATCTAGTAACATAGATGACACCG
pTCMP2::TCMP-1	Transgenic state of pTCMP2::TCMP -1 tomato plants	CTCGAGCCCTTTAAAAAGTAT	TTATCACACGCCTATGGCCATGGC

	1 tomato plants		
nYFP::TCMP-2 //BBX16::cYFP	Ratiometric BIFC	TCMP-2 cloning GGGGACAACTTTGTATAATAAAGTTGCCATGACAAATATTTTGGGACTTTGTAA BBX16 cloning GGGGACAAGTTTGTACAAAAAAGCAGGCTTTATGTGCAATGGAAGAAGAGAA	TCMP-2 cloning (with Stop codon) GGGGACCACTTTGTACAAGAAAGCTGGGTATTAAGGCAACAGGTTGCATGTAC BBX16 cloning (without Stop codon) GGGGACAACTTTGTATAGAAAAGTTGGGTGAGAAACAAAAAAGGTTCTTTCA
TCMP-2::nYFP //BBX16::cYFP	Ratiometric BIFC	TCMP-2 cloning GGGGACAACTTTGTATAATAAAGTTGCCATGACAAATATTTTGGGACTTTGTAA BBX16 cloning GGGGACAAGTTTGTACAAAAAAGCAGGCTTTATGTGCAATGGAAGAAGAGAAA	TCMP-2 cloning (without Stop codon) GGGGACCACTTTGTACAAGAAAGCTGGGTAAGGCAACAGGTTGCATGTAC BBX16 cloning (without Stop codon) GGGGACAACTTTGTATAGAAAAGTTGGGTGAGAAACAAAAAAGGTTCTTTCA
nYFP::TCMP-2 //ΔBBX16::cYF P	Ratiometric BIFC	TCMP-2 cloning GGGGACAACTTTGTATAATAAAGTTGCCATGACAAATATTTTGGGACTTTGTAA Deleted BBX16 cloning GGGGACAAGTTTGTACAAAAAAGCAGGCTTTATGTGTATTCTTTGTGGAATTTGC	TCMP-2 cloning (with Stop codon) GGGGACCACTTTGTACAAGAAAGCTGGGTATTAAGGCAACAGGTTGCATGT AC Deleted BBX16 cloning (without Stop codon) GGGGACAACTTTGTATAGAAAAGTTGGGTGAGAAACAAAAAAGGTTCTTTCA
TCMP-2::nYFP //ΔBBX16::cYF P	Ratiometric BIFC	TCMP-2 cloning GGGGACAACTTTGTATAATAAAGTTGCCATGACAAATATTTTGGGACTTTGTAA Deleted BBX16 cloning GGGGACAAGTTTGTACAAAAAAGCAGGCTTTATGTGTATTCTTTGTGGAATTTGC	TCMP-2 cloning (without Stop codon) GGGGACCACTTTGTACAAGAAAGCTGGGTAAGGCAACAGGTTGCATGTAC Deleted BBX16 cloning (without Stop codon) GGGGACAACTTTGTATAGAAAAGTTGGGTGAGAAACAAAAAAGGTTCTTTCA
p35S::TCMP2::t35S	Transgenic state of MicroTom plants	CCTCGTCAACATGGTGGAGCACGACA	AGTAAGTCCGTATTGATCGGTT
p35S::TCMP2::t35S	Transgenic state of *S. pennellii* plants	GGTTTGTGCAATGAGCCATGT	GATCTAGTAACATAGATGACACCG
p35S::*S*BBX16::t35S	Cloning	GCAGGTACCATGTGCAATGGAAGAAGAGAAA	TGCGGATCCTTAGAGAAACAAAAAAGGTTCTTT
p35S::*S*BBX17::t35S	Cloning	GCAGGTACCATGTGTTGTAGTGGAAGAAGAGAG	TTAGGATCCTCAAATAAACAGAAAAAGCTCTT
*S*BBX16 Solyc12g005750	RT-PCR	TGTGAACTTTGTAAATCAGAAGCCT	TGCCTTTGAGCAAAGAAATTAGC
*S*BBX17 Solyc07g052620	RT-PCR	GTGCCTTCTTTGCAGCGTTTG	GTTCCAAACGGGCAATCGTCG

Table S.8: List of TCMP-2 interacting candidates from Y2H screen

Locus	PBS†	Total no. of clones	No. of independent clones	Frame‡	SOL annotation
Solyc01g111600	C	6	5	IF(§)	Metal ion binding protein
Solyc02g079850	D	1		IF	Pleckstrin homology domain-containing family F member 2
Solyc03g112230	D	2	2	IF	ZZ type zinc finger domain-containing protein
Solyc06g083250	D	1		IF	Unknown Protein
Solyc12g005750	C	5	2	IF(§)	B-box Zinc finger protein CONSTANS-LIKE 4
Solyc01g008960	D	2	2	IF	Argonaute 4a
Solyc01g008280	D	1		IF	Serine/threonine-protein phosphatase 2A activator 2
Solyc01g102410	D	2	2	IF	Glutaminyl-tRNA synthetase
Solyc01G067390	D	1		IF	RNA helicase DEAH-box1
Solyc02G71980	D	1		IF	Actin-binding protein
Solyc05g056280	C	4	4	IF	RNA-binding protein Luc7-like 2
Solyc07g042190	D	1		IF	Protein of unknown function
Solyc03g123460	D	2	1	IF	Protein of unknown function
Solyc01g073890	D	1		IF	CHP-rich zinc finger protein-like
Solyc05g012610	D	1		IF	Appr-1-p processing enzyme domain protein
Solyc01g104030	D	1		IF	Inward rectifier potassium channel-like protein
Solyc09g074880	D	2	1	IF	Homology to unknown gene
Solyc06g083250	D	4	3	IF	Unknown Protein
Solyc04g015200	D	1		IF	6-phosphofructokinase 2
Solyc05g012770	D	1		IF	WRKY transcription factor 4
Solyc00g007220	D	1		IF	Ring finger protein
Solyc03g115230	D	1		IF	Heat shock protein tfhs1
Solyc02g062000	D	1		IF	RUN and FYVE domain-containing protein 1
Solyc07g021750	D	1		IF	Cytidine deaminase
Solyc08g023280	D	1		IF	Tripartite motif-containing 22
Solyc10g061930	D	1		IF	Casein kinase II subunit beta-4
Solyc05g007060	D	1		IF	Uncharacterized protein
Solyc09g075830	D	1		IF	Time for coffee
Solyc06g071450	D	1		IF(§)	RNA polymerase II transcription factor B subunit 4
Solyc07g017490	D	1		IF	Red family protein
Solyc09g007180	C	3	3	IF	Adenylate kinase
Solyc03g083000	D	1		IF	AT2G46550 protein
Solyc08g005150	D	1		IF	Ubiquitin ligase
Solyc01g008560	D	1		IF	NAD kinase 1
Solyc10g075035	D	1		IF	B3 domain-containing protein
Solyc01g110120	D	1		IF	V-type proton ATPase subunit a
Solyc03g116140	D	2	2	IF	Activating signal cointegrator 1
Solyc07g064910	D	2	1	IF	EH domain-containing protein 1
Solyc01g009780	D	2	1	IF	LITAF-domain containing protein
Solyc01g108180	D	2	1	IF	Pentatricopeptide repeat-containing protein
Solyc10g079370	D	1		IF	Transcription initiation factor IIB
Solyc04g071350	C	6	2	IF	Exocyst complex component *Sec5*
Solyc04g054760	D	1		IF	Senescence-associated family protein
Solyc06g072460	D	1		IF	Cysteine/Histidine-rich C1 domain family protein
Solyc11g066130	D	1		IF	Osmotin
Solyc07g043420	D	1		IF	2-oxoglutarate-dependent dioxygenase 2
Solyc09g008280	D	1		IF	S-adenosyl-L-methionine synthetase

†PBS (predicted biological score) shows the confidence of interaction: C, good; D, moderate.

‡Frame (IF:*In frame* with the Gal4 Activation Domain). (§), the fragment contains the full length ORF

Table S.9: List of protein sequences analyzed using MEGA5 for the phylogenetic tree construction reported in Figure 9.

Arabidopsis thaliana

Domains	Locus (gene name)	Protein sequence
1 B-box + CCT	At1g25440 (*At*BBX15-COL16)	MMKSLANAVGAKTARACDSCVKRRARWYCAADDAFLCQSCDSLVHSANPLARRHERVRLKTASPAVVKHSNHSSASPPH EVATWHHGFTRKARTPRGSGKKNNSSIFHDLVPDISIEDQTDNYELEEQLICQVPVLDPLVSEQFLNDVVEPKIEFPMIRSGL MIEEEEDNAESCLNGFFPTDMELEEFAADVETLLGRGLDTESYAMEELGLSNSEMFKIEKDEIEEEVEEIKAMSMDIFDDDRK DVDGTVPFELSFDYESSHKTSEEEVMKNVESSGECVVKVKEEEHKNVLMLRLNYDSVISTWGGQGPPWSSGEPPERDMDI SGWPAFSMVENGGESTHQKQYVGGCLPSSGFGDGGREARVSRYREKRRTRLFSKKIRYEVRKLNAEKRPRMKGRFVKRA SLAAAASPLGVNY
1 B-box + CCT	At1g68520 (*At*BBX14-COL6)	MMKSLASAVGGKTARACDSCVKRRARWYCAADDAFLCHACDGSVHSANPLARRHERVRLKSASAGKYRHASPPHQATW HQGFTRKARTPRGGKKSHTMVFHDLVPEMSTEDQAESYEVEEQLIFEVPVMNSMVEEQCFNQSLEKQNEFPMMPLSFKSS DEEDDDNAESCLNGLFPTDMELAQFTADVETLLGGGDREFHSIEELGLGEMLKIEKEEVEEEGVVTREVHDQDEGDETSPF EISFDYEYTHKTTFDEGEEDEKEDVMKNVMEMGVNEMSGGIKEEKKEKALMLRLDYESVISTWGGQGIPWTARVPSEIDLD MVCFPTHTMGESGAEAHHHNHFRGLGLHLGDAGDGGREARVSRYREKRRTRLFSKKIRYEVRKLNAEKRPRMKGRFVKR SSIGVAH
2 B-box	At2g21320 (*At*BBX18-DBB1a)	MRILCDACESAAAIVFCAADEAALCCSCDEKVHKCNKLASRHLRVGLADPSNAPSCDICENAPAFFYCEIDGSSLCLQCDMV VHVGGKRTHRRFLLLRQRIEFPGDKPNHADQLGLRCQKASSGRGQESNGNGDHDHNMIDLNSNPQRVHEPGSHNQEEGI DVNNANNHEHE
2 B-box + CCT	At3g02380 (*At*BBX3-COL2)	MLKEESNESGTWARACDTCRSAACTVYCEADSAYLCTTCDARVHAANRVASRHERVRVCQSCESAPAAFLCKADAASLCT ACDAEIHSANPLARRHQRVPILPLSANSCSSMAPSETDADNDEDDREVASWLLPNPGKNIGNQNNGFLFGVEYLDLVDYSS SMDNQFEDNQYTHYQRSFGGDGVVPLQVEESTSHLQQSQQNFQLGINYGFSSGAHYNNNSLKDLNHSASVSSMDISVVPE STASDITVQHPRTTKETIDQLSGPPTQVVQQLTPMEREARVLRYREKKKTRKFDKTIRYASRKAYAEIRPRIKGRFAKRIETEA EAEEIFSTSLMSETGYGIVPSF
2 B-box + CCT	At3g07650 (*At*BBX7-COL9)	MGYMCDFCGEQRSMVYCRSDAACLCLSCDRSVHSANALSKRHSRTLVCERCNAQPATVRCVEERVSLCQNCDWSGHNN SNNNNSSSSSTSPQQHKRQTISCYSGCPSSSELASIWSFCLDLAGQSICEQELGMMNIDDDGPTDKKTCNEDKKDVLVGSS SIPETSSVPQGKSSSAKDVGMCEDDFYGNLGMDEVDMALENYEELFGTAFNPSEELFGHGGIDSLFHKHQTAPEGGNSVQ PAGSNDSFMSSKTEPIICFASKPAHSNISFSGVTGESSAGDFQECGASSSIQLSGEPPWYPPTLQDNNACSHSVTRNNAVM RYKEKKKARKFDKRVRYASRKARADVRRRVKGRFVKAGEAYDYDPLTPTRSY
1 B-box	At3g21890 (*At*BBX30-MIP1a)	MCRGLNNEESRRSDGGGCRSLCTRPSVPVRCELCDGDASVFCEADSAFLCRKCDRWVHGANFLAWRHVRRVLCTSCQK LTRRCLVGDHDFHVVLPSVTTVGETTVENRSEQDNHEVPFVFL
1 B-box	At4g15248 (*At*BBX31-MIP1b)	MCRGFEKEEERRSDNGGCQRLCTESHKAPVSCELCGENATVYCEADAAFLCRKCDRWVHSANFLARRHLRRVICTTCRKL TRRCLVGDNFNVVLPEIRMIARIEEHSSDHKIPFVFL
2 B-box	At4g38960 (*At*BBX19-DBB1b)	MRILCDACENAAAIIFCAADEAALCRPCDEKALHMRLDISKCSESVKRVQIVETSSLIWWIKMGTFCLQSLHLVVHMCNKLAS RHVRVGLAEPSNAPCCDICENAPAFFYCEIDGSSLCLQCDMVVHVGGKRTHGRFLLLRQRIEFPGDKPKENNTRDNLQNQR VSTNGNGEANGKIDDEMIDLNANPQRVHEPSSNNNGIDVNNENNHEPAGLVPVGPFKRESEK
2 B-box + CCT	At5g15840 (*At*BBX1-CO)	MLKQESNDIGSGENNRARPCDTCRSNACTVYCHADSAYLCMSCDAQVHSANRVASRHKRVRVCESCERAPAAFLCEADD ASLCTACDSEVHSANPLARRHQRVPILPISGNSFSSMTTTHHQSEKTMTDPEKRLVVDQEEGEEGDKDAKEVASWLFPNSD KNNNNQNNGLLFSDEYLNLVDYNSSMDYKFTGEYSQHQQNCSVPQTSYGGDRVVPLKLEESRGHQCHNQQNFQFNIKYG SSGTHYNDNGSINHNAYISSMETGVVPESTACVTTASHPRTPKGTVEQQPDPASQMITVTQLSPMDREARVLRYREKRKTR KFEKTIRYASRKAYAEIRPRVNGRFAKREIEAEEQGFNTMLMYNTGYGIVPSF
2 B-box + CCT	At5g15850 (*At*BBX2-COL1)	MLKVESNWAQACDTCRSAACTVYCRADSAYLCSSCDAQVHAANRLASRHERVRVCQSCERAPAAFFCKADAASLCTTCD SEIHSANPLARRHQRVPILPISEYSYSSTATNHSCETTVTDPENRLVLGQEEEDEDEAEAASWLLPNSGKNSGNNNGFSIGD EFLNLVDYSSSDKQFTDQSNQYQLDCNVPQRSYGEDGVVPLQIEVSKGMYQEQQNFQLSINCGSWGALRSSNGSLSHMV NVSSMDLGVVPESTTSDATVSNPRSPKAVTDQPPYPPAQMLSPRDREARVLRYREKKKMRKFEKTIRYASRKAYAEKRPRI KGRFAKKKDVDEEANQAFSTMITFDTGYGIVPSF
2 B-box + CCT	At5g48250 (*At*BBX8-COL10)	MGYMCDFCGEQRSMVYCRSDAACLCLSCDRNVHSANALSKRHSRTLVCERCNAQPASVRCSDERVSLCQNCDWSGHDG KNSTTTSHHKRQTINCYSGCPSSAELSSIWSFCMDLNISSAEESACEQGMGLMTIDEDGTGEKSGVQKINVEQPETSSAAQ GMDHSSVPENSSMAKELGVCEDDFNGNLISDEVDLALENYEELFGSAFNSSRYLFEHGGIGSLFEKDEAHEGSMQQPALSN NASADSFMTCRTEPIICYSSKPAHSNISFSGITGESNAGDFQDCGASSMKQLSREPQPWCHPTAQDIIASSHATTRNNAVMR YKEKKKARKFDKRVRYVSRKERADVRRRVKGRFVKSGEAYDYDPMSPTRSY

Solanum lycopersicum

Domains	Locus (gene name)	Protein sequence
1 B-box	Solyc12g005750 (*S*lBBX16)	MCNGRREIDEEKIEELHNIIVCELCKSEAYVYCEADNAFLCKKCDKLVHTANFFAQRHIRCILCGICKKLTKRYLIGVSHEVILLK VVRCTNFDEQNCSTKVKEPFLFL
1 B-box	Solyc07g052620 (*S*lBBX17)	MCSGRREGDEKTSSTSYCKGPSKEGESIISSAITCALCSSEASVYCEADNAFLCRKCDRSVHGANFLAQRHIRCLLCSVCRK TTRRFLIGTSSELILPTIARLEQRNRSRSAESETTDYRTTPQELFLFI
2 B-box	Solyc12g089240 (*S*lBBX20)	MKIQCDVCNKKEAIVFCTADEAALCDDCDHRVHHVNKLASKHQRFSLVQPSPKQAPMCDICQERRGFLFCQQDRAIMCREC DIPIHKANEHTQKHNRYLLTGIKLSANSALYSAPSQSQSQSQSAISSADSCVSNLKSKDSTSKPVAGSVFVSPAIISNSTKGGA VSSAVESVKVVKEKVGGCNNNVQFVNGGGNNLTSSISEYLEMLPGWHVEDFLDCSTPNVYSKNIGDEDMLSFWDTDLESQ FSSFPPQNVGIWVPQAPPLQESKQETQIQFFPSQNLNFGGQIGLKESREVTNIKSSRKWTDDNSFAVPQMKPPSTSFKRTR TLW
2 B-box	Solyc04g081020 (*S*lBBX21)	MKIQCDVCNNNEASVFCVADEAALCDSCDHRVHHANKLASKHQRFSLIQPSPKQIPVCDICQERRAFLFCQQDRAILCRECD VSIHKANEHTQKHNRFLLTGVKISANSSLYTSSESVSAASCSANQDSVTNLNKPQICTKKTSPVSGSVPQQQVSVAANIGEN SYTSSISEYLEMLPGWHVEELLNASTIPTNGFCKIGDNDVFPIWDSEIESSMNSFSPENIGIWVPQAPPALTPQKNQNQVFPR NINFGGQIEFKNMKEVTSKKSSRKWRDDNSFAVPQISPSSSSISFKRSRTLW
1 B-box + CCT	Solyc05g009310 (*S*lBBX15)	MVSERKLASAMGGKTTRACDNCIKKRARWYCPADDAFLCQNCDASVHSANPLARRHERVRLKTSSLKQTSSPSSSSDDYF PDLESPLSISSVSVSVSVPSWHRGFTRKARTPRQGRKASKSAGDGDVIRKNPIHLVPEILSDENSLDENEEEQLLYRVPILDP FVGHLYSSSTAPTDADSEFKLESKEMTLQDDICNVDLNRFHEMLPSEMELAEFAADVESLLGKGLDDESFDMEGLGLLGVC NKEENSMISHEKVKIEDEGEMEVVTKTTSPTTHNHQYNHTHDHDIDINEDTFEFKFDYDSSINIIGDDEVVTNDENKKKILLNLD YEGVLKAWADQRCPWTNGERPELDSNESWPDCMGNYMGIMNENVTIVDRGREARVTRYREKRRTRLFSKKIRYEVRKLN AEKRPRMKGRFVKRANFVTTSTPNYPLVK
1 B-box + CCT	Solyc04g007210 (*S*lBBX13)	MSSEKKLANAMGAKTARACDNCIRKRARWYCAADDAFLCQSCDSSVHSANPLARRHERVRLKTSSFKSSDDFPNLESTVS GLGSGSGSGSDSIPSWHCGFTRKARTPRYGNKHAKRVKSTEEEEEEEEMKNPIQLVVPEILSDENSHDENEEEQLLYRVPIF DPFMADGSNYGNEYSSNKVDFNQDMNTFQGLLAPSEMELAEFAADVVSLLGKGLDDEESFNYMEGLGFLEKHDEKLVKVE DEGEVGFVNMISTNNQVDYSEFDMVGETFELKFDYDSQVINNLDEDNKKVEFLEINYDSGKNNNKIMLNLDYESVLKSWGD KRFPWTTGVRPEVDFNDCWPVCMGNCGKIHSYGDIAIMNGHGGGVVDEGREARVLRYKEKRRTRLFSKKIRYEVRKLNAE KRPRMKGRFVKRTNFAPTPFPSLNK
2 B-box + CCT	Solyc02g089540 (*S*lBBX3)	MLKKENSNNWARVCDSCHSATCTVYCRADSAYLCAGCDARIHTASLMASRHERVWVCEACERAPAAFLCKADAASLCASC DADIHSANPLARRHHRVPIMPIPGTIYGPPAVHTITGGSMMIGGTTGEGTEDDGFLSLNQDADDTTIDEEDEDEAASWLLLNP PVKNNNKNNNYGMLFGGEVVDDYLDLAEYGGDSQFNDQYSVNQQQQHYSVPQKSYVEDSVVPVQNGQRKSLILYQTPQQ QQSHHLNFQLGMEYDNSNTGYGYPASLSHSVSISSMDVSVVPESAQSETSNSHPRPPKGTIDLFSGPPIQIPPQLTPMDREA RVLRYREKKKNRKFEKTIRYASRKAYAETRPRIKGRFAKRTDVEAEVDQMFSTQLMTDSNYGIVPSF
2 B-box + CCT	Solyc12g096500 (*S*lBBX5)	MGTENWSLTAKLCDSCKTSPATVFCRADSAFLCLGCDCKIHAANKLASRHARVWVCEVCEQAPASVTCKADAAALCVTCD RDIHSANPLARRHERFPVVPFYDFAVAKSHGGGDTDADAVDDEKYFDSTNENPSQPEEEAEAASWILPTPKEGTDQYKSAD YLFNDMDSYLDIDLMSCEQKPHILHHQQHQHNHYSSDGVVPVQNNNETTHLPGPVVDGFPTYELDFTGSKPYMYNFTSQSI SQSVSSSSLDVGVVPDHSTMTDVSNTFVMNSSSGAIAGAGADVVPNAVSGLDREARVMRYREKRKNRKFEKTIRYASRKA YAETRPRIKGRFAKRTETEIDSLITVDASYGVVPSF

8. APPENDIX B

"TCMP-2 affects tomato flowering and interacts with BBX16, a homolog of the arabidopsis B-box MiP1b"

Barbara Molesini[1] | Valentina Dusi[1] | Federica Pennisi[1] | Gian Pietro Di Sansebastiano[2] | Serena Zanzoni[3] | Anna Manara[1] | Antonella Furini[1] | Flavio Martini[1] | Giuseppe Leonardo Rotino[4] | Tiziana Pandolfini[1]

[1]Department of Biotechnology, University of Verona, Verona, Italy; [2]DiSTeBA Department of Biological and Environmental Sciences and Technologies, University of Salento, Lecce, Italy; [3]Centro Piattaforme Tecnologiche, University of Verona, Verona, Italy; [4]CREA Research Centre for Genomics and Bioinformatics, Lodi, Italy.

Plant Direct. 2020;00:1–16. wileyonlinelibrary.com/journal/pld3 ; DOI: 10.1002/pld3.283

"How Hormones and MADS-Box Transcription Factors Are Involved in Controlling Fruit Set and Parthenocarpy in Tomato"

Barbara Molesini | Valentina Dusi | Federica Pennisi | Tiziana Pandolfini

Department of Biotechnology, University of Verona, Strada Le Grazie, 15, 37134 Verona, Italy;

Genes 2020, 11, 1441; doi:10.3390/genes11121441 www.mdpi.com/journal/genes